Molecular Biological Studies of the Photosynthetic Electron Transfer Pathway in Green Sulfur Bacteria:

An analysis of the electron donor side on the reaction center and a new approach to elucidate its symmetric pathway

緑色硫黄細菌の光合成電子伝達経路に関する分子生物学的研究:
反応中心における電子供与系の解析と対称的経路の解明に向けた新しいアプローチ

Doctoral dissertation

Chihiro Azai

May 2010

Graduate School of Science

Osaka University

Abbreviations

Abs	absorbance
BChl	bacteriochlorophyll
β-OG	n-octyl-β-D-glucopyranoside
Chl	chlorophyll
cyt	cytochrome
DTT	dithiothreitol
ESR	electron spin resonance
ET	electron transfer
FAP	filamentous anoxygenic phototroph
Fe-S	iron-sulfur
Fd	ferredoxin
FMO	Fenna-Mathews-Olson
LC	liquid chromatography
MS	mass spectrometry
OD	optical density
PAGE	polyacryl amide gel electrophorasis
PCR	polymerase chain reaction
PS I, II	Photosystem I, II
RC	reaction center
SDS	sodium dodecyl sulfate
SQR	sulfide:quinone reductase

Contents

General Introduction

An Overview of Photosynthesis

Two types of photosynthesis

Photosynthesis is one of the most important biological processes largely responsible for primary production on the earth. It converts solar energy to chemical free energy and generates physiological reducing power required for many metabolic processes including inorganic carbon assimilation. Although there are so many kinds of photosynthetic organisms, their photosynthetic reaction systems can be classified into two classical groups in terms of the oxygen-evolving ability: oxygenic and anoxygenic photosynthesis. The most flourishing and widely distributed photosynthetic organisms on the present earth are oxygenic phototrophs, such as plants, algae, and cyanobacteria, which utilize water as an electron source for their growth and evolve oxygen as a byproduct of water cleavage reaction. It is considered that oxygenic phototrophs had emerged in the ancient ocean ca. 3.5 billion years ago [1], and oxygen released from water cleavage gradually changed the anaerobic atmosphere into the present aerobic one.

On the other hand, all of prokaryotic phototrophs other than cyanobacteria, such as purple bacteria, green sulfur bacteria, heliobacteria, and filamentous anoxygenic photosynthetic bacteria (FAPs), are anoxygenic ones, which are most commonly called 'photosynthetic bacteria'[1-4]. A classification of photosynthetic organisms by means of the oxygen evolving ability and the types of reaction center complexes (as mentioned below) is summarized in Table G-1. In contrast to oxygenic phototroph, anoxygenic ones do not

evolve oxygen because they utilize organic and/or inorganic reduced compounds as photosynthetic electron sources. Architectures of their photosynthetic system are much simpler than those of oxygenic ones and are supposed to remain many primitive properties. Therefore, a research on anoxygenic photosynthetic mechanisms would provide important clues for the fundamental principle and evolutionary scenario of the light energy conversion system.

Table. G-1: ***Two types of photosynthesis and two types of RC complexes.***

	Type I RC	**Type II RC**
Oxygenic photosynthesis	**Chloroplast** (Plants, Algae) **Cyanobacteria** (Photosystem I)	(Photosystem II)
Anoxygenic photosynthesis	**Green sulfur bacteria** **Heliobacteria**	**Purple bacteria** **Filamentous anoxygenic bacteria**

Primary process of photosynthesis

The primary process of photosynthesis is a light-driven electron transfer (ET) reaction, so-called 'light reaction' or 'photosynthetic electron transport'. The overview of this process is well known as follows. The initial step of photosynthesis occurs within a photosynthetic reaction center (RC) complex in the membrane. Light energy is captured as a excited state of a light harvesting pigment and transferred to a primary electron donor (P), which is a special dimer of (bacterio)chlorophyll ((B)Chl), through excitation energy transfer reactions between pigment molecules. The photoexcited P (P*) induces an initial charge separation with a primary electron acceptor (A_0) and starts subsequent ET reactions at both acceptor and donor sides. On the acceptor side, the energized and unpaired electron on the A_0^- anion radical migrates on a series of ET cofactors (A_n) in the RC complex, and finally reduces $NADP^+$ to generate physiological reducing power, NADPH, which is required for various biosynthetic

reactions including carbon assimilation and nitrogen fixation. A schematic representation of the initial process and ETs on the acceptor side is shown below.

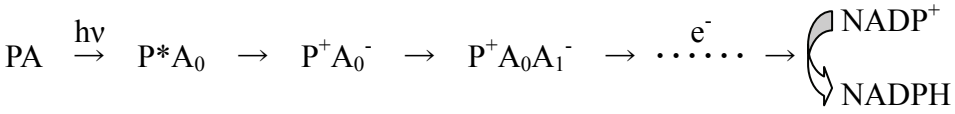

On the donor side, the photooxidized P^+ cation radical draws an electron from a secondary electron donor (D_1) due to its high electrochemical potential, and induces subsequent positive hole transfer reactions that are a series of rereduction processes with electron donors (D_n). The positive hole from P^+ is finally filled with an electron obtained by oxidizing an environmental electron donor. Some electron donors are protonated and deprotonated concomitantly with their reduction and oxidation, which cause unidirectional membrane proton translocation and/or location-specific proton release and consumption and form the difference in proton concentration across the membrane. The proton concentration difference generates a transmembrane electrochemical potential gradient, known as transmembrane proton motive force. It drives the membrane ATP synthase, F_oF_1-ATPase, to produce large amounts of free energies required for various life activities. Thus, the sequential photosynthetic ET reactions are generally coupled to ATP synthesis, which is called 'photo-phosphorylation'. A schematic representation of the donor side ETs and coupled ATP synthesis is shown below.

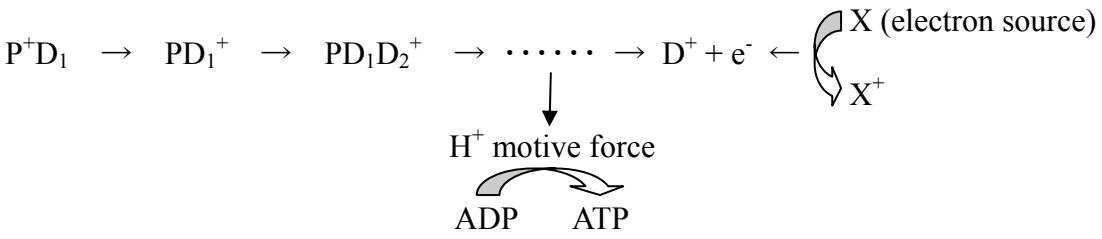

Since photosynthetic ET reactions on both sides are driven by a pair of the strong oxidant and reductant, P^+ and A_0^-, only the initial charge separation within the RC complex is

light-dependent in absolute terms. Thus, the RC complex is a central system for light-to-energy conversion and serves as an engine of photosynthesis.

Photosynthetic Reaction Centers

Two types of RC complexes and electron transport pathways

RC complexes can be classified into two types in terms of their terminal electron acceptors: type I and II RCs. Type I RC is alternatively called 'iron-sulfur (Fe-S) type' RC because it contains three low potential Fe-S clusters as terminal electron acceptors. The type I RC can generate a highly energized electron to reduce ferredoxin (Fd), which is a soluble electron carrier and used as the electron donor for $NADP^+$ reduction by ferredoxin-$NADP^+$ oxidoreductase (FNR). On the other hand, the type II RC has two pheophytin *a* and two quinone molecules as primary and terminal electron acceptors, respectively; thus, it is alternatively called 'pheophytin-quinone type' RC. Type II RC is incapable of reducing Fd, but carries out a double reduction of the terminal quinone acceptor, Q_B. The resultant quinol molecule serves as a lipophilic electron carrier and is subsequently oxidized in a membrane-bound quinol oxidoreductase such as cytochrome (cyt) bc_1 and b_6f complexes. Through quinol oxidation in this complex, the proton gradient is formed across membranes with the Q-cycle mechanism.

These two types of RCs have obviously different biochemical and physiological functions, which are closely related to overall photosynthetic transport pathways in photosynthetic organisms [3-5], as summarized in Figure G-1. Oxygenic phototrophs possess both types of RC complexes: photosystems (PSs) I and II. PS I is a type I RC which reduce Fd and oxidize soluble metal-containing carriers, cyt c_6 and/or plastocyanin; PS II is a type II RC which reduce plastoquinone molecules and oxidize water molecules. They are linked with plasoquinol-cyt c_6 and/or plasoquinol-plastocyanin oxidoreductase, cyt b_6f

complex, through a series of ET reactions. The plastoquinone serves as a mediator between PS II and cyt b_6f complex, while cyt c_6 and plastocyanin do between cyt b_6f complex and PS I. Therefore, the well-known linear ET pathway in oxygenic photosynthesis, depicted as 'z-scheme', occurs in the following sequence: water, PS II, plastquinone, cyt b_6f complex, cyt c_6 and/or plastocyanin, PS I, ferredoxin, FNR, and $NADP^+$ (Figure G-1). However, when large amounts of ATPs are required and/or excess amounts of NADPHs are accumulated in the cell, oxygenic photosysnthesis shifts to operate a cyclic ET, which occurs only between cyt b_6f complex and PS I [6-8].

In contrast to oxygenic ones, anoxygenic phototrophs have only one type of RC complexes (Table G-1): type I RCs in green sulfur bacteria and heliobacteria (RC I), and type II RCs in purple bacteria and FAPs (RC II) [3-5]. In purple bacteria, unlike PS II, RC II does not oxidize water, but instead of the oxygenic linear one, it operates a cyclic ET through quinol-cyt c_2 oxidoreductase, cyt bc_1 complex. Similarly to oxygenic photosynthesis, a quinone molecule shuttles between RC II and cyt bc_1 complex. The small soluble *c*-type cyt, cyt c_2, serves as an electron carrier from cyt bc_1 complex to RC II [9]. Therefore, the cyclic ET in purple bacteria occurs in following sequence: RC II, quinone, cyt bc_1 complex, and cyt c_2 (Figure G-1). It is also well known that the membrane-anchored cyt c_y can substitute for the function of cyt c_2 in some species of purple bacteria [10]. In the case of FAPs, a cyclic ET is thought to occur in similar manner to the purple bacterial one, but there are some significant difference in their ET components; for example, a molybdopterin oxidoreductase homologue, cyt C_p complex, would function as a quinol oxidoreductase instead of a cyt bc_1 complex, and the membrane-bound blue-copper protein, auracyanin, might transfer the electron from that complex [11,12]. The RCs of green sulfur bacteria and heliobacteria essentially function in almost the same way as PS I. Quinone molecules convey electrons derived from oxidation of environmental electron sources to a quinol oxidoreductase. As in the case of cyt c_6 in oxygenic phototrophs and cyt c_2 and c_y in purple bacteria, small *c*-type

cyts also serve as electron carriers from a quinol oxidoreductase to the RCs I in both green sulfur bacteria and heliobacteria [13-16]. The reduced Fd and/or NADPH, which is a final product on the acceptor side of the RCs I, is consumed by various biosynthetic reactions in the cell. This electron transfer pathway from quinone to Fd is recognized as a linear one (Figure G-1). Contrary to this, a cyclic ET pathway around the RC I might also be operated; quinols formed on the acceptor side diffuse in membranes to be oxidized in *bc* complex.

Symmetric and asymmetric properties of RC complexes

In all RC complexes so far investigated, the RC core protein is a dimer of transmembrane core polypeptides. It serves as a scaffold of ET cofactors including P and A_0. PS I, PS II, and RC II consist of two core polypeptides which are almost identical but partially different and are considered to have been diverged from the same polypeptide. These RCs are thus referred to as 'heterodimeric' ones. The crystal structure of heterodimeric RCs was first determined on the RC II from purple bacterium *Blastochloris viridis* (formerly *Rhodopseudomonas viridis*) [17]; this was also the crystal structure of a membrane protein that was first reported. Afterward, many three-dimensional structures have been determined in all kinds of heterodimeric RCs; for example, PS I from the cyanobacterium *Thermosynechococcus elongatus* [18] and the higher plant *Arabidopsis thaliana* [19,20], PS II from *T. elongates* [21,22], and RC II from the purple bacterium *Rhodobacter sphaeroides* [23-26]. These structures of heterodimeric RCs have revealed some noteworthy structural relationships between RC complexes; regardless of highly diverse amino acid sequences, the RC core polypeptides fold in almost the same configurations and ET cofactors are arranged to form two quasi-C_2 symmetrical ET pathways (Figure G-2). Thus, all present RCs are supposed to have been developed from the same 'homodimeric' ancestor molecule whose two core polypeptides are identical and two ET pathways are perfectly C_2-symmetrical [2,3,5].

In contrast to symmetric properties of the structures, spectroscopic studies so far have

shown that the electron migrates on only or mainly one pathway; therefore, the two ET pathways are obviously asymmetrical in terms of the function [5,27-29] (Figure G-2). This discrepancy would arise from the difference in local physicochemical environments around two pathway provided by the heterodimeric core protein. There has been, however, no direct experimental evidence to prove this idea because it is difficult to specify amino acid residues responsible for the asymmetric nature of ET pathways in the present highly diverse heterodimeric core proteins.

On the other hand, RC I of green sulfur bacteria and heliobacteria is the homodimeric RC whose core protein is made up of two identical polypeptides [14,15,30]. There would be a set of entirely C_2-symmetrical ET pathways in the RC I; therefore, those two ET pathways would show the completely same physicochemical properties. Indeed, fourier-transform infrared (FTIR) and ESR spectroscopic studies showed that the positive charge of P^+ in RC I is symmetrically distributed on the special dimer of BChl [31]. The axially-symmetrical spin distribution on the inter-polypeptide [4Fe-4S] cluster, F_X, has also been suggested in heliobacterial RC complex (unpublished data). Since the ancestral RC complex is thought to have been a homodimeric core protein and had symmetric ET pathways, RC I is expected to remain to have many ancestral features in its structure and function. Thus, RC I is a key to understand physiological meanings of heterodimerization in RCs and to explore the evolutionary process toward complicated heterodimeric RCs.

Green Sulfur Bacteria

Physiological characters of green sulfur bacteria

Green sulfur bacteria are obligatory anaerobic photoautotrophic bacteria, and classified into the phylogenetically and physiologically distinct group, *Chlorobi* [32-34]. They are gram-negative eubacteria and have no developed membrane structure as thylakoids

in chloroplasts and cyanobacteria or chromatophore in purple bacteria; therefore, a series of photosynthetic light reactions occurs in inner cellular membranes. They are usually found in anoxic and sulfide-rich freshwater, either in the bottom sediment or deep layers of the water column, or within microbial mats. Recent studies revealed that they have also been found in some extreme environment such as the anoxic layer 100 meters below the surface of the Black Sea [35], deep-sea hydrothermal vents in the Pacific Ocean [36], and the microbial mats of Octopus and Mushroom Springs in Yellow Stone National Park [37]. To adapt to such dim-light environments, all green sulfur bacteria so far characterized have developed unique light harvesting organelles attached to the membrane, called 'chlorosome' [38](Figure G-3A). Chlorosome is the vesicle that is made of a monolayer of lipid and contains self-aggregates of BChl *c*, *d*, or *e* depending on species [39,40]. It can capture the light energy and transfer the excited energy to the RC with high efficiency; it allows these organisms to grow at remarkably low light intensities (Figure G-3B). All well characterized strains fix carbon dioxides by the reductive (also called 'reverse') tricarboxylic acid (TCA) cycle instead of the common calvin cycle [41-43]. Most of strains utilize the electron derived from oxidation of inorganic sulfur compounds such as sulfide, thiosulfate, and/or elemental sulfur, and also hydrogen for their photosynthesis, while a few species can use ferrous iron [44,45].

To provide greater understandings of physiology and evolution of green sulfur bacteria especially about their photosynthesis and carbon and sulfur metabolism at the molecular level, genome sequencing projects have been performed in twelve well-characterized strains (available on the websites of Integrated Microbial Genomes resource (IMG, http://img.jgi.doe.gov) and National Center for Biotechnology Information (NCBI, http://www.ncbi.nlm.nih.gov)). Although these projects are currently at various stages, these genome analyses have provided much comprehensive information for their biodiversities. They have remarkably small 2-3 Mb genomes encoding only 1700-2800 genes, and 1400-1500 of them are common in all strains. In addition to this, the lack of the

two-component signaling system for the response to the environmental change and few transcription factors indicate that they are well adapted to a narrow-range environmental condition where light energy and nutrients are limited [4].

The one notable exception of green sulfur bacteria is *Chlorobium ferrooxidans*, which is classified into the genus *Chlorobium* based on its 16S-rRNA and *fmoA* gene sequences [33,44,45]. Unlike all other green sulfur bacteria, this strain is incapable of utilizing any reduced sulfur compounds, but uses ferrous iron (Fe^{2+}) as the sole electron source for its growth [45]. Consistent with this phenotype, many genes related to oxidation of sulfur compounds are absent in its genome [44]. However, any candidate genes responsible for oxidation of ferrous iron have not been identified yet; thus, the ferrous iron-oxidizing enzyme system and the electron transport pathway from ferrous iron to the RC have remained unknown.

Green sulfur bacterial RC complexes

The green sulfur bacterial RC complex consists of only five subunits, PscA-D and Fenna-Mathews-Olson (FMO) protein [30] (Figure G-4A). Therefore, it has a simpler architecture compared to the heterodimeric PS I of oxygenic photorophs, which are composed of twelve subunits. Functions of the subunits of the green sulfur bacterial RC complex have been well characterized by biochemical and spectroscopic studies. PscA is the core polypeptide, two of which forms the homodimeric core protein. It is partially homologous to PsaA and PsaB, core polypeptides of PS I. PscB is the functional homologue of PsaC in PS I, which contains two [4Fe-4S] clusters, F_A and F_B, as terminal electron acceptors. PscC is the membrane-bound *c*-type cyt, which is also called 'cytochrome c_z' [46,47]. It is unique subunit for the green sulfur bacterial RC complex serving as the physiological secondary electron donor. PscD is the small dispensable subunit responsible for the effective energy transfer from the chlorosome to the RC [48]. Its amino acid sequence shows a significant

similarity to PsaD in PS I; but, it is not a functional homologue. FMO protein is the water-soluble light harvesting complex attached to the RC complex. Its crystal structure was determined as the first case of pigment-containing proteins [49-51]. It forms a trimeric structure binding seven or eight BChls *a* in each monomer, and mediates energy transfer from chlorosome to the RC. Although the crystal structure of the green sulfur bacterial RC complex is still lacking, subunit organization of the green sulfur bacterial RC complex (Figure G-4A) has been constructed from the three-dimensional image of the purified RC complex by the single particle analysis using STEM (Scanning Transmission Electron Microscopy) [52] (Figure G-4B).

Most of ET cofactors in the green sulfur bacterial RC are also identified [30] (Figure G-4A). The primary electron donor is a special dimer of BChl *a* (or its epimer) with an absorption peak at 830 nm, but historically called 'P840'. The primary electron acceptor, A_0, is Chl a_{PD}, which is a close derivative of Chl *a* in oxygenic phototrophs and shows almost the same spectroscopic character as Chl *a*. The [4Fe-4S] cluster, F_X, is the electron acceptor which are formed by chelating with cysteine residues from two identical PscAs and the terminal electron acceptors, F_A/F_B, are hold in the PscB.

Meanwhile, the existence of a secondary acceptor, A_1, is still controversial in RC I. Regardless of whether type I or II RCs, all heterodimeric RCs contain two quinone molecules serving as the A_1 acceptor [5]. In PS I, two phylloquinone molecules are tightly bound to the PsaA/PsaB core protein through π-π interactions with indol rings of tryptophan residues. These tryptophan residues are conserved among all PsaA and PsaB core polypeptides of PS I, but not among those of RC I [14,15,30,53]. In homology models of RCs I, the estimated quinone-binding site seems to be rather hydrophilic than hydrophobic, suggesting that quinone molecules are loosely bound to the RC as in the case of the terminal acceptor, Q_B, in type II RC.

Spectroscopic observations concerning A_1 acceptor in RC I could not been

understood straightforward [14,15,30]. The transient spectroscopic analyses revealed that the reoxidation of A_0^- occured with the time constant $t_{1/e}$ = 600 ps in RC I, which was supposed that the ET proceeds from A_0 directly to F_X without A_1. However, this rate constant is too fast judged from the ET theory, assuming that the structure of RC I is almost the same as PS I. Stable ESR measurements at cryogenic temperature showed that semiquinone-like radicals are accumulated by cooling RC I under the light in the presence of strong reductants, indicating that there is a photoreducible quinone-like acceptor in RC I. Consistent with this observation, HPLC analyses of various RC I preparations have detected approximately one menaquinone molecule in the RC complex, but the absence or the specific extraction of the menaquinone molecule did not cause any effect on the ET reaction to F_X. Recently, the transient ESR signal of a quinoine-like A_1 acceptor was observed in the heliobacterial RC complex [57], but not in any green sulfur bacterial RC complex. The three-dimensional structure of RC I can provide some important clues to solve these discrepancy; however, any RC I has never been a successful target for the crystal structural study due to their extreme sensitivities to oxygen causing the difficulties in biochemical manipulations.

Donor-side electron transport pathways

In green sulfur bacteria, the donor side electron transport occurs in the periplasmic space and starts with the immediate electron donation from cyt c_z, PscC subunit of the RC complex, to the photooxidized P840 [46,58]. The cyt c_z is the membrane-bound mono-heme *c*-type cyt with an α-absorption peak at 551-553 nm; this wavelength is slightly different in various preparations [46,59-62]. The cyt c_z can be divided into two distinct domains: one consists of the three membrane-spanning α-helices in the N-terminal half portion, and another comprises the hydrophilic C-terminal half with a single-heme attachment site [58]. Recently, the C-terminal hydrophilic heme-containing moiety has been overexpressed in *Escherichia coli* and its crystal structure has been deterimed [61,63]. It revealed that the C-terminal

heme-binding portion is structurally related to well-known soluble electron carriers like mitochondrial cyt *c*. The ET rate from cyt c_z to P840 shows the remarkable dependence on viscosity of the reaction mixture [59], implying that the C-teminal domain of cyt c_z fluctuates on the surface of the RC complex by anchoring to membranes through its N-terminal hydrophobic domain while searching for its reaction partners around the P840.

The two different electron donors for the oxidized cyt c_z are identified by two different experiments (Figure G-1). One is a small water soluble mono-heme *c*-type cyt named cyt *c*-554 or cyt *c*-555, and described here as cyt *c*-554/555. Its α-absorption band is asymmetric and peaked at 554 or 555 nm depending on species [13,64-66]. It serves as a soluble electron carrier for periplasmic sulfur-oxidizing enzymes as mentioned below. The direct electron donation from cyt *c*-554/555 to the oxidized cyt c_z is clearly demonstrated by the *in vitro* reconstitution experiment of the purified RC complex and the cyt *c*-554 isolated from *Chlorobaculum tepidum* [66]. The other direct donor for the cyt c_z is a membrane-bound *c*-type cyt, named cyt *c*-556, which was discovered by chemically reduced-minus-oxidized difference absorption spectrum of the purified membrane [47]. The flash-excitation analysis using the membrane demonstrates that cyt *c*-556 serves as a direct electron donor for the oxidized cyt c_z and a shuttle-like carrier between the quinole oxidoreductse and the RC complex.

Since these two electron transport pathways were investigated independently, it remains unclear whether cyt *c*-554/555 shuttles between quinole oxidoreductse and the RC complex in parallel with cyt *c*-556 as in the case of cyt c_2 and c_y of purple bacteria. The recent mutagenetic study revealed the dispensability of cyt *c*-554 for the photosynthetic growth of *Chlorobaculum tepidum* by constructing the mutant lacking cyt *c*-554 [67]. However, no disruption mutant of cyt *c*-556 has been obtained yet, because its amino acid sequence information is still lacking. Thus, more information concerning ET reactions, especially when all these electron carriers coexist as *in vivo*, would be required for

understanding the physiological electron transport pathways in green sulfur bacteria.

In addition to the linear ET pathways, two cyclic ET pathways have been predicted in green sulfur bacteria. One is derived from the structural property of the quinone acceptor in RC I as mentioned above. The loosely bound quinone molecule in RC I might serve as a lipophilic mobile carrier and shuttle between the RC complex and the quinol oxidoreductase as the Q_B quinone in type II RC. Another is the NADH dehydrogenase-mediated pathway. Since a set of genes coding NADH dehydrogenase subunits (*nuo* genes) is present in green sulfur bacterial genomes [68], the complex might mediate the ET from NADH and/or NADPH to a quinone molecule. However, these cyclic ETs have never been observed so far even in biochemical or physiological ways. It remains uncertain whether these cyclic ET really operate in green sulfur bacteria or not.

Inorganic sulfur oxidation pathways

Green sulfur bacteria oxidize inorganic reduced sulfur compounds for their photoautotrophic growth. Almost all of them can oxidize sulfide (S^{2-}) and elemental sulfur (S^0) to sulfate (SO_4^{2-}). They highly prefer to use sulfide even if any other sulfur compounds are available [42,69]. At the initial stage in batch culture, they oxidize sulfide incompletely to elemental sulfur, and secrete it extracellularly as insoluble sulfur globules. Elemental sulfur of these sulfur globules are incorporated again into the cell and oxidized completely to sulfate when sulfide is depleted in the medium. Several strains of green sulfur bacteria are also capable of oxidizing thiosulfate ($S_2O_3^{2-}$) to sulfate [33,44]. Oxidation of tetrathionate ($S_4O_6^{2-}$) has been also reported in two thiosulfate-oxidizing strains [42], whereas no strain has been reported to utilize sulfite (SO_3^{2-}).

The oxidation pathways of these reduced sulfur compounds have not been completely elucidated, while many potential enzymes involved in oxidations of these sulfur compounds have been identified by biochemical and recent comparative genomic analyses [44,68].

There are two kind of enzymes responsible for sulfide oxidation in green sulfur bacteria: sulfide:quinone reductase (SQR) and flavocytochrome *c*. The SQR is a membrane-bound flavoprotein and catalyzes oxidation of sulfide to elemental sulfur with quinone as the electron acceptor. There are three *sqr* gene homologues in the *Chlorobaculum tepidum* genome; two of them are thought to contribute the sulfide-dependent growth [70]. The *sqr* gene homologue is also found in genomes of all other green sulfur bacteria. Flavocytochrome *c*, FCC, is a soluble periplasmic enzyme serving as a sulfide:cyt *c* oxidoreductase [69,71,72]. It consists of two subunits: a small *c*-type cyt subunit, FccA, and a large flavoprotein subunit, FccB. FccA and FccB are encoded in the *fccAB* gene cluster, which are also widely distributed among green sulfur bacteria.

Thiosulfate oxidation is thought to be catalyzed by Sox multienzyme system [73-75]. The constituent proteins of the Sox system are encoded by the *sox* gene cluster, which is present in all thiosulfte-oxidizing strains of green sulfur bacteria. The functions of Sox proteins are well characterized using lithoautotrophic sulfur-oxidizing bacterium *Paracoccus pantotrophus* [74,76] and purple non-sulfur bacterium *Rhodovulum sulfidophilum* [75]; the current reaction models for the thiosulfate oxidation pathway to sulfate has been proposed as shown in Figure G-5. According to this scheme, the SoxCD complex is required for complete oxidation of thiosulfate and recycling of the scaffold complex, SoxYZ; however, recent genomic analyses revealed that the *soxCD* genes are lacking in *sox* gene clusters of green sulfur bacteria [44,73]. Thus, other reaction mechanisms should be involved in complete oxidation of thiosulfate.

Since reduced sulfur compounds are used as electron sources for the photosynthesis, all these sulfur oxidation pathways are necessary to be linked to the donor-side electron transport pathways. The SQR-mediated sulfide oxidation can reduce quinone serving as a membrane electron carrier; therefore, SQR would form the membrane electron transport pathway with the quinol oxidoreductase. On the other hand, it has been considered that cyt

c-554/555 could function as the electron acceptor for both FCC and Sox system by *in vitro* reconstitution experiments studied more than 30 years ago [77-79]. A recent study also confirmed that the cyt *c*-554 enhances thiosulfate oxidation activity of the Sox system reconstituted *in vitro* [80]. However, these pathways were investigated only in biochemical ways and have never been verified *in vivo*; thus, the physiological electron carrier for each sulfur oxidation pathway has been inconclusive and the overall elecstron transport pathway from sulfur compounds to the RC complex in green sulfur bacteria has also remained unsolved.

Chlorobaculum tepidum as the model organism

Chlorobaculum tepidum (formerly *Chlorobium tepidum*), one of the best characterized strains, is commonly used as the model species of green sulfur bacteria [68,81,82]. Its complete genome sequence has been available in green sulfur bacteria in 2002 by TIGR (The Institute for Genome Research, USA) [83]. This organism is a moderately thermophilic phototroph with the optimal growth temperature at 45-48°C [81]; therefore, this is suitable for biochemical manipulations such as the preparation in anaerobic chamber, which is available only at room temperature. For this beneficial property, many successful biochemical and spectroscopic studies have been performed using its photosynthetic membrane and RC complex. Meanwhile, any molecular genetic study had never been conducted in homodimeric RC I of green sulfur bacteria as well as heliobacteria, as contrasted to huge numbers of mutagenic studies on heterodimeric RCs. However, in 2001, Frigaad and Bryant reported a natural transformation of *Chlorobaculum tepidum* by homologous recombination, and established the general gene inactivation method [84]. Since then, many mutants have been constructed by disrupting genes concerning BChl and carotenoid biosynthesis (for review, see [68]), but few were concerning the RC complex [48], electron carrier protein [67], and inorganic sulfur oxidation [70]. This situation is

presumably caused by the obligatory photoautotrophic feature of green sulfur bacteria; thus, another method such as gene expression and/or transformation system is required for further mutagenic studies targeting essential genes for photosynthesis.

Outline of the Thesis

Numerous informative data on the green sulfur bacterial photosynthetic system have been provided with many biochemical and spectroscopic studies so far. However, few new achievements have been made by such traditional methods especially concerning physiological electron transport system and the function and structure of green sulfur bacterial RC complex. The purpose of this thesis is to reveal that the molecular biological approach using *Chlorobaculum tepidum* is the most effective method and the potential breakthrough for further investigations of the green sulfur bacterial photosynthesis especially at physiological levels and also for solving long-time unsettled issues of the homodimeric RC I.

In this thesis, the author describes the results on two studies using traditional gene-inactivation mutants of *Chlorobaculum tepidum* and the new methodology for site-directed mutagenic analyses of the *Chlorobaculum tepidum* RC. Chapter I is the study concerning photosynthetic electron transport pathway in green sulfur bacteria using *Chlorobaculum tepidum* mutant lacking cyt *c*-554. This is the successful example of application of the molecular biological method to the classical biochemical and spectroscopic analysis. The results clearly demonstrate that two direct electron donors to cyt c_z, that is, cyt *c*-554 and membrane-bound cyt *c*-556, serve as the electron carriers on different electron transport pathways and form bifurcated electron donation pathways to the RC complex *in vivo*. In chapter II, the direct linking between electron transport and sulfur oxidation pathways of *Chlorobaculum tepidum* are investigated using the traditional gene-inactivation method. This is the first report on the study concerning *in vivo* electron transport pathways from sulfur

compounds to the RC complex. The meaning of the bifurcated electron transport pathways revealed in chapter I is discussed from the physiological and evolutionary aspects. In chapter III, the author proposed a new mutagenesis method, “duplication of the *pscA* gene”, which enables us to carry out any site-directed mutations in the RC core protein of *Chlorobaculum tepidum*. A small epitope tag was also found to be a useful tool for one-step preparation of the highly photoactive *Chlorobaculum tepidum* RC complex. This would prosecute some biochemical and spectroscopic studies which require large amounts of preparation, such as an X-ray crystallographic study. Furthermore, this novel method would make it possible to construct artificial heterodimeric RC complexes of *Chlorobaculum tepidum* with intentional amino acid substitutions. The author expects all these achievements in this thesis to advance much more active molecular biological researches on the photosynthesis of green sulfur bacteria for the future.

Figures

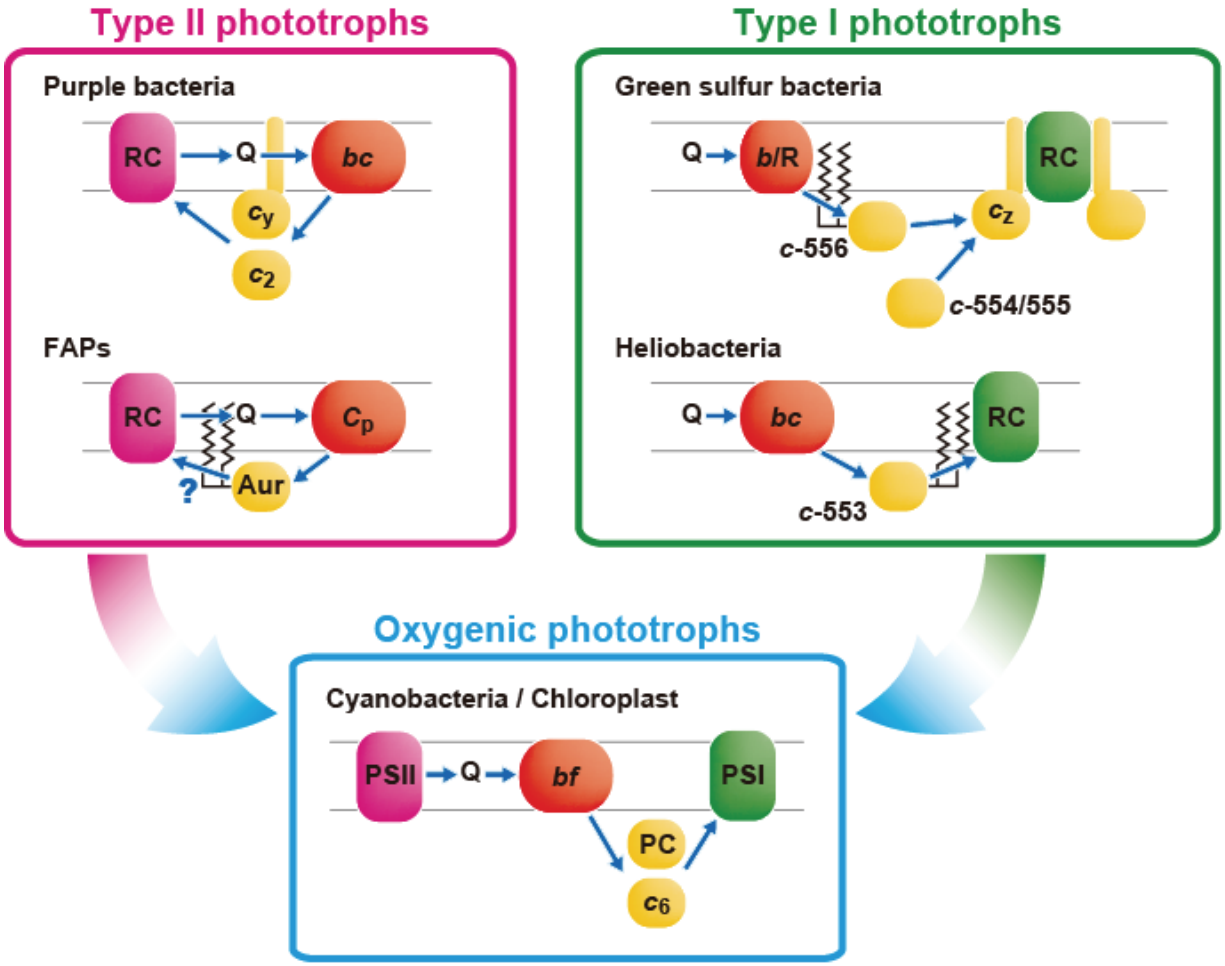

Figure G-1: ***Diagrammatic representation of photosynthetic electron transport pathways in anoxygenic and oxygenic phototrophs.*** Arrows indicate the direction of electron flows. RC, PSI, PSII, *bc* (bc_1), *b*/R, C_p, b_6f, c_2, c_y, c_z, *c*-554/555, *c*-556, *c*-553, c_6, PC, and Q represent reaction center, PS I, PS II, cyt *bc* (bc_1) complex, cyt *b*/Rieske protein, cyt C_p complex, cyt b_6f complex, cyt c_2, cyt c_y, cyt c_z, cyt *c*-554/555, cyt *c*-556, cyt *c*-553, cyt c_6, plastocyanin, and quinone pool, respectively.

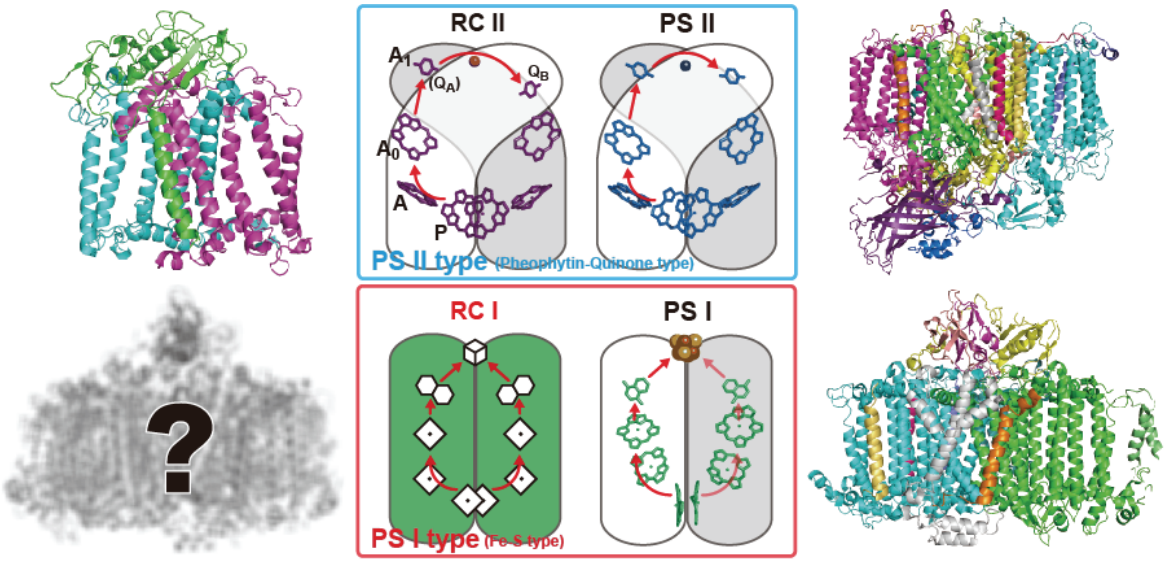

Figure G-2: ***Schematic drawing of electron transfer chains and protein structures of the four kinds of RC complexes.*** *Edges*, protein structures of RC II (PDB: 1PCR), PS II (PDB: 2AXT), and PS I (PDB: 1JB0). The crystal structure of RC I that is still unknown (left-lower edge). *Centers*, the arrangements of electron transfer cofactors in four kinds of RC complexes. Each drawn cofactor arrangements is corresponding to the protein structure drawn nearby it. Two core polypeptides in the heterodimeric RC were shown as rod-like shapes stained in different colors each other, white or gray. Arrows and their thicknesses indicate the direction and dominancy of the electron transfers, respectively. The cofactor arrangement and electron transfer pathways of RC I are shown as a possible estimation.

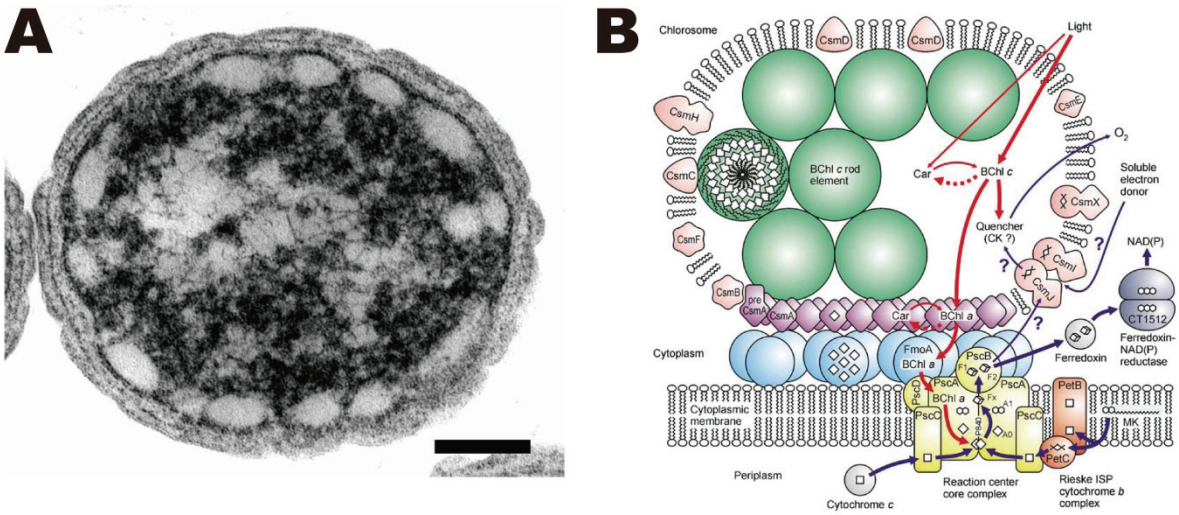

Figure G-3: ***The intracellular structure of green sulfur bacteria Chlorobaculum tepidum.*** (A) The transmission electron microscopic image of ultra-thin section of *Chlorobaculum tepidum*. The scale bar represents 100 nm. Unstained white ellipses attached to the inner membrane are chlorosomes. Reproduced from Frigaard et al. (2002: [38]). (B) The model of photosynthetic apparatus of *Chlorobium tepidum*. Red and blue arrows represent electron transfer and excitation energy transfer, respectively. Reproduced from Frigaard et al. (2003: [68]).

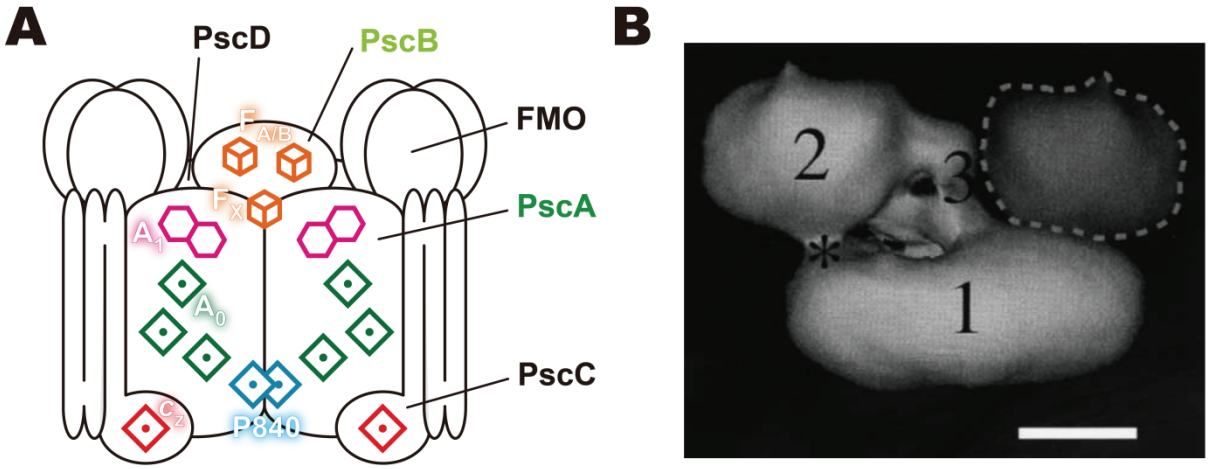

Figure G-4: ***The subunit organization of greens sulfur bacterial RC complex.*** (A) The model of subunit organization of the green sulfur bacterial RC complex. Electron acceptors identified spectroscopic studies are also shown at expected binding positions. BChl *a*, Chl *a*, and *c*-type hemes are shown as cyan, green, and red squares, respectively. Three Fe-S clusters are shown as orange cubes. The purple row of two hexagons represents naphtoquinone molecules, but its function as A_1 is still controversial. (B) Three-dimensional reconstruction of the *Chlorobaculum tepidum* PscA/PscB/PscC/PscD/FMO complex viewed from the side. Three main domains are clearly visible, labeled 1, 2 and 3. Region 1 is the membrane associated part of the complex, the homodimeric core composed of two PscA proteins together with the PscC subunit. Region 2 is the FMO trimer. The two densities distinguishable within region 3 are considered to be the PscB protein (closest to region 1) and the PscD protein (closest to region 2). The asterisk marks the possible energy transfer area. Small features, such as the apparent 1–1.5 nm cavity close to region 3, are below the resolution (about 2 nm) and arise from the threshold-based surface representation method employed. As illustrated by the outlined superposition an additional FMO trimer could be accommodated within the structure. The scale bar represents 5 nm. Reproduced from Rémingy et al (1999: [52]).

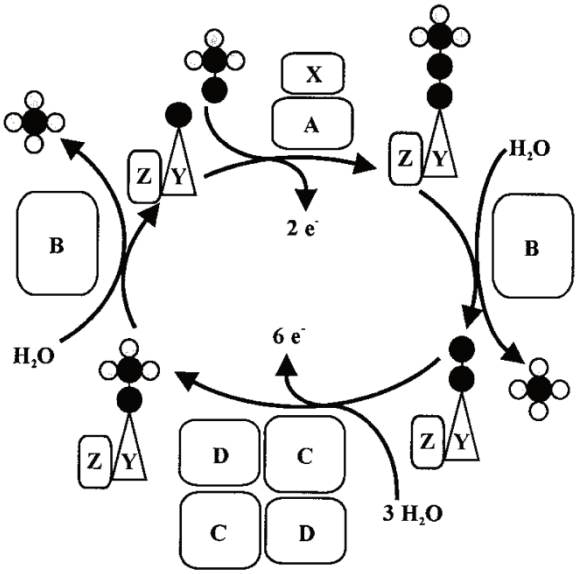

Figure G-5: ***Model of the sequence of thiosulfate oxidation reactions by Sox system in Paracoccus pantotrophus.*** Open and filled circles represent oxygen and sulfur atoms, repectively. Three components are related to the complete oxidation of thiosulfate in the Sox system. SoxYZ complex serves as a scaffold for the sequence of reactions. SoxAX complex initiates the thiosulfate oxidation to covalently conjugate thiosulfate to the thiol group of the concerved cysteine residue in the SoxY, forming SoxY-thiocysteine-S-sulfate. SoxB can hydrolyze sulfate from thiocysteine-S-sulfate and thiocysteine-sulfate. SoxCD complex completely oxidize the outer sulfur atom of SoxY-thiocysteine-S form the disulfide bond thiocysteine-S-sulfate. Reproduced from Friedrich et al (2001: [74]).

Reference

1. Olson, J. M. (2006) Photosynthesis in the Archean era, *Photosynth Res* **88**, 109-117
2. Xiong, J., and Bauer, C. E. (2002) Complex evolution of photosynthesis, *Annu Rev Plant Biol* **53**, 503-521
3. Olson, J. M., and Blankenship, R. E. (2004) Thinking about the evolution of photosynthesis, *Photosynth Res* **80**, 373-386
4. Bryant, D. A., and Frigaard, N. U. (2006) Prokaryotic photosynthesis and phototrophy illuminated, *Trends Microbiol* **14**, 488-496
5. Heathcote, P., Fyfe, P. K., and Jones, M. R. (2002) Reaction centres: the structure and evolution of biological solar power, *Trends Biochem Sci* **27**, 79-87
6. Heber, U., and Walker, D. (1992) Concerning a Dual Function of Coupled Cyclic Electron Transport in Leaves, *Plant Physiol* **100**, 1621-1626
7. Joliot, P., and Joliot, A. (2002) Cyclic electron transfer in plant leaf, *Proc Natl Acad Sci U S A* **99**, 10209-10214
8. Shikanai, T. (2007) Cyclic electron transport around photosystem I: genetic approaches, *Annu Rev Plant Biol* **58**, 199-217
9. Meyer, T. E., and Donohue, T. J. (1995) Cytochromes, iron-sufur, and copper proteins mediating wlwctron transfer from cyt bc_1 complex to photosynthetic reaction center complex. in *Anoxygenic Photosynthetic Bacteria.* (Blankenship, R. E., Madigan, M. T., and Bauer, C. E. eds.), Kluwer Academic Publishers, Dordrecht, The Netherlands. pp 725-745
10. Daldal, F., Deshmukh, M., and Prince, R. C. (2003) Membrane-anchored cytochrome c as an electron carrier in photosynthesis and respiration: past, present and future of an unexpected discovery, *Photosynth Res* **76**, 127-134
11. Tsukatani, Y., Nakayama, N., Shimada, K., Mino, H., Itoh, S., Matsuura, K., Hanada, S., and Nagashima, K. V. (2009) Characterization of a blue-copper protein, auracyanin, of the filamentous anoxygenic phototrophic bacterium Roseiflexus castenholzii, *Arch Biochem Biophys* **490**, 57-62
12. Yanyushin, M. F., del Rosario, M. C., Brune, D. C., and Blankenship, R. E. (2005) New class of bacterial membrane oxidoreductases, *Biochemistry* **44**, 10037-10045
13. Azai, C., Tsukatani, Y., Itoh, S., and Oh-Oka, H. (2010) C-type cytochromes in the photosynthetic electron transfer pathways in green sulfur bacteria and heliobacteria, *Photosynth Res*
14. Heinnickel, M., and Golbeck, J. H. (2007) Heliobacterial photosynthesis, *Photosynth Res* **92**, 35-53
15. Oh-oka, H. (2007) Type 1 reaction center of photosynthetic heliobacteria, *Photochem*

Photobiol **83**, 177-186

16. Oh-oka, H., and Blankenship, R. E. (2004) Green bacteria: secondary electron donor (cytochromes). in *Encyclopedia of biological chemistry.* (Lennarz, W. J., and Lane, M. D. eds.), Academic Press, Oxford. pp 521-524
17. Deisenhofer, J., Epp, O., Miki, K., and Michel, H. (1985) Structure of the protein subunits in the photosynthetic reaction centre of Rhodopseudomonas viridis at 3Å resolution, *Nature* **318**, 618-626
18. Jordan, P., Fromme, P., Witt, H. T., Klukas, O., Saenger, W., and Krauss, N. (2001) Three-dimensional structure of cyanobacterial photosystem I at 2.5 A resolution, *Nature* **411**, 909-917
19. Ben-Shem, A., Frolow, F., and Nelson, N. (2003) Crystal structure of plant photosystem I, *Nature* **426**, 630-635
20. Amunts, A., Drory, O., and Nelson, N. (2007) The structure of a plant photosystem I supercomplex at 3.4 A resolution, *Nature* **447**, 58-63
21. Guskov, A., Kern, J., Gabdulkhakov, A., Broser, M., Zouni, A., and Saenger, W. (2009) Cyanobacterial photosystem II at 2.9-A resolution and the role of quinones, lipids, channels and chloride, *Nat Struct Mol Biol* **16**, 334-342
22. Loll, B., Kern, J., Saenger, W., Zouni, A., and Biesiadka, J. (2005) Towards complete cofactor arrangement in the 3.0 A resolution structure of photosystem II, *Nature* **438**, 1040-1044
23. Allen, J. P., Feher, G., Yeates, T. O., Komiya, H., and Rees, D. C. (1987) Structure of the reaction center from Rhodobacter sphaeroides R-26: the protein subunits, *Proc Natl Acad Sci U S A* **84**, 6162-6166
24. Allen, J. P., Feher, G., Yeates, T. O., Komiya, H., and Rees, D. C. (1987) Structure of the reaction center from Rhodobacter sphaeroides R-26: the cofactors, *Proc Natl Acad Sci U S A* **84**, 5730-5734
25. Yeates, T. O., Komiya, H., Rees, D. C., Allen, J. P., and Feher, G. (1987) Structure of the reaction center from Rhodobacter sphaeroides R-26: membrane-protein interactions, *Proc Natl Acad Sci U S A* **84**, 6438-6442
26. Ermler, U., Fritzsch, G., Buchanan, S. K., and Michel, H. (1994) Structure of the photosynthetic reaction centre from Rhodobacter sphaeroides at 2.65 A resolution: cofactors and protein-cofactor interactions, *Structure* **2**, 925-936
27. Li, Y., van der Est, A., Lucas, M. G., Ramesh, V. M., Gu, F., Petrenko, A., Lin, S., Webber, A. N., Rappaport, F., and Redding, K. (2006) Directing electron transfer within Photosystem I by breaking H-bonds in the cofactor branches, *Proc Natl Acad Sci U S A* **103**, 2144-2149
28. Diner, B. A., and Rappaport, F. (2002) Structure, dynamics, and energetics of the primary photochemistry of photosystem II of oxygenic photosynthesis, *Annu Rev Plant Biol* **53**, 551-580

29. Wakeham, M. C., and Jones, M. R. (2005) Rewiring photosynthesis: engineering wrong-way electron transfer in the purple bacterial reaction centre, *Biochem Soc Trans* **33**, 851-857
30. Hauska, G., Schoedl, T., Remigy, H., and Tsiotis, G. (2001) The reaction center of green sulfur bacteria(1), *Biochim Biophys Acta* **1507**, 260-277
31. Noguchi, T. (2010) Fourier transform infrared spectroscopy of special pair bacteriochlorophylls in homodimeric reaction centers of heliobacteria and green sulfur bacteria, *Photosynth Res*
32. Overmann, J. (2000) The family Chlorobiaceae. in *The Prokaryotes: an Evolving Electronic Resource for the Microbiological Community.*, 3rd edn., Springer, New York, http://link.springer-ny.com/link/service/books/10125
33. Imhoff, J. F. (2003) Phylogenetic taxonomy of the family Chlorobiaceae on the basis of 16S rRNA and fmo (Fenna-Matthews-Olson protein) gene sequences, *Int J Syst Evol Microbiol* **53**, 941-951
34. Garrity, G. M., and Holt, J. G. (2001) Phylum BXI. *Chlorobi* phy. nov. in *Bergey's Manual of Systematic Bacteriology* (Boone, D. R., and Castenholz, R. W. eds.), 2nd edn., Springer, New York. pp 601-623
35. Overmann, J., Cypionka, H., and Pfenning, N. (1992) An extremely low-light-adapted phototrophic sulfur bacterium from the Black Sea., *Limnol Oceanogr* **37**, 150-155
36. Beatty, J. T., Overmann, J., Lince, M. T., Manske, A. K., Lang, A. S., Blankenship, R. E., Van Dover, C. L., Martinson, T. A., and Plumley, F. G. (2005) An obligately photosynthetic bacterial anaerobe from a deep-sea hydrothermal vent, *Proc Natl Acad Sci U S A* **102**, 9306-9310
37. Ward, D. M., Ferris, M. J., Nold, S. C., and Bateson, M. M. (1998) A natural view of microbial biodiversity within hot spring cyanobacterial mat communities, *Microbiol Mol Biol Rev* **62**, 1353-1370
38. Frigaard, N. U., Voigt, G. D., and Bryant, D. A. (2002) Chlorobium tepidum mutant lacking bacteriochlorophyll c made by inactivation of the bchK gene, encoding bacteriochlorophyll c synthase, *J Bacteriol* **184**, 3368-3376
39. Olson, J. M. (1998) Chlorophyll organization and function in green photosynthetic bacteria, *Photochem Photobiol* **67**, 61-75
40. Blankenship, R. E., Olson, J. M., and Miller, M. (1995). in *Anoxygenic Photosynthetic Bacteria.* (Blankenship, R. E., Madigan, M. T., and Bauer, C. E. eds.), Kluwer Academic Publishers, Dordrecht, The Netherlands. pp 399-435
41. Evans, M. C., Buchanan, B. B., and Arnon, D. I. (1966) A new ferredoxin-dependent carbon reduction cycle in a photosynthetic bacterium, *Proc Natl Acad Sci U S A* **55**, 928-934
42. Brune, D. C. (1989) Sulfur oxidation by phototrophic bacteria, *Biochim Biophys Acta* **975**, 189-221

43. Buchanan, B. B., and Arnon, D. I. (1990) A reverse KREBS cycle in photosynthesis: consensus at last, *Photosynth Res* **24**, 47-53
44. Frigaard, N. U., and Bryant, D. A. (2008) Genomic insight into the sulfur metabolism of phototropic green sulfur bacteria. in *Sulfur Metabolism in Phototrophic Organisms* (Rüdiger, H. ed.), Springer, New York. pp 337-355
45. Heising, S., Richter, L., Ludwig, W., and Schink, B. (1999) Chlorobium ferrooxidans sp. nov., a phototrophic green sulfur bacterium that oxidizes ferrous iron in coculture with a "Geospirillum" sp. strain, *Arch Microbiol* **172**, 116-124
46. Oh-oka, H., Kamei, S., Matsubara, H., Iwaki, M., and Itoh, S. (1995) Two molecules of cytochrome c function as the electron donors to P840 in the reaction center complex isolated from a green sulfur bacterium, Chlorobium tepidum, *FEBS Lett* **365**, 30-34
47. Oh-oka, H., Iwaki, M., and Itoh, S. (1998) Membrane-bound cytochrome cz couples quinol oxidoreductase to the P840 reaction center complex in isolated membranes of the green sulfur bacterium Chlorobium tepidum, *Biochemistry* **37**, 12293-12300
48. Tsukatani, Y., Miyamoto, R., Itoh, S., and Oh-Oka, H. (2004) Function of a PscD subunit in a homodimeric reaction center complex of the photosynthetic green sulfur bacterium Chlorobium tepidum studied by insertional gene inactivation. Regulation of energy transfer and ferredoxin-mediated NADP+ reduction on the cytoplasmic side, *J Biol Chem* **279**, 51122-51130
49. Olson, J. M. (2004) The FMO Protein, *Photosynth Res* **80**, 181-187
50. Matthews, B. W., Fenna, R. E., Bolognesi, M. C., Schmid, M. F., and Olson, J. M. (1979) Structure of a bacteriochlorophyll a-protein from the green photosynthetic bacterium Prosthecochloris aestuarii, *J Mol Biol* **131**, 259-285
51. Tronrud, D. E., Wen, J., Gay, L., and Blankenship, R. E. (2009) The structural basis for the difference in absorbance spectra for the FMO antenna protein from various green sulfur bacteria, *Photosynth Res* **100**, 79-87
52. Remigy, H. W., Stahlberg, H., Fotiadis, D., Muller, S. A., Wolpensinger, B., Engel, A., Hauska, G., and Tsiotis, G. (1999) The reaction center complex from the green sulfur bacterium Chlorobium tepidum: a structural analysis by scanning transmission electron microscopy, *J Mol Biol* **290**, 851-858
53. Heathcote, P., Jones, M. R., and Fyfe, P. K. (2003) Type I photosynthetic reaction centres: structure and function, *Philos Trans R Soc Lond B Biol Sci* **358**, 231-243
54. Trost, J. T., Brune, D. C., and Blankenship, R. E. (1992) Protein sequences and redox titrations indicate that the electron acceptors in reaction centers from heliobacteria are similar to Photosystem I, *Photosynth Res* **32**, 11-22
55. Kramer, D. M., Schoepp, B., Liebl, U., and Nitschke, W. (1997) Cyclic electron transfer in Heliobacillus mobilis involving a menaquinol-oxidizing cytochrome bc complex and an RCI-type reaction center, *Biochemistry* **36**, 4203-4211
56. Hohmann-Marriott, M. F., and Blankenship, R. E. (2007) Variable fluorescence in

green sulfur bacteria, *Biochim Biophys Acta* **1767**, 106-113

57. Miyamoto, R., Mino, H., Kondo, T., Itoh, S., and Oh-Oka, H. (2008) An electron spin-polarized signal of the P800+A1(Q)- state in the homodimeric reaction center core complex of Heliobacterium modesticaldum, *Biochemistry* **47**, 4386-4393
58. Okkels, J. S., Kjaer, B., Hansson, O., Svendsen, I., Moller, B. L., and Scheller, H. V. (1992) A membrane-bound monoheme cytochrome c551 of a novel type is the immediate electron donor to P840 of the Chlorobium vibrioforme photosynthetic reaction center complex, *J Biol Chem* **267**, 21139-21145
59. Oh-oka, H., Iwaki, M., and Itoh, S. (1997) Viscosity dependence of the electron transfer rate from bound cytochrome c to P840 in the photosynthetic reaction center of the green sulfur bacterium Chlorobium tepidum, *Biochemistry* **36**, 9267-9272
60. Oh-oka, H., Kakutani, S., Kamei, S., Matsubara, H., Iwaki, M., and Itoh, S. (1995) Highly purified photosynthetic reaction center (PscA/cytochrome c551)2 complex of the green sulfur bacterium Chlorobium limicola, *Biochemistry* **34**, 13091-13097
61. Higuchi, M., Hirano, Y., Kimura, Y., Oh-oka, H., Miki, K., and Wang, Z. Y. (2009) Overexpression, characterization, and crystallization of the functional domain of cytochrome c(z) from Chlorobium tepidum, *Photosynth Res* **102**, 77-84
62. Okamura, N., Shimada, K., and Matsuura, K. (1994) Photo-oxidation of membrane-bound and soluble cytochrome *c* in the green sulfur bacterium *Chlorobium tepidum*., *Photosynth Res* **41**, 125-134
63. Hirano, Y., Higuchi, M., Azai, C., Oh-Oka, H., Miki, K., and Wang, Z. Y. (2010) Crystal structure of the electron carrier domain of the reaction center cytochrome c(z) subunit from green photosynthetic bacterium Chlorobium tepidum, *J Mol Biol* **397**, 1175-1187
64. Yamanaka, T., and Okunuki, K. (1968) Comparison of Chlorobium thiosulphatophilum cytochrome c-555 with c-type cytochromes derived from algae and nonsulphur purple bacteria, *J Biochem* **63**, 341-346
65. Meyer, T. E., Bartsch, R. G., Cusanovich, M. A., and Mathewson, J. H. (1968) The cytochromes of Chlorobium thiosulfatophilum, *Biochim Biophys Acta* **153**, 854-861
66. Itoh, M., Seo, D., Sakurai, H., and Setif, P. (2002) Kinetics of electron transfer between soluble cytochrome c-554 and purified reaction center complex from the green sulfur bacterium Chlorobium tepidum, *Photosynth Res* **71**, 125-135
67. Tsukatani, Y., Miyamoto, R., Itoh, S., and Oh-oka, H. (2006) Soluble cytochrome c-554, CycA, is not essential for photosynthetic electron transfer in Chlorobium tepidum, *FEBS Lett* **580**, 2191-2194
68. Frigaard, N. U., Chew, A. G., Li, H., Maresca, J. A., and Bryant, D. A. (2003) Chlorobium tepidum: insights into the structure, physiology, and metabolism of a green sulfur bacterium derived from the complete genome sequence, *Photosynth Res* **78**, 93-117

69. Brune, D. C. (1995) Sulfur compounds as photosynthetic electron donors. in *Anoxygenic Photosynthetic Bacteria* (Blankenship, R. E., Madigan, M. T., and Bauer, C. E. eds.), Kluwer Academic Publishers, Dordrecht, The Netherlands. pp 847-870
70. Chan, L. K., Morgan-Kiss, R. M., and Hanson, T. E. (2009) Functional analysis of three sulfide:quinone oxidoreductase homologs in Chlorobaculum tepidum, *J Bacteriol* **191**, 1026-1034
71. Fukumori, Y., and Yamanaka, T. (1979) Flavocytochrome c of Chromatium vinosum. Some enzymatic properties and subunit structure, *J Biochem* **85**, 1405-1414
72. Yamanaka, T. (1976) The subunits of Chlorobium flavocytochrome c, *J Biochem* **79**, 655-660
73. Friedrich, C. G., Bardischewsky, F., Rother, D., Quentmeier, A., and Fischer, J. (2005) Prokaryotic sulfur oxidation, *Curr Opin Microbiol* **8**, 253-259
74. Friedrich, C. G., Rother, D., Bardischewsky, F., Quentmeier, A., and Fischer, J. (2001) Oxidation of reduced inorganic sulfur compounds by bacteria: emergence of a common mechanism?, *Appl Environ Microbiol* **67**, 2873-2882
75. Bamford, V. A., Bruno, S., Rasmussen, T., Appia-Ayme, C., Cheesman, M. R., Berks, B. C., and Hemmings, A. M. (2002) Structural basis for the oxidation of thiosulfate by a sulfur cycle enzyme, *EMBO J* **21**, 5599-5610
76. Friedrich, C. G., Quentmeier, A., Bardischewsky, F., Rother, D., Kraft, R., Kostka, S., and Prinz, H. (2000) Novel genes coding for lithotrophic sulfur oxidation of Paracoccus pantotrophus GB17, *J Bacteriol* **182**, 4677-4687
77. Kusai, A., and Yamanaka, T. (1973) A Novel function of cytochrome C (555, Chlorobium thiosulfatophilum) in oxidation of thiosulfate, *Biochem Biophys Res Commun* **51**, 107-112
78. Kusai, A., and Yamanaka, T. (1973) Cytochrome c (553, Chlorobium thiosulfatophilum) is a sulphide-cytochrome c reductase, *FEBS Lett* **34**, 235-237
79. Kusai, K., and Yamanaka, T. (1973) The oxidation mechanisms of thiosulphate and sulphide in Chlorobium thiosulphatophilum: roles of cytochrome c-551 and cytochrome c-553, *Biochim Biophys Acta* **325**, 304-314
80. Ogawa, T., Furusawa, T., Nomura, R., Seo, D., Hosoya-Matsuda, N., Sakurai, H., and Inoue, K. (2008) SoxAX binding protein, a novel component of the thiosulfate-oxidizing multienzyme system in the green sulfur bacterium Chlorobium tepidum, *J Bacteriol* **190**, 6097-6110
81. Wahlund, T. M., Woese, C. R., Castenholz, R. W., and Madigan, M. T. (1991) A thermophilic green sulfur bacterium from New Zealand hot springs, Chlorobium tepidum sp. nov., *Arch. Microbiol.* **56**, 81-90
82. Frigaard, N. U., and Bryant, D. A. (2004) Seeing green bacteria in a new light: genomics-enabled studies of the photosynthetic apparatus in green sulfur bacteria and filamentous anoxygenic phototrophic bacteria, *Arch Microbiol* **182**, 265-276

83. Eisen, J. A., Nelson, K. E., Paulsen, I. T., Heidelberg, J. F., Wu, M., Dodson, R. J., Deboy, R., Gwinn, M. L., Nelson, W. C., Haft, D. H., Hickey, E. K., Peterson, J. D., Durkin, A. S., Kolonay, J. L., Yang, F., Holt, I., Umayam, L. A., Mason, T., Brenner, M., Shea, T. P., Parksey, D., Nierman, W. C., Feldblyum, T. V., Hansen, C. L., Craven, M. B., Radune, D., Vamathevan, J., Khouri, H., White, O., Gruber, T. M., Ketchum, K. A., Venter, J. C., Tettelin, H., Bryant, D. A., and Fraser, C. M. (2002) The complete genome sequence of Chlorobium tepidum TLS, a photosynthetic, anaerobic, green-sulfur bacterium, *Proc Natl Acad Sci U S A* **99**, 9509-9514

84. Frigaard, N. U., and Bryant, D. A. (2001) Chromosomal gene inactivation in the green sulfur bacterium Chlorobium tepidum by natural transformation, *Appl. Environ. Microbiol.* **67**, 2538-2544

CHAPTER I

Parallel Electron Donation Pathways to Cytochrome c_z in the Photosynthetic Reaction Center Complex of *Chlorobaculum tepidum*

Summary

In this chapter, the author studied the regulation mechanism of electron donations from menaquinol:cytochrome *c* oxidoreductase and cytochrome *c*-554 to the type I homodimeric photosynthetic reaction center (RC) complex of the green sulfur bacterium *Chlorobaculum tepidum.* Flash-induced absorption changes of multiple cytochromes were measured in the membranes prepared from a mutant devoid of cytochrome *c*-554 or in the reconstituted membranes by exogenously adding cytochrome *c*-555 purified from other *Chlorobaculum parvum*. The results indicated that the photo-oxidized cytochrome c_z bound to the RC complex was rereduced rapidly by cytochrome *c*-555 as well as by the menaquinol:cytochrome *c* oxidoreductase and that cytochrome *c*-555 did not function as a shuttle-like electron carrier between the menaquinol:cytochrome *c* oxidoreductase and cytochrome c_z. It was also shown that the rereduction rate of cytochrome c_z by cytochrome *c*-555 was as high as that by the menaquinol:cytochrome *c* oxidoreductase. The two electron transfer pathways linked to sulfur metabolisms seem to function independently to donate electrons to the RC complex.

Introduction

Green sulfur bacteria are strictly anaerobic photoautotrophs that have homodimeric type I reaction center (RC) complex, as do heliobacteria [1,2], and utilize inorganic sulfur compounds (sulfide, thiosulfate, and/or sulfur) as the electron sources for photosynthetic CO_2 fixation [3]. The primary electron donor P840, a special pair of bacteriochlorophyll *a*, in the RC complex initiates the light-driven electron-transfer reaction as the first step in the conversion of light energy into chemical free energy. It is important for the photo-oxidized $P840^+$ to be rereduced rapidly to achieve highly efficient solar energy conversion.

In a thermophilic green sulfur bacterium, *Chlorobaculum* (*Cba.*) *tepidum*, $P840^+$ is rereduced by one of RC subunits, a PscC subunit, which is also called as cytochrome (cyt) c_z [4,5]. It has been demonstrated that two molecules of cyt c_z are contained in the RC complex [6]. Cyt c_z has three membrane-spanning α-helices in its N-terminus and a heme-containing moiety in its C-terminus [5,7]. The C-terminal domain protrudes into the periplasmic space and carries electrons directly from menaquinol:cyt *c* oxidoreductase to P840 [4]. It is supposed to be fluctuated as evidenced by the extraordinary dependence of its reaction rates on solvent viscosity [7]. This unique feature of cyt c_z appears to be similar to that of cyt c_y which serves as a shuttle to mediate electron transfer between cytochrome bc_1 complex and the type II RC in *Rhodobacter* species of purple non-sulfur bacteria [8].

The oxidized cyt c_z^+ then accepts electrons from cyt *c*-554 as well as menaquinol:cyt *c* oxidoreductas [4,9]. Cyt *c*-554 is a soluble mono-heme cytochrome with a molecular mass of approximately 10 kDa [10,11], which is named cyt *c*-555 after its α-absorption peak shift in the case of *Cba. parvum* [12]. Cyt *c*-554 has been shown to function as an immediate electron donor to cyt c_z^+ by an *in vitro* reconstitution study using the purified RC complex from *Cba. tepidum* [9]. On the other hand, a study using membranes free from soluble cyt *c*-554, as confirmed by heme-staining analysis on SDS-PAGE, demonstrated a direct electron

donation from the menaquinol oxidoreductase to cyt c_z [4].

An ascorbate-reduced absorption spectrum of another cyt, which exhibited an α-absorption peak at 556 nm, was also detected in the membrane preparation [4]. Flash-induced absorption changes indeed revealed the presence of a shoulder at around 556 nm in the different spectrum of cyt c_z, which became more prominent by the addition of stigmatellin. Since the activity of the menaquinol:cyt *c* oxidoreductase was inhibited by antimycin A, It is suggested that cyt *c*-556 played a role similar to that of a cyt c_1 subunit in the cyt bc_1 complex [4]. The menaquinol:cyt *c* oxidoreductase in *Cba. tepidum* could thus be classified to the *bc*-type one although the gene encoding probable cyt c_1 has yet been unidentified in the genome of green sulfur bacteria

Tsukatani *et al.* have recently demonstrated that the electron transfer from menaquinol:cyt *c* oxidoreductase to cyt c_z occurred directly in the crude membrane extract prepared from a cyt *c*-554-deleted mutant of *Cba. tepidum* [13]. However, it still remains uncertain whether soluble cyt *c*-554 can mediate electron transfer reaction *in vivo* between menaquinol:cyt *c* oxidoreductase and cyt c_z as in the case of purple non-sulfur bacteria, where cyt c_2 shuttles electrons between the bc_1-type ubiquinol oxidoreductase and the type II RC complex [14]. To address this issue, in the present study, the author carried out the *in vitro* reconstitution experiments using membranes prepared from the cyt *c*-554-deleted mutant by exogenously adding cytochrome *c*-555 purified from *Cba. parvum*. The results indicated that cyt c_z accepted electrons from both menaquinol:cyt *c* oxidoreductase and cyt *c*-554/555 independently. Cyt *c*-554/555 never serves as a shuttle-like mediator between menaquinol:cyt *c* oxidoreductase and cyt c_z but seems to be connected to thiosulfate oxidation pathway.

Materials and methods

Isolation of photosynthetic membranes from the mutant cells lacking cyt c-554

A deletion mutant of cyt *c*-554 of *Cba. tepidum* (Δ*cycA*) was constructed in the previous study [13], and the photosynthetic membranes of the mutant were prepared according to the procedure described previously [4] in an anaerobic chamber (Coy Laboratory Products, Ann Arbor, MI, USA).

Purification of cyt c-554/555

Soluble cyt *c*-554/555 was purified from the wild-type strain of *Cba. tepidum* and *Cba. parvum* basically according to the previous reports [4,9] with a few modifications described below. Harvested cells were disrupted by three-time passages through a French pressure cell at 20,000 psi (138 MPa). Cell debris was removed by centrifugation at 10,000 *g* for 15 min, and the supernatant was again centrifuged at 110,000 *g* for 1h. The resultant supernatant was fractionated by ammonium sulfate (40-80% saturation). The precipitated fraction by 80% ammonium sulfate was suspended in a 20 mM Tris-HCl buffer (pH 8.0), dialyzed against the same buffer, and applied on an anion-exchange column (DEAE-Toyopearl 650M) equilibrated with the same buffer. The flow-through fraction was then subjected to CM-cellulose column chromatography. After washing the column with a 20 mM Tris-HCl buffer (pH 8.0), the cyt *c* molecules were eluted with a linear gradient of 0-500 mM NaCl in the same buffer. Elution enriched with cytochromes was concentrated by ultrafiltration (Viva-spin, VIVA Science, 5000 MW cut-off) and applied on a gel-permeation column (Sephacryl S-100 HR 26/60, Amersham Pharmacia) equilibrated with a 50 mM Tris-HCl buffer (pH 8.0) containing 100 mM NaCl. The cyt *c*-554/555 fraction was concentrated by ultrafiltration (YM-3, Amicon), and its resultant concentration was estimated by assuming an absorption coefficient at the α-peak to be 23.8 $mM^{-1}cm^{-1}$ [9]. SDS-PAGE analysis of the purified protein followed by heme staining

showed no band except that of the 10-kDa cyt *c*-554/555.

Flash-induced absorption changes

Flash-induced absorption changes were measured with a split beam spectrophotometer at 295 K as described previously [15]. Membrane preparations were suspended in 50 mM Tris-HCl (pH 8.0) supplemented with 1 mM EDTA, 2 mM dithiothreitol, and 10 mM sodium ascorbate. The concentration of the membranes was adjusted to give an absorbance of 1.5 at 810 nm (equivalent to a 0.3 μM P840 concentration) by assuming the antenna size in the RC complex (BChl *a*/P840 ratio) to be 50 [16,17] and the extinction coefficient (ε_{810}) for BChl *a* at 810 nm to be 100 $mM^{-1}cm^{-1}$ [18]. For the reconstitution experiments, the purified cyt *c*-554/555 was added to the membrane suspension to give a final concentration of 1 μM or 10 μM.

Results

Flash-induced absorption changes of cytochromes in membranes

The absorption changes of multiple heme components were measured in the cyt *c*-554/555-reconstituted system using membranes from the Δ*cycA* mutant of *Cba. tepidum*. Soluble cyt *c*-555 purified from the closely related species *Cba. parvum*, which showed its α-absorption peak at 555 nm, was used for the reconstitution instead of cyt *c*-554 of *Cba. tepidum*, which has its peak at 554 nm. This is because the former is suitable for the present reconstitution experiments in order to distinguish its spectral changes from the overlapping absorption changes of cyt c_z with the α-absorption peak at 552-553 nm [4,7]. Control experiments using the latter gave similar results, although it was rather difficult to distinguish the kinetics of each *c*-type cytochrome accurately (not shown).

In order to quantitatively analyze the reactions of cyt c_z, added cyt *c*-555, and cyts *c*-556 and *b* in the menaquinol:cyt *c* oxidoreductase, which gave specific peaks at 552, 555, 556, and 563 nm, respectively, in their α-absorption regions, the author measured the flash-induced absorption changes at 552 nm (for all the *c*-type cytochromes in Figure I-1), 547 nm (for cyt c_z in Figure I-2A), 558 nm (for cyts *c*-555 and *c*-556 in Figure I-2B), and 563 nm (for cyt *b* in Figure I-3) as the difference with respect to those at 540 nm (also see Figure I-4). The reaction ascribable to the externally added cyt *c*-555 was assumed mainly from the dependency on its concentration.

Flash-induced absorption changes of c-type cytochromes

Figure I-1 shows the flash-induced absorption changes (mainly of cyt c_z) in membranes monitored at 552 -(minus) 540 nm over 80 ms. The present measurement with a time resolution of 1 ms did not reveal the precise time course of the immediate oxidation of cyt c_z by $P840^+$ and its rereduction by cyt *c*-556 in menaquinol:cyt *c* oxidoreductase ($t_{1/e}$ = 150

μs), as demonstrated previously [4]. However, the kinetics could still exhibit rapid oxidations of *c*-type hemes and their subsequent rereductions, as mentioned below.

The decay kinetics of trace a in Figure I-1A represents the case without added cyt *c*-555. Its kinetics was fitted by two exponential decay components with half times ($t_{1/2}$) of 1.5 and 15 ms with the estimated contributions of 60 and 40%, respectively. The 1.5 ms component, which was fully removed in the presence of stigmatellin, as shown in trace b, could be assigned to represent the electron donation from the Rieske Fe-S center in the menaquinol:cyt *c* oxidoreductase because stigmatellin was known to inhibit the rereduction of cyt *c* by the Rieske Fe-S center. The result was consistent with the previous study, which estimated the equilibration time of electrons between the Rieske Fe-S center and heme *c*-556 in the menaquinol:cyt *c* oxidoreductase to be around 560 μs [4]. The slow 15-ms component would represent the electron transfer rate to Rieske Fe-S center by menaquinol oxidation in the Q_o site, which was suggested to proceed with a $t_{1/2}$ of approx. 20 ms (see below and [4]). In fact, the contribution of this component to the total amplitude of absorption changes decreased in the presence of stigmatellin (Figure I-1A, trace b.)

The decay kinetics in the presence of stigmatellin was fitted by two exponential components with $t_{1/2}$ of 15 and 200 ms with relative contributions of 16 and 84%, respectively (Figure I-1A, trace b). The lack of the 1.5 ms phase as well as the significant suppression of the 15 ms phase indicated almost complete inhibition of the electron donation from the menaquinol:cyt *c* oxidoreductase, as mentioned above. The 200 ms component seemed to be ascribable to the rereductions of hemes *c* by ascorbate added in the reaction medium and/or by the back-reaction from photo-reduced terminal Fe-S centers (F_A/F_B) in the RC complex [19].

When the membranes were reconstituted with cyt *c*-555 (Figure I-1B), the amplitudes of the absorption changes immediately after the flash excitation were slightly larger, and no fast recovery phases were observed both in the absence and presence of stigmatellin (Figure I-1B, traces a and b). These kinetic profiles could be interpreted as that the added cyt *c*-555

rereduced the photo-oxidized cyt c_z^+ concomitantly with cyt *c*-555 oxidation and its subsequent slow rereduction ($t_{1/2}$ > 100 ms) probably by ascorbate.

Effects of cyt c-555 addition on the flash-induced absorption changes of cyts c

Flash-induced absorption changes of cyt c_z and cyt *c*-555 were measured at 547 - 540 nm and at 558 - 540 nm, respectively, in the presence of different concentrations of cyt *c*-555 (Figure I-2). At 547 - 540 nm, the absorption bleach and subsequent recovery were observed in the absence of cyt *c*-555 after the flash excitation, indicating the rapid oxidation and rereduction of cyt c_z (Figure I-2A, trace a). The addition of cyt *c*-555 somewhat slowed down the rereduction process, especially at 10 μM of cyt *c*-555 (Figure I-2A, traces b and c) (see below for its interpretation).

The absorption changes monitored at 558 - 540 nm, where cyt c_z had a small contribution, were different from those at 547 - 540 nm (Figure I-2B). Without cyt *c*-555, a small transient negative change, probably due to the photo-oxidized $P840^+$ and its subsequent rereduction by cyt c_z, was detected immediately after the flash excitation, followed by a subtle absorption increase (Figure I-2B, trace a). This absorption increase seemed to be due to the overlap of the reduced cyt *b* in the menaquinol:cyt *c* oxidoreductase along with the recovery of P840. In the presence of 10 μM cyt *c*-555 (Figure I-2B, trace c), a slow absorption decrease with $t_{1/2}$ = 3 ms was detected after the flash excitation, whose half-time appeared to be almost the same as the one for the decay kinetics of the oxidized cyt c_z^+ (see Figure I-2A, trace c) and represented the increase of the oxidized cyt $c\text{-}555^+$. However, the absorption decrease at 558 - 540 nm never completely recovered within 100 ms, suggesting that the oxidized state of cyt $c\text{-}555^+$ remained for a relatively long time without its prompt rereduction process. In the presence of 1 μM of cyt *c*-555, an intermediate kinetic profile was observed, as shown in trace b of Figure I-2B. All of the above results thus imply that electrons can be donated to the RC from both cyt *c*-555 and menaquinol:cyt *c* oxidoreductase.

Effects of cyt c-555 addition on the flash-induced absorption changes of cyt b

Flash-induced absorption changes of cyt *b* were monitored at 563 - 540 nm (Figure I-3). In the absence of cyt *c*-555 (Figure I-3A, trace a), the flash excitation induced an absorption increase with $t_{1/2}$ = approx. 1 ms, followed by the recovery with $t_{1/2}$ = 9 ms, suggesting the transient reduction of cyt *b* due to a turnover of menaquinol:cyt *c* oxidoreductase. In the presence of antimycin A, which is an inhibitor for the Q_i site of cyt bc_1-type complex, cyt *b* was fully reduced due to the inhibition of the reoxidation of reduced cyt *b*. The kinetics was fitted with two exponential components with $t_{1/2}$ = 2 and 26 ms in relative contributions of 25 and 75%, respectively (Figure I-3A, trace b). The phenomenon of the oxidant-induced reduction of cyt *b* presented here confirmed that the oxidized cyt c_z^+ could be rereduced by the menaquinol:cyt *c* oxidoreductase without cyt *c*-555, as previously demonstrated [4]. The amplitude of cyt *b* reduction in the presence of antimycin A was almost comparable with that of the flash-oxidized cyt c_z^+ (data not shown). This indicates the tight coupling between the menaquinol:cyt *c* oxidoreductase and the RC complex.

In the presence of cyt *c*-555 (Figure I-3B, trace a), a transient but smaller absorption increase was still observed at 563 - 540 nm. The addition of antimycin A (Figure I-3B, trace b) increased the extent of cyt *b* reduction to be a level about a half that in the absence of cyt *c*-555 (Figure I-3A, trace b). In other words, about a half of the flash-oxidized cyt c_z^+ could be rereduced directly by the menaquinol:cyt *c* oxidoreductase, and the rest could be rereduced by externally added cyt *c*-555, as described in detail below.

All the results shown in Figures I-1 to I-3 therefore suggest that both cyt *c*-555 and menaquinol:cyt *c* oxidoreductase can efficiently donate electrons to cyt c_z.

Time-resolved difference absorption spectra

Figure I-4 exhibits the flash-induced time-resolved difference absorption spectra in

membranes with and without exogenous cyt *c*-555. In membranes alone, a spectrum obtained at 1 ms after the flash excitation showed a negative peak at 552 nm, indicating the rapid oxidation of cyt c_z (Figure I-4A). The peak became smaller and was shifted to 554 nm at 10 ms, probably due to some contribution of the oxidized cyt *c*-556^+ in the menaquinol:cyt *c* oxidoreductase.

The 1 ms spectrum in the presence of cyt *c*-555 showed a broad peak at 552 - 556 nm, clearly indicating the oxidation of cyt *c*-555 by cyt c_z^+ (Figure I-4B). The peak position shifted gradually to the longer wavelength side with time and, finally, to 555 nm at 10 ms, suggesting a more contribution of the oxidized cyt *c*-555^+. The large extent of cyt *c*-555^+, which remained at 10 ms, implied the slow rereduction rate of cyt *c*-555^+. It could be assumed that cyt *c*-555 rapidly rereduced c_z^+ and that the resultant cyt *c*-555^+ was rereduced by ascorbate added in the reaction medium under the present experimental conditions. It was also noted that the extent of cyt *b* reduction was decreased to about half (Figure I-4B). This suggests that the rereduction of cyt c_z^+ by cyt *c*-555 decreased the extent of cyt *b* reduction, although the oxidation/reduction of cyt *c*-556 in menaquinol:cyt *c* oxidoreductase could not be recognized in these spectral changes.

The addition of antimycin A in the presence of cyt *c*-555 did not significantly change the kinetics of *c*-type cytochromes (compare Figure I-4C to 4B). The amplitude of the reduced cyt *b* in Figure I-4C was almost the same as that in Fig. 4B and smaller than that in Fig. 4A, indicating that antimycin A did not affect the extent of reduced cyt *b* in the presence of cyt *c*-555. It was essentially consistent with the kinetic data obtained in Figure I-3. Therefore, it is natural to consider that cyt *c*-555 decreased the extent of photo-reduced cyt *b*, implying that two electron donors, cyt *c*-555 and menaquinol:cyt *c* oxidoreductase, function in parallel to rereduce cyt c_z^+ and that cyt *c*-555^+ cannot be rereduced by the menaquinol:cyt *c* oxidoreductase.

In the presence of stigmatellin, which inhibits the Q_o site of menaquinol:cyt *c*

oxidoreductase, the flash excitation induced a difference spectrum with a larger negative peak at around 553 nm at 1 ms (Figure I-4D). Then, the peak at 10 ms shifted to 555 nm along with only a small decrease in the amplitude of the spectrum. On the other hand, the absorption increase at 563 nm was significantly smaller compared to those in Figure I-4A to 4C. These effects were ascribable to the suppression of the electron donation from the Q_o site in the menaquinol:cyt *c* oxidoreductase, resulting in the suppression of the oxidant-induced reduction of cyt *b* as well as the rereduction of cyt c_z^+ and cyt *c*-556^+ [4]. The large negative absorption band with an apparent peak at 555 nm at 3-10 ms suggests oxidations of multiple *c*-type cytochromes, as explained by a simulation in the Discussion.

Discussion

Electron transfers from menaquinol:cyt c oxidoreductase and cyt c-554/555 to cyt c_z

Water-soluble cyt *c*-554/555 has been shown to function as the direct electron donor to cyt c_z of the RC complex [9]. It has also been demonstrated that cyt *c-556* in the menaquinol:cyt *c* oxidoreductase donates electrons to cyt c_z in the membrane preparation isolated from the wild-type cells of *Cba. tepidum* [4]. However, the issue concerning whether cyt *c*-554/555 functions as a shuttle-type electron carrier between the menaquinol:cyt *c* oxidoreductase and cyt c_z remains to be resolved.

In purple non-sulfur photosynthetic bacteria, a membrane-anchored cyt c_y donates electrons to the type II RC [20]. *Rhodobacter capsulatus* possesses cyt c_y and soluble periplasmic cyt c_2, both of which function as parallel electron carriers from cyt bc_1 complex to the RC in photosynthetically grown cells [8,21]. Although two cytochromes might have different physiological roles, both mutants defective in cyt c_y and cyt c_2, respectrively, can still grow phototrophically [8].

Cyt c_z in green sulfur bacteria, on the other hand, is also a membrane-bound monoheme *c*-type cytochrome with three putative membrane-spanning helices [5,7]. This structure and its function as an electron donor to P840 in the green sulfur bacterial RC complex somehow resemble those of cyt c_y [4]. It could therefore be expected that cyt *c*-554/555 mediated the electron transfer reaction between menaquinol:cyt *c* oxidoreductase and the RC complex as was the case with cyt c_2 [20]. However, the results in this study clearly demonstrated that the oxidized cyt *c*-555 was not rereduced under the present experimental condition in which the menaquinol:cyt *c* oxidoreductase was fully operating as the electron donor to cyt c_z (Figure I-2B). The reduction of cyt *b* in the menaquinol:cyt *c* oxidoreductase was indeed shown to be depressed to almost half by the addition of 10 μM cyt *c*-555 (see Figure I-3B), strongly indicating that electron transfer reaction between cyt *c*-556

and cyt c_z was hindered by externally added cyt *c*-555.

A heme-containing moiety of cyt c_z, which is exposed to a periplasmic space, has been assumed to be fluctuated to search for its reaction partners, the RC core protein and cyt *c*-556, both of which reside in membranes [4,7]. It is thus conceivable that the C-terminal domain of cyt c_z could take different orientations during a series of reaction processes; it would associate with cyt *c*-554/555 in a manner to obey the second order reaction mode (see Figure I-5, inset). The probable complex formation between cyt c_z and cyt *c*-554/555 would then block the electron transfer from cyt *c*-556 to cyt c_z, resulting in the partial suppression of cyt *b* reduction. This implies that two paths of electron flow from cyt *c*-554/555 and the menaquinol:cyt *c* oxidoreductase could be balanced dependent upon their respective redox states as mentioned below. It seems unlikely that the direct contact of cyt *c*-554/555 with cyt *c*-556 inhibited the reduction of cyt *b*, because the *in vitro* kinetic analysis demonstrated that cyt *c*-554 donated electrons to cyt c_z to rereduce the oxidized $P840^+$ [9].

The author made an electron transfer scheme (Figure I-5) including cyt c_z, cyt *c*-554/555, and menaquinol:cyt *c* oxidoreductase based on the results in the present study. The E_m values of P840 and cyt c_z are known to be 230 - 240 and 170 - 180 mV, respectively [22-24]. Although E_m of cyt *c*-556 in the menaquinol:cyt *c* oxidoreductase has not been measured, it has been estimated to be close to the value of 160 mV of a Rieske FeS center [4,25]. The E_m value of cyt *c*-554/555 has been reported to be 130 or 148 mV by two research groups [9,11], which is lower than the estimated E_m value of cyt *c*-556 in the menaquinol:cyt *c* oxidoreductase. At 10 ms after the flash excitation in the presence of stigmatellin (see Figure I-4E), the redox equilibration between cyt c_z and the other three redox centers, P840, *c*-556, and *c*-554/555, would be attained as follows.

(1) (cyt c_z /cyt c_z)$^+$ + P840 ⇔ (cyt c_z /cyt c_z) + $P840^+$

(2) cyt c_z^+ + cyt *c*-556 ⇔ cyt c_z + cyt *c*-556^+

(3) cyt c_z^+ + *c*-554/555 ⇔ cyt c_z + *c*-$554/555^+$

Based on the E_m values listed above, the redox state of each heme *c* was calculated by a Nernst equation (ΔE_m = RT/F ln *K*) and the relative amounts of oxidized cyts c_z^+, *c*-556$^+$, and *c*-554/555$^+$ were estimated to be 0.2 : 0.25 : 0.55, respectively, at the equilibrium. The difference absorption spectrum measured at 10 ms in the presence of stigmatellin was simulated by summing up the estimated spectrum of each component shown in Figure I-4E. In this calculation, P840 was assumed to be the almost fully reduced state at 10 ms because this approximation had little effect within experimental errors and made the result much simpler. The spectrum thus obtained reproduced well the difference absorption spectrum obtained in the present measurement (see a gray curve in Figure I-4D). This result suggests that the three *c-type* cyts indeed functions to reduce P840$^+$ and are almost equilibrated to each other as expected from their redox potentials. However, more accurate kinetic data will be required for determination of the precise contribution of each *c*-type heme to the difference absorption spectrum in the future.

The second-order rate constant of the electron transfer from cyt *c*-554 to cyt c_z was calculated to be 1.7 x 10^7 M^{-1} s^{-1} *in vitro* using the isolated RC complex reconstituted with cyt *c*-554 [9]. In the present study, the electron transfer rate from cyt *c*-555 to cyt c_z in membranes gave $t_{1/2}$ = 3 ms at 10 μM of cyt *c*-555 (Figure I-2B, trace c). The observed rate would be rational because the excess amount of cyt *c*-555 was added with respect to P840 concentration (roughly estimated to be about 0.3 μM). Cyt c_z^+ was rereduced by both cyt *c*-555 and menaquinol:cyt *c* oxidoreductase at an almost 1:1 ratio under the present condition. A simple interpretation for the independent electron donation would be that the C-terminal domain of cyt c_z has different orientations to make contact with both electron donors as discussed above.

Although there is no available data concerning the *in vivo* concentration of cyt *c*-554/555 in green sulfur bacteria, the amounts of cyt c_2 in *Rps. viridis* and *Rba. sphaeroides* cells have been estimated to be in the millimolar range [26,27]. If one considers that the

concentration of cyt *c*-554/555 *in vivo* is similar, the maximum rate constant of electron transfer from cyt *c*-554/555 to cyt c_z would be several to tens μs, which would be significantly faster than that of the electron transfer rate from menaquinol:cyt *c* oxidoreductase to cyt c_z ($t_{1/e}$ = 150 μs). This implies that cyt *c*-554/555 can be quite an efficient electron donor to cyt c_z and can compete against menaquinol:cyt *c* oxidoreductase when the reduced form of cyt *c*-554/555 is abundant in amount. This will be discussed below in terms of sulfur oxidations.

Reaction of bc-type menaquinol:cyt c oxidoreductase in Cba. tepidum

The chemically reduced-minus-oxidized difference spectra of chlorosome-depleted membrane preparations of *Cba. tepidum* suggested the presence of cyt *c*-556 [4]. However, the assignment of cyt *c*-556 has not been very clear up to now because of the possibility of the contamination of membranes by a residual amount of cyt *c*-554. Although a complete elimination of cyt *c*-554 in the membrane preparation was confirmed by SDS-PAGE and heme staining analyses [4], the detection of a low-molecular-weight (approx. 10,000) heme-*c* protein is very difficult in general. It is clear, on the other hand, that the membranes isolated from the Δ*cycA* mutant of *Cba. tepidum* do not contain any cyt *c*-554. The results in the present study, thus, clearly demonstrate a direct tight coupling between the menaquinol:cyt *c* oxidoreductase and cyt c_z of the RC complex without any involvement of soluble electron carriers. Furthermore, the presence of cyt *c*-556 was an indispensable component for a good simulation of the spectrum as shown in Figure I-4D. The time-dependent shift of the peak wavelength in the 552-556 nm region in Figure I-4A also indicated the reduction of cyt c_z^+ by another cytochrome, probably cyt *c*-556, with a peak at a longer wavelength. All of these results strongly suggest that cyt *c*-556 serves as the immediate electron donor to cyt c_z^+ like cyt c_1 in the bc_1-type oxidoreductase.

In the *Chlorobi*, genes encoding subunits of menaquinol:cyt *c* oxidoreductase are arranged in the genome in a way different from those in other phylum of bacteria, such as

Proteobacteria, Firmicutes, and Cyanobacteria [28]. In most Proteobacteria, the cyt bc_1 complex minimally consists of three subunits, the Rieske iron-sulfur protein, cyt *b*, and cyt c_1, which are encoded by the *fbcF*, *fbcB*, and *fbcC* genes, respectively [29]. These genes comprise one transcriptional unit called the *fbc* operon. On the other hand, genes for cyanobacterial cyt b_6f complex are split into two units. One unit has *fbcC* followed by the *fbcF* gene, and another has the genes coding for cyt b_6 and subunit IV. In green sulfur bacteria, the *fbcF* and *fbcB* genes form a transcriptional unit, but no *c*-type cyt gene has been found at the downstream or upstream of this unit. However, genomic analyses have enabled us to find five candidates of genes encoding membrane-bound *c*-type cyts with small molecular masses of 15-20 kDa from the genome of *Cba. tepidum*, which might be cyt *c*-556 as judged from its molecular mass [4]. The author assumes gene *CT0073* to be the best candidate because it is located upstream of the gene encoding cyt *c*-554/555 (*CT0075*). It is, however, rather questionable whether the gene annotated as *CT0074* (encoding only 46 amino acids) is a genuine gene or not. In fact, the homologues of *CT0073* but not of *CT0074* could be found in almost all other genome-sequenced green sulfur bacteria and are arranged in the same way; the homologues of *CT0073* and *CT0075* are adjacent to each other (see Figure II-4 in chapter II). The product of the *CT0073* homologues thus seems to be cyt *c-556*, which is functionally related to cyt *c*-554/555. It is noteworthy that the thiol group of the 18th cyteine residue in the CT0073 could be modified with fatty acid chains after the cleavage of its signal peptide, as predicted by the ScanProsite analysis of prokaryotic membrane lipoproteins (PROSITE profile: PS51257) on the ExPASy web server [30]. Cyt *c*-556 might thus be anchored into membranes and may serve as an electron carrier, substituting for cyt c_1 in the ordinary cyt bc_1 complex.

Photosynthetic electron transfer chains and sulfur metabolism

Cyt *c*-554/555 is likely to serve as the electron acceptor from sulfur metabolism

operated by Sox (sulfur oxidation) proteins [12,31]. The Sox system is known to be essential for both thiosulfate and sulfide oxidations in a purple bacterium, *Rhodovulum sulfidophilum* [32], and probably in a chemolithotroph, *Paracoccus pantotrophus* [33]. A soluble small cytochrome has been considered to function as an electron acceptor from SoxA, which is involved in thiosulfate oxidation [33,34] (Figure I-5). On the other hand, *Cba. thiosulfatiphilum* is known to show an activity of a membrane-associated sulfide:quinone reductase (SQR) [35]. SQR oxidizes sulfide and reduces a quinone pool in the membrane, and the electrons are donated to P840 in the RC complex via menaquinol:cyt *c* oxidoreductase. The genome sequence analysis of *Cba. tepidum* has revealed the three paralogues of the gene encoding SQR (*CT0117*, *CT0876*, and *CT1087*) [36], while a recent study has demonstrates that two of them, CT0117 and CT1087, are required for sulfide-dependent growth of *Cba. tepidum* [37].

Sulfur oxidations are therefore expected to be linked closely *in vivo* to the two electron transfer paths of the menaquinol:cyt *c* oxidoreductase and cyt *c*-554/555. As mentioned in chapter II, electrons from thiosulfate oxidation are transferred to the RC complex mainly via cyt *c*-554/555 and the path of cyt *c*-554/555 would be dominant when thiosulfate is rich in media. Contrary to this, the activity of menaquinol:cyt *c* oxidoreductase would be increased when the redox state of quinone pool is shifted to the reduced side under the sulfide-rich condition. The balance of electron flows between menaquinol:cyt *c* oxidoreductase and cyt *c*-554/555 would thus be coordinately regulated dependent upon chemical species of sulfur compounds in a natural habitat.

Figures

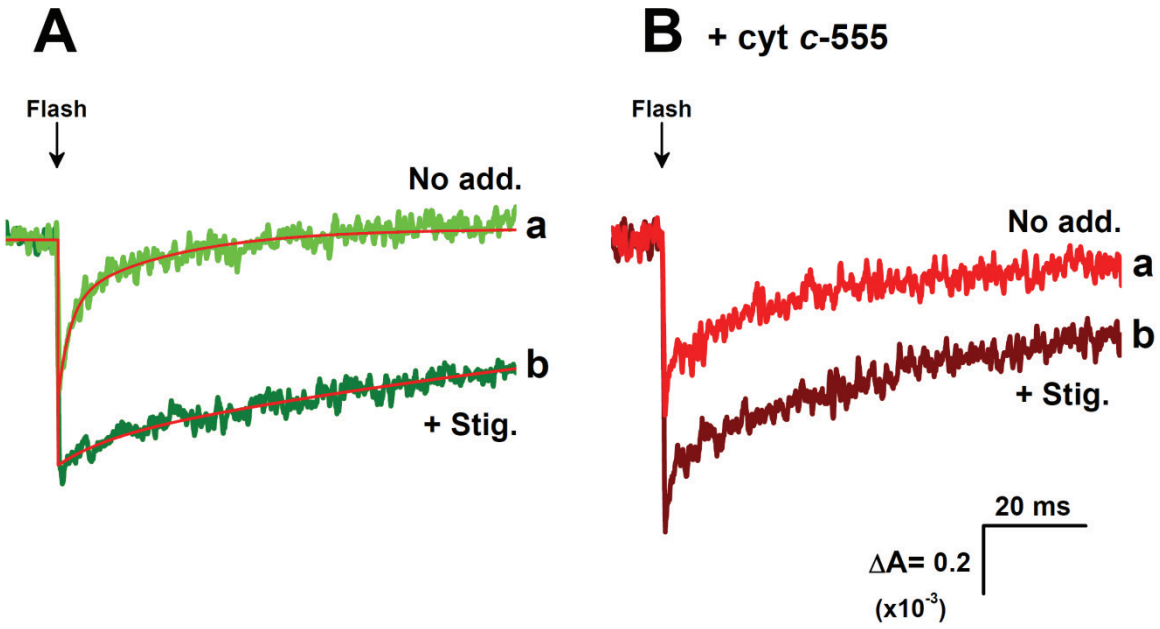

Figure I-1. Flash-induced absorption changes monitored at 552 - 540 nm (*c*-type cyts) in membranes isolated from Δ*cycA* mutant cells of *Cba. tepidum* (A) without or (B) with externally added cyt *c*-555 purified from *Cba. parvum*. Traces a and b represent kinetics in the absence and presence of 20 μM stigmatellin, respectively. Measurements were done at 295 K. The concentrations of membranes and cyt *c*-555 were adjusted to be A_{810} = 1.5 (approx. 0.3 μM P840) and 10 μM, respectively. Thin lines indicate the results of kinetic analyses by curve-fitting programs.

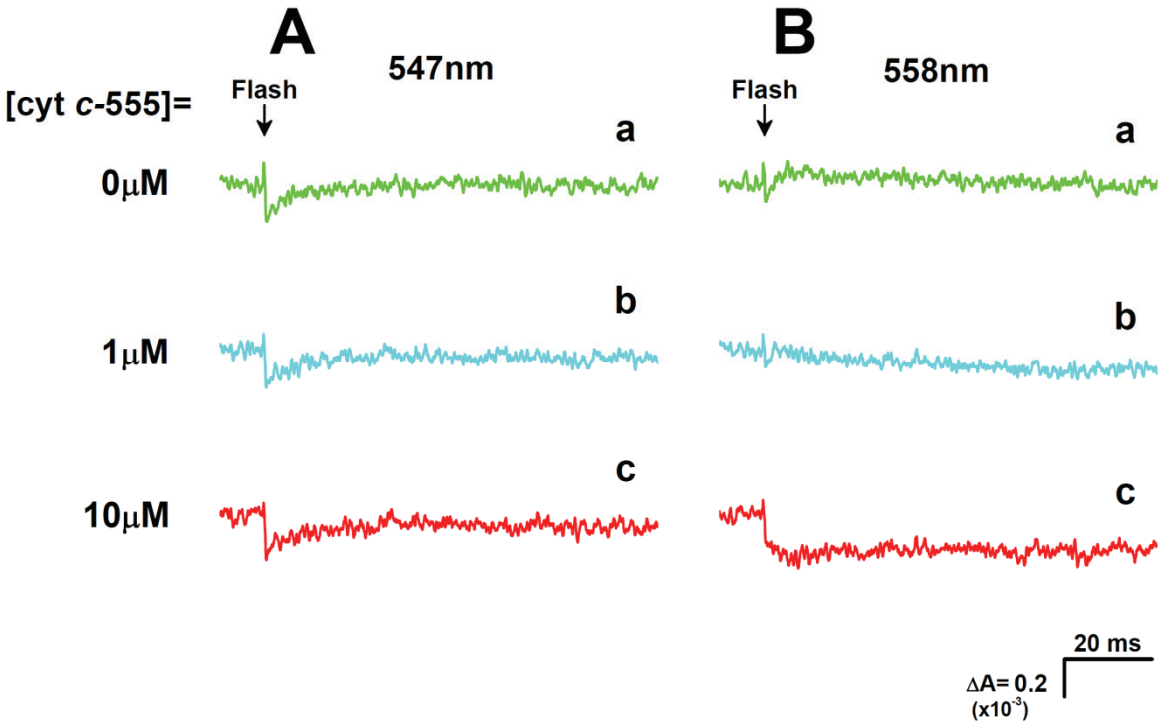

Figure I-2. Flash-induced absorption changes monitored at (A) 547 - 540 nm (cyt c_z) and (B) 558 - 540 nm (mainly cyt *c*-555) in membranes. Traces a, b, and c represent no addition and additions of 1 μM and 10 μM cyt *c*-555, respectively. Measurements were done at 295 K. The concentration of membranes was adjusted to be A_{810} = 1.5 (approx. 0.3 μM P840).

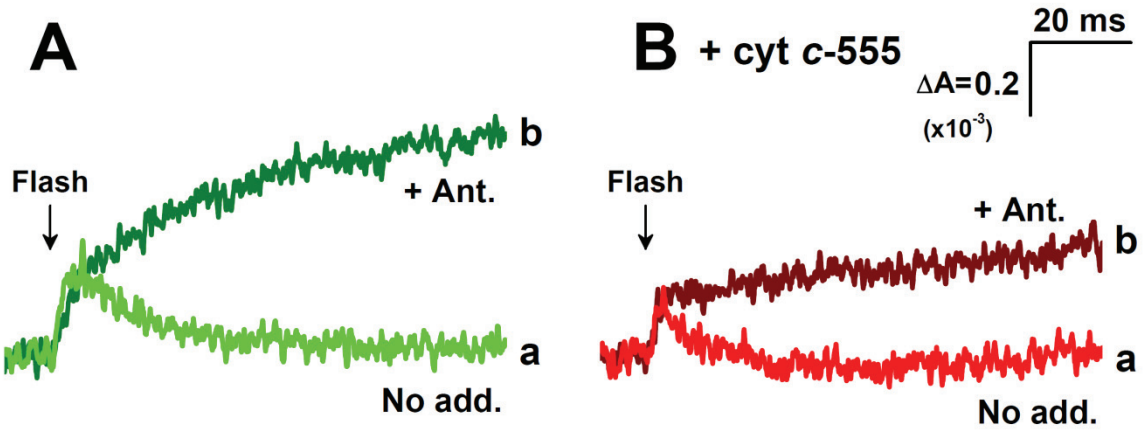

Figure I-3. Flash-induced absorption changes monitored at 563 - 540 nm (cyt *b*) in membranes (A) without or (B) with externally added cyt *c*-555. Traces a and b represent kinetics in the absence and presence of 20 μM antimycin A, respectively. Measurements were done at 295 K. The concentrations of membranes and cyt *c*-555 were adjusted to be A_{810} = 1.5 (approx. 0.3 μM P840) and 10 μM, respectively.

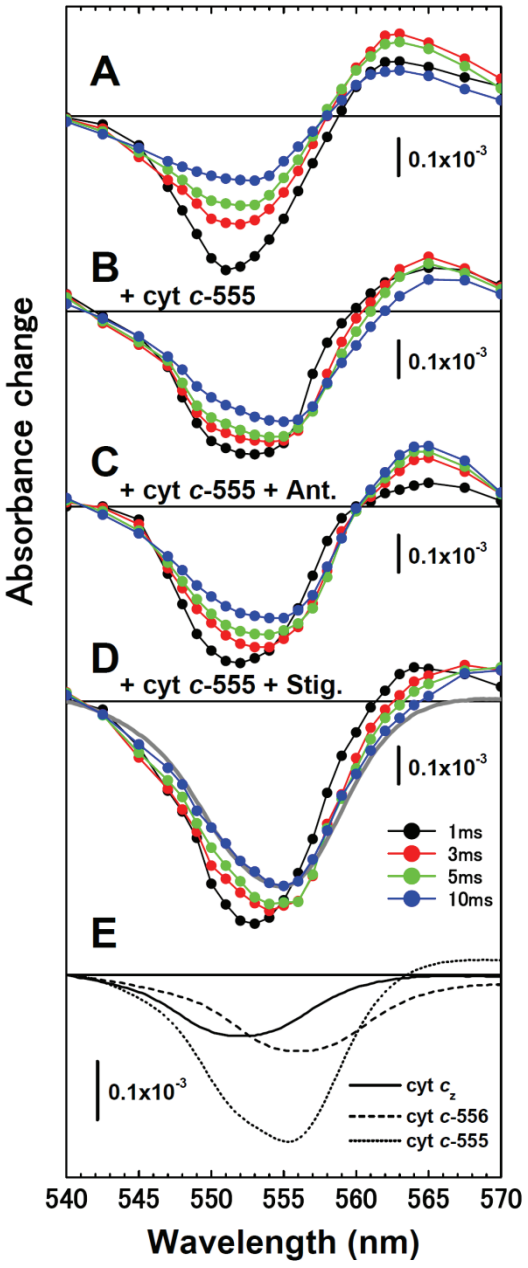

Figure I-4. Time-resolved difference absorption spectra of *c*- and *b*-type cytochromes in membranes (A) without and (B)-(D) with cyt *c*-555 after flash excitation. The oxidized-minus-reduced difference spectra of cyt c_z, cyt *c*-556, and cyt *c*-555 are also shown in (E). C and D, in the presence of 20 μM antimycin A and 20 μM stigmatellin, respectively. Times after the flash excitation are indicated in the figure. Measurements were done at 295 K. The concentrations of membranes and cyt *c*-555 were adjusted to be A_{810} = 1.5 (approx. 0.3 μM P840) and 10 μM, respectively. A difference absorption spectrum of cyt c_z was obtained from [4]. That of cyt *c*-555 was obtained in the present study. An expected spectrum of cyt *c*-556 was simply obtained by shifting the spectrum of cyt c_z to the red side by 4 nm. A spectrum after the redox equilibration was simulated by estimating the contributions of cyt c_z, cyt *c*-556, and cyt *c*-555 to be 0.2 : 0.25 : 0.55 as described in text and depicted as a gray curve in (D).

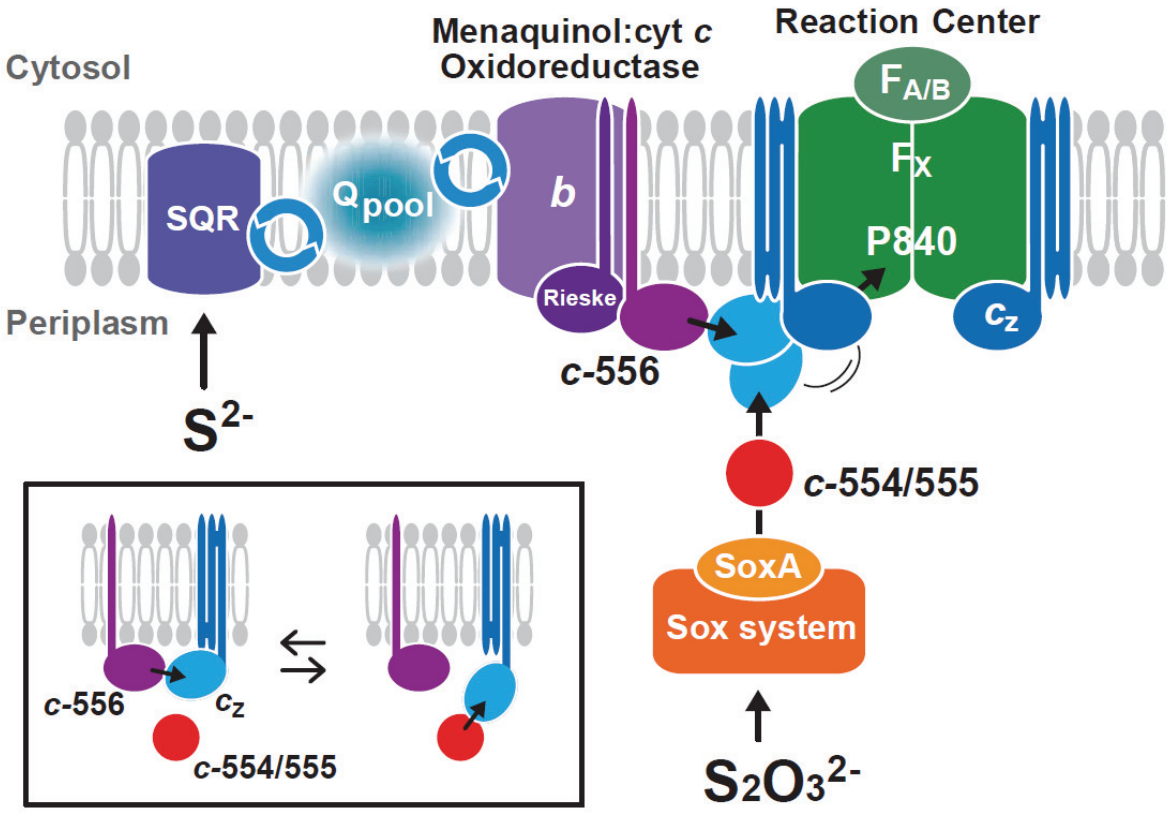

Figure I-5. Schematic illustration of electron transfer pathways around the oxidizing side of the *Cba. tepidum* RC. Electron flows are represented by arrows. A heme-binding portion of membrane-bound cyt c_z is assumed to be exposed into the solvent and fluctuates during reaction to contact with its reaction partners, cyt *c*-556 and cyt *c*-554/555. Sulfide and thiosulfate serve as the electron sources for photosynthesis in *Cba. tepidum*. *SQR*, sulfide-quinone reductase; *Q*, quinone. (*inset*) A model to represent two different orientations of the C-teminal domain of cyt c_z, which associates with cyt *c*-556 and cyt *c*-554/555.

References

1. Hauska, G., Schoedl, T., Remigy, H., and Tsiotis, G. (2001) The reaction center of green sulfur bacteria(1), *Biochim Biophys Acta* **1507**, 260-277
2. Oh-oka, H. (2007) Type 1 reaction center of photosynthetic heliobacteria, *Photochem Photobiol* **83**, 177-186
3. Trüper, H. G., Lorenz, M., Schedel, M., and Steinmentz, M. (1988) Metabolism of thiosulfate in *Chlorobium*. in *Green Photosynthetic Bacteria* (Olson, J. G., Ormerod, J., Amesz, E., Stackebrant, H. G., and Trüper, H. G. eds.), Plenum Press, New York. pp 189-200
4. Oh-oka, H., Iwaki, M., and Itoh, S. (1998) Membrane-bound cytochrome cz couples quinol oxidoreductase to the P840 reaction center complex in isolated membranes of the green sulfur bacterium Chlorobium tepidum, *Biochemistry* **37**, 12293-12300
5. Okkels, J. S., Kjaer, B., Hansson, O., Svendsen, I., Moller, B. L., and Scheller, H. V. (1992) A membrane-bound monoheme cytochrome c551 of a novel type is the immediate electron donor to P840 of the Chlorobium vibrioforme photosynthetic reaction center complex, *J Biol Chem* **267**, 21139-21145
6. Oh-oka, H., Kamei, S., Matsubara, H., Iwaki, M., and Itoh, S. (1995) Two molecules of cytochrome c function as the electron donors to P840 in the reaction center complex isolated from a green sulfur bacterium, Chlorobium tepidum, *FEBS Lett* **365**, 30-34
7. Oh-oka, H., Iwaki, M., and Itoh, S. (1997) Viscosity dependence of the electron transfer rate from bound cytochrome c to P840 in the photosynthetic reaction center of the green sulfur bacterium Chlorobium tepidum, *Biochemistry* **36**, 9267-9272
8. Jenney, F. E., Jr., and Daldal, F. (1993) A novel membrane-associated c-type cytochrome, cyt cy, can mediate the photosynthetic growth of Rhodobacter capsulatus and Rhodobacter sphaeroides, *EMBO J* **12**, 1283-1292
9. Itoh, M., Seo, D., Sakurai, H., and Setif, P. (2002) Kinetics of electron transfer between soluble cytochrome c-554 and purified reaction center complex from the green sulfur bacterium Chlorobium tepidum, *Photosynth Res* **71**, 125-135
10. Remigy, H. W., Aivaliotis, M., Ioannidis, N., Jeno, P., Mini, T., Engel, A., Jaquinod, M., and Tsiotis, G. (2003) Characterization by Mass Spectroscopy of a 10 kDa c-554 Cytochrome from the Green Sulfur Bacterium Chlorobium tepidum, *Photosynth Res* **78**, 153-160
11. Selvaraj, F., Devine, F., Zhu, W., Brune, D. C., Lince, M. T., and Blankenship, R. E. (1998) Purification and properties of cytochrome c-553 from the green sulfur bacterium *Chlorobium tepidum*. in *Photosynthesis: Mechanism and Effects* (Garab, G. ed.), Kluwer Academic Publishers, Dordrecht, The Nertherlands. pp 1593-1596

12. Oh-oka, H., and Blankenship, R. E. (2004) Green bacteria: secondary electron donor (cytochromes). in *Encyclopedia of biological chemistry.* (Lennarz, W. J., and Lane, M. D. eds.), Academic Press, Oxford. pp 521-524
13. Tsukatani, Y., Miyamoto, R., Itoh, S., and Oh-oka, H. (2006) Soluble cytochrome c-554, CycA, is not essential for photosynthetic electron transfer in Chlorobium tepidum, *FEBS Lett* **580**, 2191-2194
14. Meyer, T. E., and Donohue, T. J. (1995) Cytochromes, iron-sufur, and copper proteins mediating wlwctron transfer from cyt bc_1 complex to photosynthetic reaction center complex. in *Anoxygenic Photosynthetic Bacteria.* (Blankenship, R. E., Madigan, M. T., and Bauer, C. E. eds.), Kluwer Academic Publishers, Dordrecht, The Netherlands. pp 725-745
15. Iwaki, M., Itoh, S., Kamei, S., Matsubara, H., and Oh-oka, H. (1999) Time-resolved spectroscopy of chlorophyll-a like electron acceptor in the reaction center complex of the green sulfur bacterium Chlorobium tepidum, *Plant Cell Physiol* **40**, 1021-1028
16. Takaichi, S., and Oh-oka, H. (1999) Pigment composition in the reaction center complex from the thermophilic green sulfur bacterium, Chlorobium tepidum: Carotenoid glucoside esters, menaquinone and chlorophylls, *Plant Cell Physiol* **40**, 691-694
17. Tsukatani, Y., Miyamoto, R., Itoh, S., and Oh-Oka, H. (2004) Function of a PscD subunit in a homodimeric reaction center complex of the photosynthetic green sulfur bacterium Chlorobium tepidum studied by insertional gene inactivation. Regulation of energy transfer and ferredoxin-mediated NADP+ reduction on the cytoplasmic side, *J Biol Chem* **279**, 51122-51130
18. Olson, J. M., Philipson, K. D., and Sauer, K. (1973) Circular dichroism and absorption spectra of bacteriochlorophyll-protein and reaction center complexes from Chlorobium thiosulfatophilum, *Biochim Biophys Acta* **292**, 206-217
19. Sakurai, H., Kusumoto, N., and Inoue, K. (1996) Function of the reaction center of green sulfur bacteria, *Photochem Photobiol* **64**, 5-13
20. Daldal, F., Deshmukh, M., and Prince, R. C. (2003) Membrane-anchored cytochrome c as an electron carrier in photosynthesis and respiration: past, present and future of an unexpected discovery, *Photosynth Res* **76**, 127-134
21. Hochkoeppler, A., Jenney, F. E., Jr., Lang, S. E., Zannoni, D., and Daldal, F. (1995) Membrane-associated cytochrome cy of Rhodobacter capsulatus is an electron carrier from the cytochrome bc1 complex to the cytochrome c oxidase during respiration, *J Bacteriol* **177**, 608-613
22. Fowler, C. F., Nugent, N. A., and Fuller, R. C. (1971) The isolation and characterization of a photochemically active complex from Chloropseudomonas ethylica, *Proc Natl Acad Sci U S A* **68**, 2278-2282
23. Okamura, N., Shimada, K., and Matsuura, K. (1994) Photo-oxidation of

membrane-bound and soluble cytochrome *c* in the green sulfur bacterium *Chlorobium tepidum*., *Photosynth Res* **41**, 125-134

24. Prince, R. C., and Olson, J. M. (1976) Some thermodynamic and kinetic properties of the primary photochemical reactants in a complex from a green photosynthetic bacterium, *Biochim Biophys Acta* **423**, 357-362
25. Knaff, D. B., and Malkin, R. (1976) Iron-sulfur proteins of the green photosynthetic bacterium Chlorobium, *Biochim Biophys Acta* **430**, 244-252
26. Crofts, A. R., and Wraight, C. A. (1983) The Electrochemical Domain of Photosynthesis, *Biochim Biophys Acta* **726**, 149-185
27. Ortega, J. M., Drepper, F., and Mathis, P. (1999) Electron transfer between cytochrome c(2) and the tetraheme cytochrome c in Rhodopseudomonas viridis, *Photosynth Res* **59**, 147-157
28. Schutz, M., Brugna, M., Lebrun, E., Baymann, F., Huber, R., Stetter, K. O., Hauska, G., Toci, R., Lemesle-Meunier, D., Tron, P., Schmidt, C., and Nitschke, W. (2000) Early evolution of cytochrome bc complexes, *J Mol Biol* **300**, 663-675
29. Gray, K. A., and Daldal, F. (1995) Mutational studies of the cytochrome bc_1 complexes. in *Anoxygenic Photosynthetic Bacteria* (Blankenship, R. E., Madigan, M. T., and Bauer, C. E. eds.), Kluwer Academic Publishers, Dordrecht, The Nertherland. pp
30. de Castro, E., Sigrist, C. J., Gattiker, A., Bulliard, V., Langendijk-Genevaux, P. S., Gasteiger, E., Bairoch, A., and Hulo, N. (2006) ScanProsite: detection of PROSITE signature matches and ProRule-associated functional and structural residues in proteins, *Nucleic Acids Res* **34**, W362-365
31. Meyer, T. E., and Cusanovich, M. A. (2003) Discovery and characterization of electron transfer proteins in the photosynthetic bacteria, *Photosynth Res* **76**, 111-126
32. Appia-Ayme, C., Little, P. J., Matsumoto, Y., Leech, A. P., and Berks, B. C. (2001) Cytochrome complex essential for photosynthetic oxidation of both thiosulfate and sulfide in Rhodovulum sulfidophilum, *J Bacteriol* **183**, 6107-6118
33. Friedrich, C. G., Rother, D., Bardischewsky, F., Quentmeier, A., and Fischer, J. (2001) Oxidation of reduced inorganic sulfur compounds by bacteria: emergence of a common mechanism?, *Appl Environ Microbiol* **67**, 2873-2882
34. Bamford, V. A., Bruno, S., Rasmussen, T., Appia-Ayme, C., Cheesman, M. R., Berks, B. C., and Hemmings, A. M. (2002) Structural basis for the oxidation of thiosulfate by a sulfur cycle enzyme, *EMBO J* **21**, 5599-5610
35. Shahak, Y., Arieli, B., Padan, E., and Hauska, G. (1992) Sulfide quinone reductase (SQR) activity in Chlorobium, *FEBS Lett* **299**, 127-130
36. Eisen, J. A., Nelson, K. E., Paulsen, I. T., Heidelberg, J. F., Wu, M., Dodson, R. J., Deboy, R., Gwinn, M. L., Nelson, W. C., Haft, D. H., Hickey, E. K., Peterson, J. D., Durkin, A. S., Kolonay, J. L., Yang, F., Holt, I., Umayam, L. A., Mason, T., Brenner, M., Shea, T. P., Parksey, D., Nierman, W. C., Feldblyum, T. V., Hansen, C. L., Craven,

M. B., Radune, D., Vamathevan, J., Khouri, H., White, O., Gruber, T. M., Ketchum, K. A., Venter, J. C., Tettelin, H., Bryant, D. A., and Fraser, C. M. (2002) The complete genome sequence of Chlorobium tepidum TLS, a photosynthetic, anaerobic, green-sulfur bacterium, *Proc Natl Acad Sci U S A* **99**, 9509-9514

37. Chan, L. K., Morgan-Kiss, R. M., and Hanson, T. E. (2009) Functional analysis of three sulfide:quinone oxidoreductase homologs in Chlorobaculum tepidum, *J Bacteriol* **191**, 1026-1034

CHAPTER II

Sulfur Oxidation in Mutants of *Chlorobaculum tepidum* Devoid of Cytochrome *c*-554 and SoxB

Summary

In this chapter, the sulfur oxidation pathways of green sulfur bacteria were studied using e *Chlorobaculum tepidum* mutants. A mutant devoid of cytochrome *c*-554 in *Chlorobaculum tepidum* exhibited a decreased growth rate but normal growth yield when compared to the wild type. From quantitative determinations of sulfur compounds in media, the mutant was found to oxidize thiosulfate more slowly than the wild type but completely to sulfate as the wild type. This indicates that cytochrome *c*-554 would increase the rate of thiosulfate oxidation by serving as an efficient electron carrier but is not indispensable for thiosulfate oxidation itself. On the other hand, mutants in which a portion of the *soxB* gene was replaced with the *aacC1* cassette did not grow at all in a medium containing only thiosulfate as an electron source. Both of them exhibited partial growth yields in media containing only sulfide when compared to the wild type. This indicates that SoxB is not only essential for thiosulfate oxidation but also responsible for sulfide oxidation. An alternative electron carrier or electron transfer path would thus be operating between the Sox system and the reaction center complex in the mutant devoid of cytochrome *c*-554. Cytochrome *c*-554 might function in any other pathway(s) as well as the thiosulfate oxidation one, since even green sulfur bacteria that cannot oxidize thiosulfate contain a homologous gene encoding this electron carrier.

Introduction

Green sulfur bacteria are strictly anaerobic phototrophic organisms that utilize reduced sulfur compounds (sulfide, thiosulfate, and/or elemental sulfur) as electron sources for carbon dioxide fixation [1-3]. All these sulfur compounds are oxidized to sulfate, and liberated electrons are finally supplied to the light-driven energy conversion system, where the type 1 reaction center (RC) generates a strong reductant, reduced ferredoxin, to produce NADPH through ferredoxin-$NADP^+$ oxidoreductase [4,5]. Reduced ferredoxin also serves as an electron donor for the reductive carboxylation reactions in the reverse tricarboxylic acid cycle [6].

Two electron-donating paths to cytochrome (cyt) c_z of the RC complex are known to function in the green sulfur bacterium, *Cba. tepidum* [7]; one is through soluble cyt *c*-554, which contains a single *c*-type heme with an apparent molecular mass of about 10 kDa, and another is through membrane-bound menaquinol:cyt *c* oxidoreductase (CT0302-0303) (this soluble cyt *c* is named cyt *c*-555 after its α-absorption peak shift in the case of *Cba. parvum*; cyt *c*-554/555 is used when there is no need to distinguish them by their α-absorption peaks in the context). In chapter I, it was demonstrated by the reconstitution experiments that cyt *c*-554 was not a shuttle carrier between menaquinol:cyt *c* oxidoreductase and cyt c_z, contrary to the case of purple bacterial cyt c_2. Cyt *c*-554 was, therefore, considered to be involved only in the electron transfer from thiosulfate oxidation, as suggested by several *in vitro* biochemical experiments that were carried out in the early 1970s [4,8,9], although there has been no concrete *in vivo* evidence for this.

On the other hand, a subject concerning thiosulfate oxidation system, as well as its related electron transfer path(s), has not been resolved yet in green sulfur bacteria. A Sox multienzyme system, which is known to be involved in thiosulfate oxidation, has been elucidated to consist of at least four components (SoxAX, YZ, CD, and B) in the

chemolithotrophic bacterium *Paracoccus pantotrophus* [10]. This type of multienzyme system seems to be widely distributed in thiosulfate-utilizing bacteria [11]. The genomic analysis of *Cba. tepidum* has also revealed the presence of the *sox* gene cluster, which is presumably involved in thiosulfate oxidation [12,13]. However, contrary to the case in *P. pantotrophus*, the *soxCD* genes, which are responsible for the oxidation of the outer sulfur atom covalently bound to a cysteine residue in SoxY, are missing in the *Cba. tepidum* genome [14]. Other reaction mechanisms not involving SoxC/D have therefore been suggested to enable thiosulfate oxidation to sulfate [13]. A recent work has demonstrated that SoxK (CT1020), which made a ternary complex along with SoxAX (CT1019, CT1016), was necessary to exhibit a maximal reduction rate of cyt *c*-554 when the thiosulfate oxidation activity was measured in an *in vitro* reconstitution system [15].

Tsukatani *et al.* previously reported that cyt *c*-554 is not essential for the phototrophic growth of *Cba. tepidum* [16]. As a full growth of the insertion mutant of the *cycA* gene (*CT0075*) encoding cyt *c*-554 (Δ*cycA* mutant) was observed in a medium containing both sulfide and thiosulfate, the author simply considered that a tight coupling reaction between menaquinol:cyt *c* oxidoreductase and the RC complex, which enabled electron supply from sulfide oxidation by a membrane-bound sulfide:quinone reductase (SQR; CT0117, CT1087), would sustain its photosynthetic growth [17,18]. In this study, a mutant devoid of SoxB (CT1021) (Δ*soxB* mutant) and a double mutant of cyt *c*-554 and SoxB (Δ*cycAsoxB* mutant) were constructed in order to reinvestigate the intrinsic role of cyt *c*-554 *in vivo* with modern molecular biological techniques in combination with traditional assays of sulfur compound concentrations in media. The author examined the capabilities of three mutant strains so far obtained to oxidize both sulfide and thiosulfate in media. A complete oxidation of thiosulfate was unexpectedly observed in the Δ*cycA* mutant. The present results indicate that cyt *c*-554 is an efficient but not essential electron carrier for the thiosulfate oxidation in *Cba. tepidum*. The functions of cyt *c*-554/555 in green sulfur bacterial species which cannot oxidize

thiosulfate were also disscued from evolutionary aspects.

Materials and methods

Bacterial strains and growth conditions

The strain WT2321 of *Cba. tepidum* [19] was used as the wild type and host for transformation. The Δ*cycA* strain was obtained in previous work [16]. Pf-7 medium [20], which contained 4 mM thiosulfate and 2.5 mM sulfide as electron sources, was used for the growth analyses shown in Figure 2. However, in order to measure sulfur compounds more precisely as well as to get full growth of culture, an additional buffering reagent, 3-(N-morpholino)propanesulfonic acid (MOPS), was added to Pf-7 medium at a final concentration of 10 mM [21] and the concentration of thiosulfate contained was increased to 9 mM, which was then designated as Pf-7-MOPS. As the upper limit of sulfide tolerance for *Cba. tepidum* was reported to be about 4 mM [20], the concentration of sulfide in Pf-7-MOPS was adjusted at 2.5 mM. Pf-7-MOPS containing only thiosulfate or sulfide as a sole electron source was prepared basically according to the method described by Frigaard and Bryant [21] as follows. One liter of Pf-7-MOPS medium without $Na_2S_2O_3 \cdot 5H_2O$, $Na_2S \cdot 9H_2O$, and $NaHCO_3$ was autoclaved at 121°C for 20 min and cooled in an anaerobic chamber (Coy Laboratory Products, Ann Arbor, MI) overnight in order to completely remove any residual oxygen from the medium. In an anaerobic chamber, 2.3 g of $Na_2S_2O_3 \cdot 5H_2O$ or 0.6 g of $Na_2S \cdot 9H_2O$ was dissolved into a freshly prepared solution of 2.0 g of $NaHCO_3$ in 50 ml. After filter sterilization, each solution was added to the medium to make a 9 mM thiosulfate- or 2.5 mM sulfide-containing medium. Growth on agar CP plates was carried out as described previously [21,22].

Plasmid construction for natural transformation

A 2.7-kb DNA fragment containing the *soxB* gene was amplified by polymerase chain reaction (PCR) using an SOB-F primer (5'-*ACATGCCATGG*TCATCTTCGCCGCTGATC)

and an SOB-R primer (5'-*GCTCTAGA*AGGTAAAGCCCTGCTTGG), both of which were designed on the basis of the complete genomic sequence of *Cba. tepidum* [12]. In these primer sequences, heterologous bases are italicized, and recognition sites are underlined, respectively, an *Nco*I site for SOB-F and an *Xba*I site for SOB-R. Plasmid pSB was produced by digesting this DNA fragment with *Nco*I and *Xba*I and cloning the product thus obtained into the same recognition sites of pKF3 (Takara Bio Inc.). Plasmid pSB was then cut at two *Hin*dIII sites located at both ends of the *soxB* gene and ligated with the gentamycin resistance (Gm^r) cassette, which was produced by *Hin*dIII digestion of pUCGM [23], as shown in Figure II-1A. The resultant plasmid, pSB-Gm^r, was prepared in a large amount with a MIDI-prep kit (Invitrogen). About 1 μg of pSB-Gm^r was linearized by cutting at the *Nco*I site and applied to natural transformation in strain WT2321 of the *Cba. tepidum* and the Δ*cycA* strain as described previously [21]. The transformants grown on selective (Gm^r) CP plates were restreaked three times onto Gm^r CP plates. Single colonies on the third plate were inoculated into the liquid media, and the grown cells were inoculated again into selective liquid media containing appropriate antibiotics (gentamycin for the Δ*soxB* strain and streptomycin/gentamycin for the Δ*cycAsoxB* strain). These growth cultures were used for further investigations.

Genomic DNAs of all the strains were prepared according to the method described previously [22]. Plasmid constructions and other routine molecular biological procedures were carried out using chemically competent *Escherichia coli* DH5α as a host.

Growth rate measurements

The wild-type and mutant strains of *Cba. tepidum* were routinely grown at 40°C in a home-built growth chamber illuminated from the front with a light intensity of 30 μmol of photons m^{-2} s^{-1} using incandescent lamps, although the optimum temperature for growth is 47°C [20]. In the case of the growth measurements of mutants, no antibiotic was added into

liquid media in order to avoid any influence to their growth behavior. It has recently been demonstrated that temperature for growth affects cellular physiology, that is, compositions of bacteriochlorophyll *c* homologs and physical properties of chlorosomes [24]. Although the phenotypes observed in this study were expected to be more severe at the optimum temperature, the same conclusions concerning sulfur oxidation would be drawn from experiments at different temperatures.

For a quick estimation of the growth rate, the optical density at 660 nm was routinely monitored using a photometer (mini photo 518R, TAITEC). For a more reliable estimation, the protein content in each culture was determined basically according to the method described by Mukhopadhyay et al. [25]. Inoculation was done by transferring an aliquot amount (1 μg protein) of early stationary-phase cells, which were grown preliminarily under the same condition, into a freshly prepared medium in a 30-ml screw-capped tube without a headspace. Each culture was kept in the dark for 1 - 2 hrs before measurements started. The average value of five independent measurements was plotted against the time elapsed. The optical density was not monitored consecutively in each tube, but it was discarded after measurement in order to avoid any interference of growth.

Quantitative determinations of sulfur compounds

After centrifugation of each culture, the resultant supernatant was kept at -80°C until use except for sulfide determination. The content of the sulfur compounds in the supernatant was determined as follows: the sulfide content was estimated by the formation of methylene blue [26], the thiosulfate content, by cyanolysis in the presence of Cu^{2+} ion followed by Fe-SCN complex formation [27], and the sulfate content, by the formation of $BaSO_4$ precipitates after the reaction with $BaCl_2$ under acidic conditions [28]. As Pf-7-MOPS contained 0.8 mM $MgSO_4$, it was impossible to clarify physiological meanings of values less than 0.8 mM obtained in the present measurement (see Table II-1).

The elemental sulfur was also quantified after hexane extraction of the centrifugation pellet, followed by further extraction with methanol and subsequent measurement of the absorption of the finally obtained extract at 260 nm [29]. The hot cyanolysis method was also applied to estimate it and almost the same result was obtained [30] (data not shown).

Although a freshly prepared liquid medium (both Pf-7 and Pf-7-MOPS) contained 2.5 mM sulfide, the actual measurement value of sulfide immediately after inoculation was found to be only 1 mM due to its volatilization and/or oxidation during a centrifugation step to collect the supernatant (see Figure II-2B). The initial sulfide content was therefore confirmed to be about 2.4 mM by a direct addition of reagents into the medium in a culture tube after the removal of its screw cap and a subsequent color development in it (see Table II-1). The cyanolysis method tends to react slightly with elemental sulfur and/or polysulfide derived from sulfide oxidation by air [27], which would, thus, overestimate the thiosulfate content to be 0.1-0.3 mM in sulfide-containing media (also see Table II-1).

Results

Construction of Cba. tepidum mutants

The *soxB* gene was disrupted in both the *Cba. tepidum* wild type and the Δ*cycA* strain by replacing the central portion of a *soxB* gene with the *aacC1* gentamycin cassette as depicted in Figure II-1A. The insertion of the *aacC1* gene into the correct locus in the genomic DNA was verified by PCR analyses using a primer set of SOB-F/SOB-R. Although 2.7-kb fragments containing a full size of the *soxB* gene were amplified from the wild type and Δ*cycA* strain, products with a size of 2.0 kb were obtained from the Δ*soxB* and Δ*cycAsoxB*::*aacC1* strains (Figure II-1B). This was interpreted to be due to the deletion of a 1.6-kb fragment within the coding region of the *soxB* gene when an *aacC1* cassette with the size of 0.9 kb was inserted (see Figure II-1A). On the other hand, a primer set of C554F/C554R, which was applied to cause the insertional disruption of the *cycA* gene in the previous study [16], confirmed that both mutants were never affected by the present transformation procedures. Furthermore, the same results were also obtained in mutants after several generations of cultivation in non-selective Pf-7 and/or Pf-7-MOPS media (data not shown), indicating that the *aacC1* cassette was stably incorporated into the genome.

Growth rates and oxidations of sulfide and thiosulfate in complete media

Figure II-2A shows the growth profiles of the wild type and three mutants (Δ*cycA*, Δ*soxB*, and Δ*cycAsoxB* strains) cultivated in Pf-7 medium [20], which contains both sulfide and thiosulfate (Figure II-2A). All of them grew almost at the same rate during the initial 15 hrs, and their doubling times were estimated to be 2 hrs, nearly the same as that reported originally in *Cba. tepidum* under optimal conditions [20]. During this period, sulfide was consumed completely in all cultures, while the thiosulfate contents remained almost unchanged (Figure II-2, B and C). Although sulfide appeared to be exhausted more slowly in

the cultures of the disruption mutants of the *soxB* gene (Δ*soxB* and Δ*cycAsoxB* strains) than in those of the wild type and the Δ*cycA* strain, their growth rates did not clearly reflect these small distinctions.

After 15 hrs, the wild type and the Δ*cycA* strain still continued to grow to attain their full growth, although the Δ*cycA* strain was slightly retarded compared to the wild type ($P < 0.001$) (Figure II-2A). The doubling time of the wild type was thus almost the same as before, while that of the mutant strain was estimated to be about 4.5 hrs. In agreement with their respective growth profiles, the wild type consumed thiosulfate more rapidly than the Δ*cycA* strain (Figure II-2C), and no significant difference was observed between their final cell yields.

On the other hand, the Δ*soxB* and Δ*cycAsoxB* strains ceased to grow after 15 hrs, when sulfide in their cultures was completely exhausted, and their final cell yields were estimated to be less than one tenth of that of the wild type (Figure II-2, A and B; also see Table II-1). Since the SoxB is a component in a multienzyme system involved in thiosulfate oxidation, it was conceivable that both mutants could not utilize thiosulfate as an electron source [11]. In fact, the thiosulfate contents in their cultures were constant during the measurements of their growths, as shown in Figure 2C.

Utilization of sulfide and thiosulfate as electron sources

It still remained unknown to what degree the mutants could efficiently utilize sulfide and thiosulfate for their photosynthetic growths. The growth profiles, therefore, were observed after transferring into freshly prepared media containing only sulfide or thiosulfate as the sole electron source (Figure II-3). Cell numbers were roughly estimated by measuring optical densities at 660 nm for the sake of convenience because there was no need to discriminate subtle differences in growth rates. The final cell yields were nevertheless measured by determining the protein contents in order to avoid overestimates due to light

scattering (Table II-1). The sulfur content in each culture after the stationary phase was also measured to estimate the degree of oxidation of the two electron sources.

When 9 mM thiosulfate was provided as the sole electron source, the Δ*soxB* and Δ*cycAsoxB* strains did not grow completely (Figure II-3A), and no consumption of thiosulfate was observed in either culture (Table II-1). The Δ*cycA* strain grew more slowly than the wild type, as expected from the result obtained in the Pf-7 medium, and required much more time to attain full growth (Figures II-2A and II-3A). This could be interpreted as a result reflecting the relatively slower oxidation rate of thiosulfate in the mutant compared to that in the wild type (Figure II-2C). The cell yield of the Δ*cycA* strain was, however, almost the same as that of the wild type in Pf-7-MOPS medium with or without thiosulfate (Table II-1). The entire consumption of thiosulfate by both the wild type and the Δ*cycA* strain indicated that they could utilize thiosulfate for their photosynthetic growth and completely oxidize it to sulfate. In fact, the amounts of sulfate accumulated after their full growths were nearly equivalent to those of thiosulfate added into freshly prepared media in terms of the sulfur contents (Table II-1).

On the other hand, when 2.5 mM sulfide was added to the media as a sole electron source, all four strains showed a similar growth profile (Figure II-3B). It is well known that polysulfide and/or elemental sulfur globules, which are the products of sulfide oxidation, are excreted outside of the cells during phototrophic growth and then oxidized further to sulfate [31]. The small bulges in the growth curves of the wild type and the Δ*cycA* strain, which could be observed at around 15 hrs in Figure II-3B, were thus ascribable to their transient appearance detected as a scattering artifact. From the amounts of sulfate accumulated in the cultures after full growth, most of the sulfide added into freshly prepared media seemed to be completely oxidized to sulfate by the wild type and the *cycA*::*aadA* strain (Table II-1). Although the Δ*soxB* and Δ*cycAsoxB* strains could consume sulfide judging from Figure II-2B, they were found to oxidize it only partially (Table II-1). Almost the same amount of sulfate

was detected in the Δ*soxB* strain as compared to that in the control medium, and a half amount of sulfate expected from a complete sulfide oxidation seemed to be accumulated in the Δ*cycAsoxB* strain. In fact, the final cell yields of the wild type and the Δ*cycA* strain were about 2 times larger than those of the Δ*soxB* and Δ*cycAsoxB* strains (Table II-1), in agreement with the incomplete oxidation of sulfide to sulfate by the latter two mutants. In the present experiment, the maximal sulfide concentration in media was limited to 2.5 mM because of its toxic effect on cells at higher concentrations.

Discussion

The physiological function of cyt c-554

The Δ*cycA* strain could grow even in the medium containing only thiosulfate as an electron source but exhibited a rather retarded growth rate compared to that of the wild type (Figure II-3A), which was attributable to a relatively slower oxidation rate of thiosulfate by the mutant than the wild type (Figure II-2C). However, it is noteworthy that the mutant still retained a capability to completely oxidize thiosulfate to sulfate. This was also supported by the fact that the final cell yield of the Δ*cycA* strain was almost the same as that of the wild type, implying that the mutant can utilize all the reducing power derived from thiosulfate oxidation for its own growth. Therefore, the present results have clearly demonstrated that cyt *c*-554 functions as an efficient electron carrier between the Sox system and cyt c_z as expected but is not indispensable for thiosulfate oxidation.

In the medium containing both sulfide and thiosulfate, the wild type as well as the Δ*cycA* strain utilized sulfide exclusively during the early stage of growth and then oxidized thiosulfate after sulfide exhaustion (see Figure II-2) [32]. This suggests that an activity of thiosulfate oxidation might be somehow regulated, presumably by the redox state of the quinone pool, because the sulfide oxidation by SQR could control its redox balance. It is noteworthy that the Δ*cycA* strain commenced thiosulfate consumption about 10 hrs later after the wild type did (Figure II-2C). In accordance with this, the mutant strain also resumed its growth after a time lag in media containing only thiosulfate as an electron donor as well (Figure II-3A). It may suggest that an electron-carrying component other than cyt *c*-554 or an alternative electron transfer path was induced to oxidize thiosulfate, although there is no genetic information at present from the relevant genomic analysis. Recently, the RT-PCR analysis of three SQR homologs has indicated that the transcription level of *CT1087* increased

when sulfide was supplemented to cultures [17]. It will therefore be interesting issues to study regulation mechanisms of sulfur oxidation pathway in detail.

In vivo mechanisms of sulfur oxidation in Cba. tepidum

It has been demonstrated *in vitro* that the Sox multienzyme system, which oxidizes sulfite, thiosulfate, sulfur, and/or sulfide, consists of four protein components, namely, SoxAX, SoxYZ, SoxB, and SoxCD, in *Paracoccus pantotrophus* [10]. On the other hand, the genome sequence analysis of *Cba. tepidum* has revealed that no orthologs of the *soxC* and *D* genes, which encode sulfur dehydrogenase (SoxCD), are found in the *sox* gene cluster or at other locations [12]. The present results clearly demonstrate that the *soxB* gene is indispensable for the oxidation of thiosulfate (see Figure II-3A and Table II-1), suggesting that some other component(s) than the SoxCD or a different oxidation mechanism must be operating in *Cba. tepidum*. Although an alternative carrier would also accept electrons from this Sox system, it is not at all clear at present what could play the role of cyt *c*-554 in the Δ*cycA* strain.

Furthermore, an additional interesting phenotype was recognized in mutants devoid of SoxB, i.e., neither the Δ*soxB* strain nor the Δ*cycAsoxB* one oxidized sulfide completely to sulfate (Table II-1). They did not also excrete any polysulfide/sulfur globules outside of the cells (Table II-1), although the cultures of the *soxB* mutants appeared to become somewhat turbid and show some kind of aggregations. One possible interpretation might be that the Sox system in *Cba. tepidum* is somehow involved in the oxidation of intermediate(s) produced during sulfide oxidation. This should be resolved by a more intensive analysis of all possible intermediate(s) and/or *in vitro* reconstitution experiments in the future.

The mechanisms of sulfur oxidation as well as its metabolic pathways remain enigmatic in green sulfur bacteria, although several *in vitro* reconstitution experiments had

intensively been conducted in the early 1970s [8,9]. Recent work has demonstrated that SoxK, whose gene is located between the *soxA* and *soxB* genes in the genome of *Cba. tepidum* [13], drastically enhanced the thiosulfate-dependent reduction of cyt *c*-554 by forming a ternary complex with SoxAX, when added into a reaction mixture containing SoxYZ (CT1017-1018) and SoxB [15]. However, it still remains an unknown and critical issue how thiosulfate is completely oxidized to sulfate *in vivo*. Now that genomic databases are available in some sulfur-oxidizing bacteria, comparative studies as well as molecular genetic analyses using *Cba. tepidum* will clarify the components involved in sulfide and/or thiosulfate oxidation and enable us to envisage the entire picture of the sulfur metabolism in green sulfur bacteria in the near future.

Evolutionary aspects of green sulfur bacterial cyts c

Recent genomic analyses of twelve species of green sulfur bacteria have revealed that an orthologous gene encoding a low-molecular-weight, soluble monoheme cyt *c*-554/555 is distributed in all of them (Figure II-4A) [33]. Although their deduced amino acid sequences exhibit a relatively wide range of identities (41–91%) to each other, the identities in species containing the Sox gene cluster exhibit a higher identity proportion (approximately 64–91%). An orthologous gene encoding cyt *c*-556 is also distributed as probable membrane-bound *c*-type cyt in all species, and their amino acid sequences exhibit 31–75% identity to each other. Except for *Chloroherpeton thalassium* [34] and *Chlorobium* (*Chl.*) *chlorochromatii* [35], the gene for cyt *c*-556 is located immediately upstream of the gene for cyt *c*-554/555; however, in the *Cba. tepidum* genome only, an ORF (*CT0074*) is located between two genes for cyts *c*-554/555 and *c*-556, although the annotation of *CT0074* is doubtful. These genomic organizations strongly suggest that the ET pathways involving both cyts *c*-554/555 and *c*-556 are evolutionarily conserved in green sulfur bacteria regardless of their capability for thiosulfate oxidation.

The cluster analysis of green sulfur bacterial cyts c_z, *c*-554/555, and *c*-556, as well as heliobacterial cyt *c*-553, has clarified three major groups, as shown in Figure II-4B. Cyts *c*-554/555 and *c*-556 are closely related to each other but distantly related to cyt c_z, suggesting that the former two share a paralogous relationship with each other as electron donors to cyt c_z. Cyts *c*-554/555 in four thiosulfate-oxidizing species (*Cba. tepidum*, *Cba. parvum*, *Chl. phaeovibriodes*, and *Chl. clathratiforme*; see [1,13]) do not form a monophyletic cluster, implying that they might have evolved independently in accordance with physiological demands of individual species. Furthermore, cyt *c*-554/555 of *Chl. ferroxidans* shows a high sequence identity (approximately 69%) compared to those of thiosulfate-oxidizing species. *Chl. ferroxidans*, which does not use reduced sulfur compounds (sulfide, thiosulfate, and elemental sulfur) as electron sources but oxidizes ferrous ion to ferric ion [36], contains neither the sox gene cluster nor other relevant genes [13]. This could imply two possibilities concerning the function of cyt *c*-554/555. One is that cyt *c*-554/555 has the same function as an electron carrier among all species of green sulfur bacteria; *Cba. tepidum* cyt *c*-554 not only accepts electrons from the Sox system but would also operate in (an)other unknown but common pathway(s). The other is that cyt *c*-554/555 has different functions depending on the species; *Cba. tepidum* cyt *c*-554 accepts electrons from the Sox system, while *Chl. ferroxidans* cyt *c*-554/555 would do so from the oxidation system of ferrous ion. At present, there is no biochemical and/or molecular biological data concerning cyt *c*-554/555 from *Chl. ferroxidans* or any other species which cannot oxidize thiosulfate at all. In general, cyts would be evolutionarily “adaptive” or “flexible” to physiological variations and have different functions depending on species [37].

Tables

Table II-1: ***Cell yields and concentrations of sulfur compounds in stationary phase cultures (after 72 hrs of growth) of the wild type and three mutants***

Strains	Electron sources in Pf-7-MOPS	Cell yields (µg protein/ml)	Sulfide concentrations (mM)	Thiosulfate concentrations (mM)	Elemental sulfur concentrations (mM)	Sulfate concentrations (mM)
wild type	sulfide/ thiosulfate	184.3 (±28.8)	N.D.[a]	N.D.[a]	0.1 (±0.0)	21.6 (±1.2)
	thiosulfate	211.0 (±10.9)	N.D.[a]	N.D.[a]	0.9 (±0.1)	17.4 (±1.9)
	sulfide	31.9 (±0.9)	N.D.[a]	N.D.[a]	0.1 (±0.0)	3.0 (±0.1)
Δ*cycA*	sulfide/ thiosulfate	170.5 (±22.6)	N.D.[a]	N.D.[a]	0.1 (±0.0)	22.1 (±1.0)
	thiosulfate	211.6 (±11.3)	N.D.[a]	N.D.[a]	0.4 (±0.0)	18.9 (±1.1)
	sulfide	33.0 (±2.0)	N.D.[a]	N.D.[a]	0.1 (±0.0)	2.8 (±0.1)
Δ*soxB*	sulfide/ thiosulfate	11.8 (±0.5)[b]	N.D.[a]	9.5 (±0.1)[b]	N.D.[a]	0.4 (±0.0)[b]
	thiosulfate	N.D.[a]	N.D.[a]	9.2 (±0.1)[b]	N.D.[a]	0.1 (±0.0)[b]
	sulfide	14.7 (±0.9)[b]	N.D.[a]	0.3 (±0.0)	N.D.[a]	0.9 (±0.1)[b]
Δ*cycAsoxB*	sulfide/ thiosulfate	21.1 (±3.3)[b,c]	N.D.[a]	9.1 (±0.6)[b]	N.D.[a]	1.2 (±0.1)[b,c]
	thiosulfate	N.D.[a]	N.D.[a]	9.2 (±0.0)[b]	N.D.[a]	0.1 (±0.0)[b]
	sulfide	19.3 (±2.6)[b,c]	N.D.[a]	0.2 (±0.0)	N.D.[a]	1.7 (±0.1)[b,c]
none[d]	sulfide/ thiosulfate	-	2.1 (±0.1)	9.2 (±0.1)	N.D.[a]	0.1 (±0.0)
	thiosulfate	-	N.D.[a]	9.0 (±0.1)	N.D.[a]	0.1 (±0.0)
	sulfide	-	2.4 (±0.1)	0.1 (±0.0)	N.D.[a]	0.7 (±0.0)

[a] Not detectable.

[b] $P < 0.001$, for comparison to the wild type within the same condition.

[c] $P < 0.05$, for comparison to the soxB::aacC1 strain within the same condition.

[d] Concentrations of sulfur compounds were measured in freshly prepared media as described in the text. Note that Pf-7-MOPS contains 0.8 mM

Figures

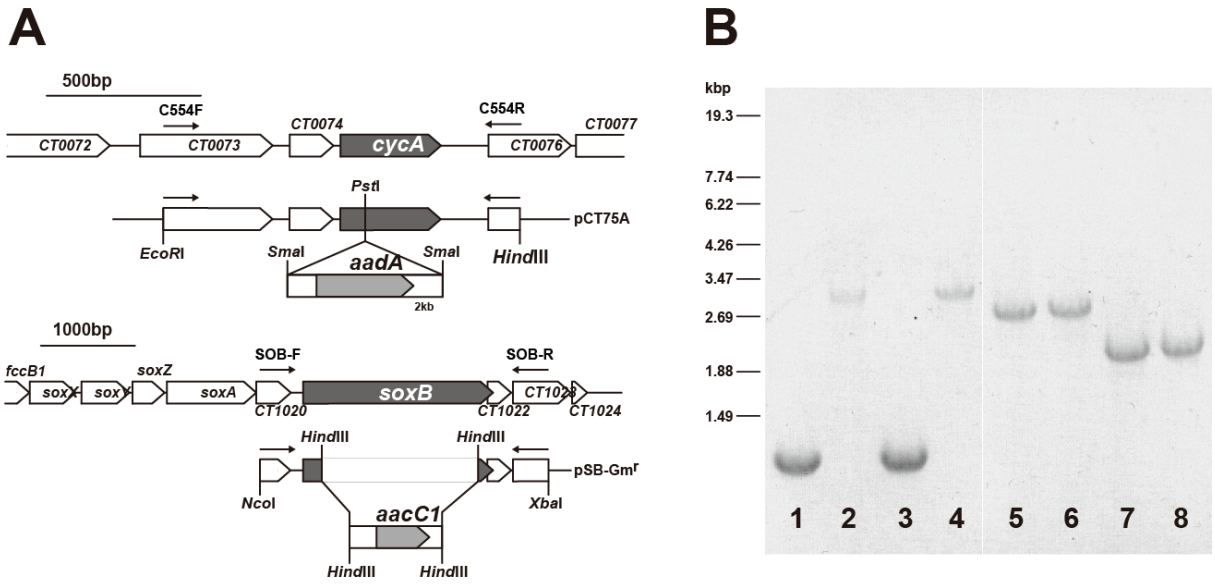

Figure II-1. (A) Schematic map for the construction of Δ*cycA* (upper) and Δ*soxB* (lower) mutants. Genes are indicated by rectangles. The arrows represent the oligonucleotide primers used for the cloning and confirmation of mutations. Plasmids were digested at the AhdI site for natural transformation and then introduced into *Cba. tepidum*. (B) PCR analysis of the genomes from the wild type (lanes 1 and 5), Δ*cycA* strain (lanes 2 and 6), Δ*soxB* strain (lanes 3 and 7), and Δ*cycAsoxB* strain (lanes 4 and 8). The loci of *cycA* and *soxB* were amplified by PCR with the primer sets of C554F and C554R (lanes 1-4) and of SOB-F and SOB-R (lanes 5-8), respectively. The numbers indicate the lengths of the DNA fragments in kilobases.

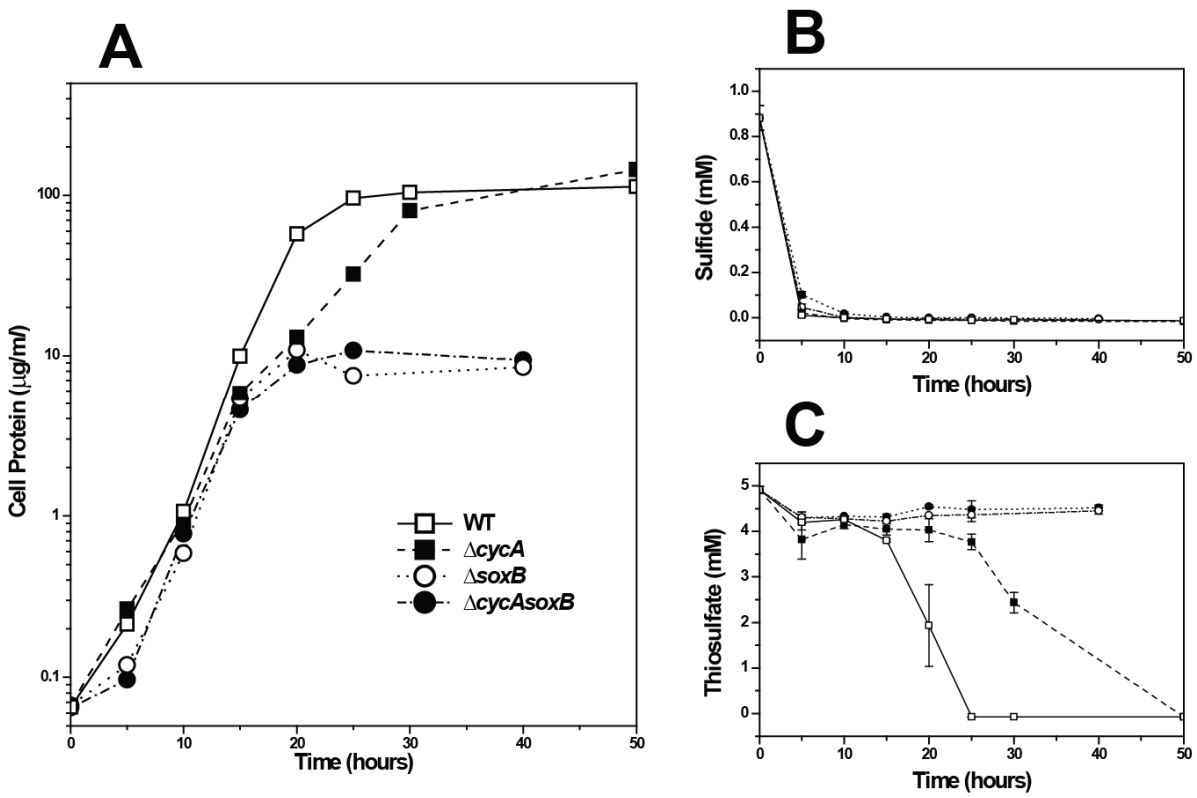

Figure II-2. (A) Growth profiles for the wild type (open squares), Δ*cycA* strain (closed squares), Δ*soxB* strain (open circles), and Δ*cycAsoxB* strain (closed circles) cultivated in Pf-7 media at 40°C. (B) and (C) Sulfide and thiosulfate consumptions during the cultivation of wild type and three mutants. The symbols are the same as in (A). The average of five independent measurements of the cell density (μg protein/ml) and the sulfide and thiosulfate concentrations [24] in media were plotted against time. Standard deviations are also indicated by bars in (B) and (C), but too small to be noted other than three points indicated in (C). Measurement values were missing at 30 hrs in the wild type and Δ*cycA* mutant in (C) because they were plotted at 40 hrs instead.

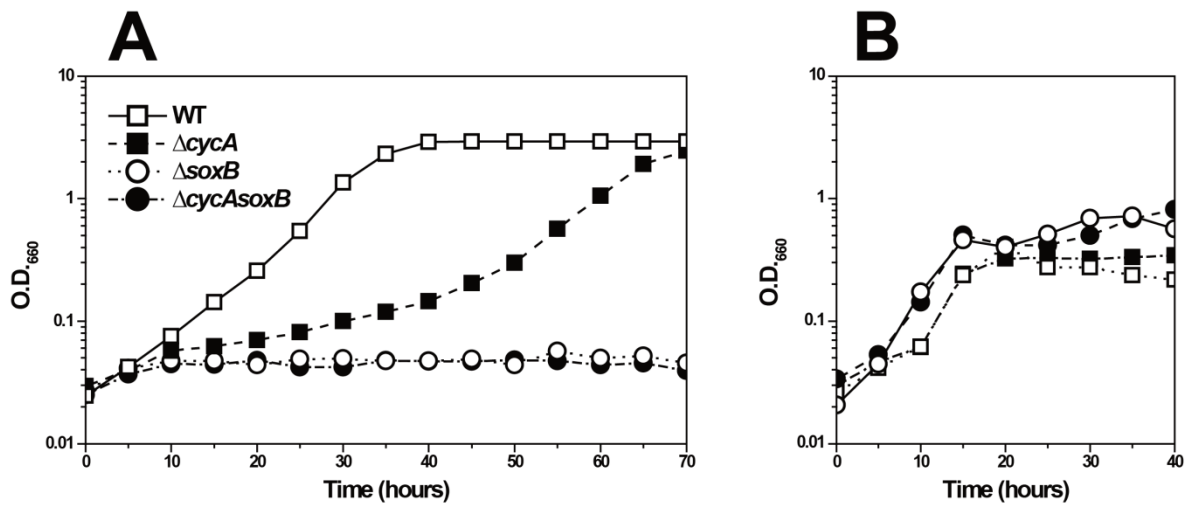

Figure II-3. Growth profiles for the wild type (open squares), Δ*cycA* strain (closed squares), Δ*soxB* strain (open circles), and Δ*cycAsoxB* strain (closed circles) cultivated in Pf-7-MOPS media with (A) thiosulfate or (B) sulfide at 40°C. The average of five independent measurements of the cell density at 660 nm was plotted against time.

A

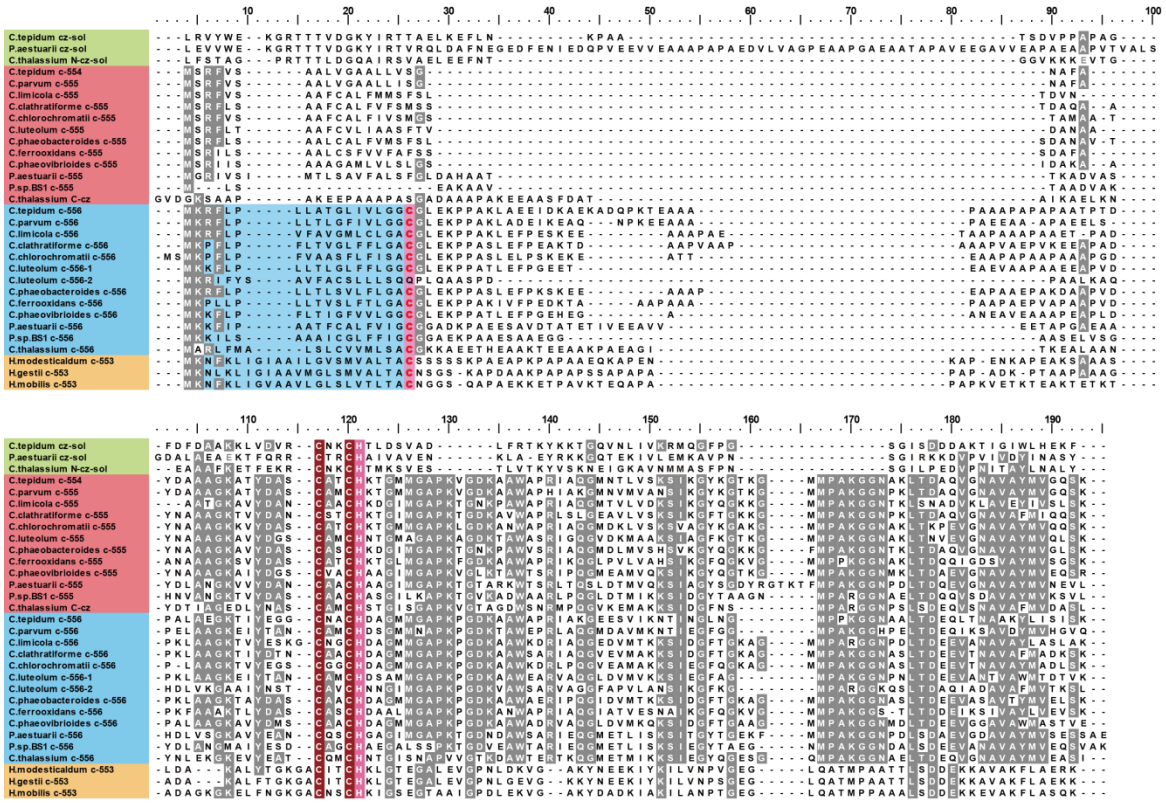

B

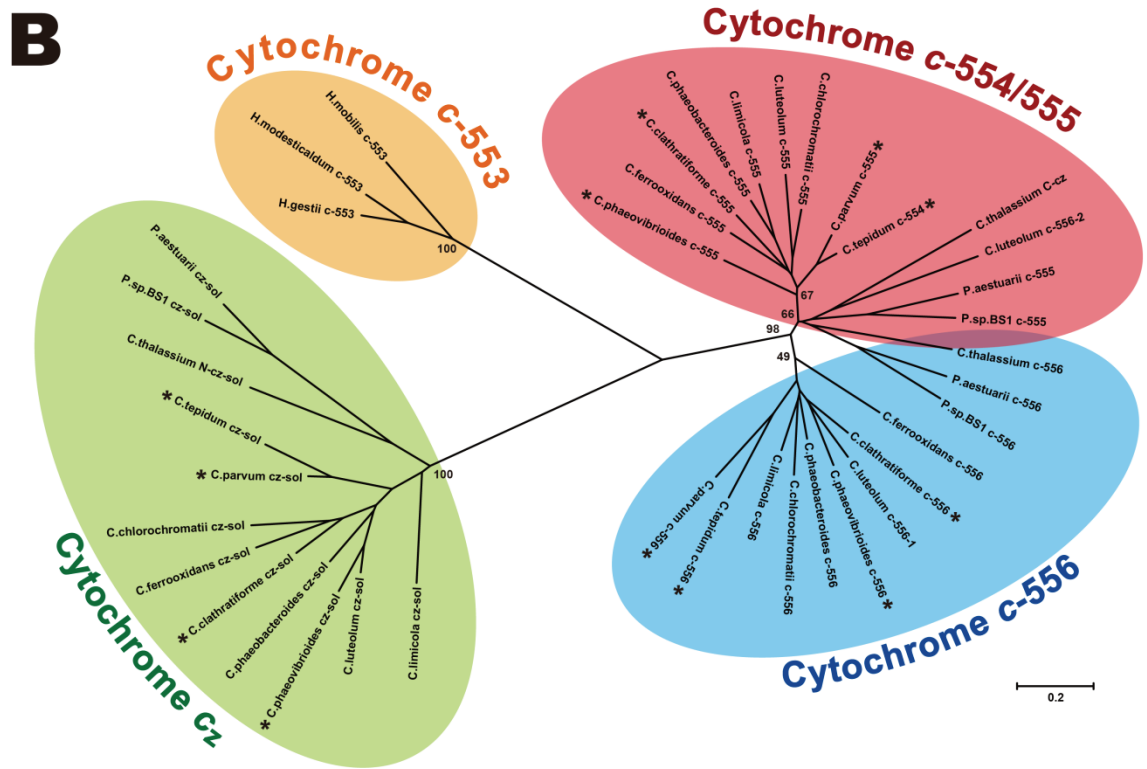
Cytochrome c-553
H.mobilis c-553
H.modesticaldum c-553
H.gestii c-553
100
Cytochrome c-554/555
C.phaeobacteroides c-555
C.limicola c-555
C.luteolum c-555
C.chlorochromati c-555
C.clathratiforme c-555
C.parvum c-555
C.tepidum c-554
C.ferrooxidans c-555
C.phaeovibrioides c-555
C.thalassium C-cz
C.luteolum c-556-2
P.aestuarii c-555
P.sp.BS1 c-555
67
66
98
49
C.thalassium c-556
P.aestuarii c-556
P.sp.BS1 c-556
C.ferrooxidans c-556
C.clathratiforme c-556
C.luteolum c-556-1
C.phaeovibrioides c-556
C.phaeobacteroides c-556
C.chlorochromati c-556
C.limicola c-556
C.tepidum c-556
C.parvum c-556
Cytochrome c-556
P.aestuarii cz-sol
P.sp.BS1 cz-sol
C.thalassium N-cz-sol
C.tepidum cz-sol
C.parvum cz-sol
100
C.chlorochromatii cz-sol
C.ferrooxidans cz-sol
C.clathratiforme cz-sol
C.phaeobacteroides cz-sol
C.phaeovibrioides cz-sol
C.luteolum cz-sol
C.limicola cz-sol
Cytochrome cz
0.2

Figure II-4. (A) Multiple alignment of amino acid sequences of green sulfur and heliobacterial *c*-type cyts (cyts c_z, *c*-554/555, *c*-556 and *c*-553) constructed with a Clustal W program. The typical binding motif for *c*-type heme, C-X-X-C-H, is completely conserved in all cyts *c*, and the relevant cysteine and histidine residues are boxed in wine red and pink, respectively. The blue-shaded region is a signal-like peptide sequence for lipidation. The conserved cysteine residues just after the signal sequences are written in red and shaded in pink. (B) Cluster analysis of green sulfur and heliobacterial *c*-type cyts. The unrooted phylogenetic tree was constructed by neighbor-joining method with MEGA4 [38]. The bootstrap values were calculated with 1000 replications and are shown by the sides of the branches. The asterisks represent green sulfur bacteria capable of thiosulfate oxidation. The mature proteins start from the 23rd tyrosine and 18th cysteine residues for cyts *c*-554/555 and *c*-556, respectively, in *Cba. tepidum* and from the 23rd cysteine residue for cyt *c*-553 in *Hbt. modesticaludam*. In the case of cyt c_z, the sequence of its C-terminal hydrophilic and soluble heme-containing domain (referred to as "cz-sol") [39,40], which corresponds to the one from the 96th amino acid in *Cba. tepidum*, was used for the analysis. Sequence data of cyt *c*-554/555 and *c*-556 homologues were obtained from the JGI microbial genomic database (http://img.jgi.doe.gov) by blast searches using *Cba. tepidum* *c*-554 (CT0075) and *c*-556 (CT0073) as queries. Although two candidates for cyt *c*-556 in the *Chl. luteolum* genome (*C. luteolum* *c*-556-1 and -2) were hit with high scores, the conserved cysteine residue was found only in the *Chl. luteolum* *c*-556-1. In *Chloroherpeton thalassium*, an *orf* gene (Ctha_1874) seems to encode a fused protein of cyt c_z and cyt *c*-554/555 at the N-terminal and C-terminal halves, respectively. These halves are therefore tentatively referred to as "N-c_z" and "C-c_z", respectively. Other sequence data were obtained from the JGI microbial genomic database and the Genbank database.

References

1. Imhoff, J. F. (2003) Phylogenetic taxonomy of the family Chlorobiaceae on the basis of 16S rRNA and fmo (Fenna-Matthews-Olson protein) gene sequences, *Int J Syst Evol Microbiol* **53**, 941-951
2. Pfennig, N. (1989) Green Bacteria. in *Bergy's Manual of Systematic Bacteriology* (Staley, J. T., Bryant, M. P., Pfenning, N., and Holt, J. C. eds.), Williams and Wilkins, Baltimore, MD. pp 1682-1707
3. Trüper, H. G., Lorenz, M., Schedel, M., and Steinmentz, M. (1988) Metabolism of thiosulfate in *Chlorobium*. in *Green Photosynthetic Bacteria* (Olson, J. G., Ormerod, J., Amesz, E., Stackebrant, H. G., and Trüper, H. G. eds.), Plenum Press, New York. pp 189-200
4. Oh-oka, H., and Blankenship, R. E. (2004) Green bacteria: secondary electron donor (cytochromes). in *Encyclopedia of biological chemistry.* (Lennarz, W. J., and Lane, M. D. eds.), Academic Press, Oxford. pp 521-524
5. Seo, D., and Sakurai, H. (2002) Purification and characterization of ferredoxin-NAD(P)(+) reductase from the green sulfur bacterium Chlorobium tepidum, *Biochim Biophys Acta* **1597**, 123-132
6. Yoon, K. S., Bobst, C., Hemann, C. F., Hille, R., and Tabita, F. R. (2001) Spectroscopic and functional properties of novel 2[4Fe-4S] cluster-containing ferredoxins from the green sulfur bacterium Chlorobium tepidum, *J Biol Chem* **276**, 44027-44036
7. Oh-oka, H., Iwaki, M., and Itoh, S. (1998) Membrane-bound cytochrome cz couples quinol oxidoreductase to the P840 reaction center complex in isolated membranes of the green sulfur bacterium Chlorobium tepidum, *Biochemistry* **37**, 12293-12300
8. Kusai, A., and Yamanaka, T. (1973) Cytochrome c (553, Chlorobium thiosulfatophilum) is a sulphide-cytochrome c reductase, *FEBS Lett* **34**, 235-237
9. Kusai, K., and Yamanaka, T. (1973) The oxidation mechanisms of thiosulphate and sulphide in Chlorobium thiosulphatophilum: roles of cytochrome c-551 and cytochrome c-553, *Biochim Biophys Acta* **325**, 304-314
10. Rother, D., Henrich, H. J., Quentmeier, A., Bardischewsky, F., and Friedrich, C. G. (2001) Novel genes of the sox gene cluster, mutagenesis of the flavoprotein SoxF, and evidence for a general sulfur-oxidizing system in Paracoccus pantotrophus GB17, *J Bacteriol* **183**, 4499-4508
11. Friedrich, C. G., Rother, D., Bardischewsky, F., Quentmeier, A., and Fischer, J. (2001) Oxidation of reduced inorganic sulfur compounds by bacteria: emergence of a common mechanism?, *Appl Environ Microbiol* **67**, 2873-2882
12. Eisen, J. A., Nelson, K. E., Paulsen, I. T., Heidelberg, J. F., Wu, M., Dodson, R. J.,

Deboy, R., Gwinn, M. L., Nelson, W. C., Haft, D. H., Hickey, E. K., Peterson, J. D., Durkin, A. S., Kolonay, J. L., Yang, F., Holt, I., Umayam, L. A., Mason, T., Brenner, M., Shea, T. P., Parksey, D., Nierman, W. C., Feldblyum, T. V., Hansen, C. L., Craven, M. B., Radune, D., Vamathevan, J., Khouri, H., White, O., Gruber, T. M., Ketchum, K. A., Venter, J. C., Tettelin, H., Bryant, D. A., and Fraser, C. M. (2002) The complete genome sequence of Chlorobium tepidum TLS, a photosynthetic, anaerobic, green-sulfur bacterium, *Proc Natl Acad Sci U S A* **99**, 9509-9514

13. Frigaard, N. U., and Bryant, D. A. (2008) Genomic insight into the sulfur metabolism of phototropic green sulfur bacteria. in *Sulfur Metabolism in Phototrophic Organisms* (Rüdiger, H. ed.), Springer, New York. pp 337-355
14. Frigaard, N. U., and Bryant, D. A. (2004) Seeing green bacteria in a new light: genomics-enabled studies of the photosynthetic apparatus in green sulfur bacteria and filamentous anoxygenic phototrophic bacteria, *Arch Microbiol* **182**, 265-276
15. Ogawa, T., Furusawa, T., Nomura, R., Seo, D., Hosoya-Matsuda, N., Sakurai, H., and Inoue, K. (2008) SoxAX binding protein, a novel component of the thiosulfate-oxidizing multienzyme system in the green sulfur bacterium Chlorobium tepidum, *J Bacteriol* **190**, 6097-6110
16. Tsukatani, Y., Miyamoto, R., Itoh, S., and Oh-oka, H. (2006) Soluble cytochrome c-554, CycA, is not essential for photosynthetic electron transfer in Chlorobium tepidum, *FEBS Lett* **580**, 2191-2194
17. Chan, L. K., Morgan-Kiss, R. M., and Hanson, T. E. (2009) Functional analysis of three sulfide:quinone oxidoreductase homologs in Chlorobaculum tepidum, *J Bacteriol* **191**, 1026-1034
18. Shahak, Y., Arieli, B., Padan, E., and Hauska, G. (1992) Sulfide quinone reductase (SQR) activity in Chlorobium, *FEBS Lett* **299**, 127-130
19. Wahlund, T. M., and Madigan, M. T. (1995) Genetic transfer by conjugation in the thermophilic green sulfur bacterium Chlorobium tepidum, *J Bacteriol* **177**, 2583-2588
20. Wahlund, T. M., Woese, C. R., Castenholz, R. W., and Madigan, M. T. (1991) A thermophilic green sulfur bacterium from New Zealand hot springs, Chlorobium tepidum sp. nov., *Arch. Microbiol.* **56**, 81-90
21. Frigaard, N. U., and Bryant, D. A. (2001) Chromosomal gene inactivation in the green sulfur bacterium Chlorobium tepidum by natural transformation, *Appl. Environ. Microbiol.* **67**, 2538-2544
22. Tsukatani, Y., Miyamoto, R., Itoh, S., and Oh-Oka, H. (2004) Function of a PscD subunit in a homodimeric reaction center complex of the photosynthetic green sulfur bacterium Chlorobium tepidum studied by insertional gene inactivation. Regulation of energy transfer and ferredoxin-mediated NADP+ reduction on the cytoplasmic side, *J Biol Chem* **279**, 51122-51130
23. Schweizer, H. D. (1993) Small broad-host-range gentamycin resistance gene cassettes

for site-specific insertion and deletion mutagenesis, *Biotechniques* **15**, 831-834

24. Morgan-Kiss, R. M., Chan, L. K., Modla, S., Weber, T. S., Warner, M., Czymmek, K. J., and Hanson, T. E. (2009) Chlorobaculum tepidum regulates chlorosome structure and function in response to temperature and electron donor availability, *Photosynth Res* **99**, 11-21
25. Mukhopadhyay, B., Johnson, E. F., and Ascano, M., Jr. (1999) Conditions for vigorous growth on sulfide and reactor-scale cultivation protocols for the thermophilic green sulfur bacterium chlorobium tepidum, *Appl Environ Microbiol* **65**, 301-306
26. Trüper, H. G., and Schlegel, H. G. (1964) Sulphur Metabolism in Thiorhodaceae. I. Quantitative Measurements on Growing Cells of Chromatium Okenii, *Antonie Van Leeuwenhoek* **30**, 225-238
27. Westley, J. (1987) Thiocyanate and thiosulfate, *Methods Enzymol* **143**, 22-25
28. Söbo, B. (1987) Sulfate: turbidimetric and nephelometric methods, *Methods Enzymol* **143**, 3-6
29. Stal, L. J., Vangemerden, H., and Krumbein, W. E. (1984) The Simultaneous Assay of Chlorophyll and Bacteriochlorophyll in Natural Microbial Communities, *J Microbiol Methods* **2**, 295-306
30. Schedel, M., and Truper, H. G. (1980) Anaerobic Oxidation of Thiosulfate and Elemental Sulfur in Thiobacillus denitrificans, *Arch Microbiol* **124**, 205-210
31. Brune, D. C. (1989) Sulfur oxidation by phototrophic bacteria, *Biochim Biophys Acta* **975**, 189-221
32. Chan, L. K., Weber, T. S., Morgan-Kiss, R. M., and Hanson, T. E. (2008) A genomic region required for phototrophic thiosulfate oxidation in the green sulfur bacterium Chlorobium tepidum (syn. Chlorobaculum tepidum), *Microbiology* **154**, 818-829
33. Azai, C., Tsukatani, Y., Itoh, S., and Oh-Oka, H. (2010) C-type cytochromes in the photosynthetic electron transfer pathways in green sulfur bacteria and heliobacteria, *Photosynth Res*
34. Gibson, J., Pfennig, N., and Waterbury, J. B. (1984) Chloroherpeton thalassium gen. nov. et spec. nov., a non-filamentous, flexing and gliding green sulfur bacterium, *Arch Microbiol* **138**, 96-101
35. Vogl, K., Glaeser, J., Pfannes, K. R., Wanner, G., and Overmann, J. (2006) Chlorobium chlorochromatii sp. nov., a symbiotic green sulfur bacterium isolated from the phototrophic consortium "Chlorochromatium aggregatum", *Arch Microbiol* **185**, 363-372
36. Heising, S., Richter, L., Ludwig, W., and Schink, B. (1999) Chlorobium ferrooxidans sp. nov., a phototrophic green sulfur bacterium that oxidizes ferrous iron in coculture with a "Geospirillum" sp. strain, *Arch Microbiol* **172**, 116-124
37. Meyer, T. E., and Cusanovich, M. A. (2003) Discovery and characterization of electron transfer proteins in the photosynthetic bacteria, *Photosynth Res* **76**, 111-126

38. Tamura, K., Dudley, J., Nei, M., and Kumar, S. (2007) MEGA4: Molecular Evolutionary Genetics Analysis (MEGA) software version 4.0, *Mol Biol Evol* **24**, 1596-1599

39. Higuchi, M., Hirano, Y., Kimura, Y., Oh-oka, H., Miki, K., and Wang, Z. Y. (2009) Overexpression, characterization, and crystallization of the functional domain of cytochrome c(z) from Chlorobium tepidum, *Photosynth Res* **102**, 77-84

40. Hirano, Y., Higuchi, M., Azai, C., Oh-Oka, H., Miki, K., and Wang, Z. Y. (2010) Crystal structure of the electron carrier domain of the reaction center cytochrome c(z) subunit from green photosynthetic bacterium Chlorobium tepidum, *J Mol Biol* **397**, 1175-1187

CHAPTER III

Molecular Biological Approaches toward the Elucidation of the Electron Transfer Pathway in the Photosynthetic Reaction Center Complex of *Chlorobaculum tepidum*

Summary

A rapid isolation method and a gene manipulation method has been required for structural and functional analyses at a molecular level of the homodimeric type I photosynthetic reaction center (RC) complex. The author constructed the green sulfur bacterium *Cba. tepidum* mutant in which the *6xHis-tag-pscA* gene encoding the His-tagged RC core protein was incorporated into a coding region of the *recA* gene, causing the duplication of *pscA* gene concomitantly with the disruption of the *recA* gene. The inactivation of the *recA* gene strongly suppressed homologous recombination in *Cba. tepidum*. Although the mutant expressed both non- and His-tagged RC core proteins, the highly pure and photoactive His-tagged RC complex was isolated in one-step by Ni^{2+}-affinity chromatography. The LC-MS/MS analysis revealed that the His-tagged RC complex was a mixture of the His-tagged homodimer and non-/His-tagged heterodimer. Furthermore, low-temperature ESR analyses indicated that there were a series of electron transfer components, iron-sulfur centers and quinones, in that complex. In this chapter, the author proposes "the *pscA* gene duplication method" as the most promising method for a site-directed mutagenesis of the homodimeric RC including intentional heterodimerization.

Introduction

Photosynthetic reaction centers (RCs) are pigment-associated membrane protein complexes which produce energized electrons through a series of redox reactions driven by a capture of solar energy. All RCs so far found in photosynthetic organisms have been classified into two types based on their terminal electron acceptors: type I (Fe-S-type) and type II (quinone-type) RCs [1]. Oxygenic cyanobacteria and chloroplasts of plants and algae utilize both of them, photosystem (PS) I and II, which form the linear electron transport pathway through the cytochrome (cyt) b_6f complex, while all anoxygenic photosynthetic bacteria use only one type of them. Purple photosynthetic bacteria and filamentous anoxygenic photosynthetic bacteria have type II RCs which do not evolve oxygen. Green sulfur bacteria and heliobacteria, which are strictly anaerobic photosynthetic bacteria, have type I RCs. Unlike all other RCs, their RCs consist of two identical core polypeptides, thus called "homodimeric" type I RCs [2,3].

Crystal structures of the "heterodimeric" type I and II RCs, which consist of a set of two almost identical, but partially different core polypeptides, clarified that all of their core polypeptides form quite similar heterodimers sharing the common folding motif of membrane-spanning α-helices as well as the spatial configuration of electron transfer (ET) components [1]. Those ET components make up two symmetrically-arranged ET chains along a pseudo-C_2 axis parallel to the membrane normal, while ET reactions itself occur via only one of two chains in all of heterodimeric type I and II RCs [1,4-6]. This functional asymmetry is thought to be due to the heterogeneity of local environments on two chains provided by heterodimeric core protein. These heterodimeric RCs would be originated from a common homodimeric ancestor whose two electron transfer chains are equally redox active [7]. From that point of view, the detail structural and functional information of homodimeric type I RCs will lead to understandings of the mechanisms and evolution of RCs due to

retaining the ancestral features, homodimeric structures. However, the information about ET pathways as well as its molecular organization in green sulfur bacterial and heliobacterial RCs is very scarce due to the difficulty in large-scale preparation and spectroscopic analyses of them. The main reason for this lies in its extreme instability under oxygenic conditions where iron-sulfur (Fe-S) centers are easily destroyed [2,3].

The green sulfur bacterial RC complex is composed of four subunits: PscA, PscB, PscC, PscD, and the Fenna-Mathews-Olson (FMO) protein [2]. A pair of PscA makes up a homodimeric core protein which contains the primary electron donor, P840; the primary electron acceptor (A_0), Chl a_{PD}; and the interpolypeptide Fe-S centers, F_X. PscB is a functional homologue of PsaC of PS I, binding two Fe-S centers which serve as the terminal electron acceptors, F_A and F_B. But, they are different in amino acid sequences as well as association properties with the RC [8]. PscC is a unique subunit of green sulfur bacterial RC complex, which is also called cyt c_z. Cyt c_z has three membrane-spanning α-helices in its N-terminus, and binds a *c*-type heme in its C-terminal water-soluble domain. Two cyt c_z are tightly bound to the RC complex and serve as the direct electron donor to the photooxidized P840 [9,10]. That electron donation rate extraordinarily depends on solvent viscosity due to the fluctuation of the C-terminal domain [11]. FMO is the BChl *a* containing protein bridging the excitation energy transfer from the chlorosome, which is an extramembranous antenna system, to the RC core complex [7]. Three FMO form a functional trimer with each monomer binding 7 or 8 BChl *a* [12,13]. PscD is required for the efficient energy transfer from the chlorosome to the RC via FMO protein, but not for photosynthetic growth [14]. Unlike these unambiguous identifications of biochemical components in the green sulfur bacterial RC complex, the existence of quinone molecules which function as a secondary electron acceptor (A_1) in all other kinds of RCs is still controversial [2]. In the case of heliobacteria, the transient ESR signal of $P800^+A_1^-$ with A/E/A/E pattern has been obtained under similar experimental condition in the RC core complex of heliobacterium

Heliobacterium modesticaldum [15]. Although menaquinone molecules have been present in some preparations of green sulfur bacterial RC [16,17], there is no evidence for its function as secondary electron acceptor (A_1); no flash-induced transient reduction signal of menaquinone has been observed [17,18].

Molecular genetic methods are thus expected to be the most promising approach to resolve the issues. In the case of heterodimeric type I and type II RCs, there have been many successful reports of site-directed mutagenesis to the RC core proteins (reviewed in [5,6,19]). For example, in the purple bacterial RC, the spin distribution and also redox potential of the primary electron donor have been modified by substitution of the leucine proximal to the BChl *a* [20]. In other instances, the substitutions of the axial ligand for the primary electron donor have been reported in all three types of heterodimeric RC [21-23]. In the case of the homodimeric type I RC, the meso-thermophilic green sulfur bacterium *Cba. tepidum* is amenable to a genetic manipulation and the information of its genome sequences is available [24-26]; however, any mutant strain having the mutated RC core protein has never been obtained so far, presumably because of its lethal effect. The author thus proposes another strategy to obtain any mutated RC complex, "the *pscA* gene duplication method"; the *tag-pscA* gene encoding the RC core protein with an affinity tag attached to its N-terminus is incorporated into the *recA* locus, which causes the disruption of the *recA* gene concomitantly with the duplication of the *pscA* gene (Figure III-1). This strategy includes two different ideas. First, since the *recA* gene is responsible for homologous DNA recombination and repair [27], its disruption mutant could be a suitable host for the expression of externally incorporated homologous genes. In various bacterial strains, RecA protein triggers SOS response to DNA damage by its protease activity specific to LexA protein which is the direct repressor of SOS genes including the *recA* gene [28]. However, there is neither any typical LexA homologue in the *Cba. tepidum* genome nor LexA-binding consensus sequences, SOS-box or LexA-box, in upstream region of the *recA* gene [28]. Thus, the disruption of the

Cba. tepidum recA gene is expected to affect only on homologous DNA recombination system, but not on response system to DNA damage. Second, since the authentic *pscA* gene expresses the wild-type RC core protein, the mutant expressing the mutagenized *tag-pscA* gene is expected to grow even in the presence of nonfunctional RC complex. The mutated RC complex would be obtained by a specific adsorption to the affinity column. Another usefulness of the *pscA* gene duplication is a method for the intentional heterodimerization of the homodimeric RC. According to the *pscA* gene duplication, any given mutation is supposed to be only on the His-tagged PscA. In principle, it is thus possible to construct the heterodimeric RC that is intentionally changed from the homodimeric one with any site-directed mutation of interest (Figure III-1, lower).

The successful *pscA* gene duplication requires two conditions. First, the disruption of the *recA* gene has to cause a deficiency the homologous recombination in the *Cba. tepidum*, but not affect the structure and function of its RC complex. According to the whole genome analysis of *Cba. tepidum*, no other *orf* but *CT1930* is expected to be the *recA* gene [26]. Since any *recA*-disruption mutant of *Cba. tepidum* has never been isolated so far, the effects on the homologous recombination as well as the photosynthetic system should be investigated in the *Cba. tepidum*. Second, the affinity tag must be available for isolation of the *Cba. tepidum* RC complex. The successful isolation of the tagged RC complex is reported in all three kinds of heterodimeric RCs [29-37], but not in any homodimeric RC. In this study, as a model case of the *pscA* gene duplication, the author introduced the *6xHis-tag-pscA* gene instead of the mutagenized one and succeeded in one-step purification of the highly-photoactive His-tagged RC complex containing a series of electron transfer components. Furthermore, the constructed mutant expressed not only the His-tagged PscA homodimer but also non-/His-tagged PscA heterodimer.

Experimental procedures

Strains and culture conditions

The strain WT2321 [38] of *Cba. tepidum* was used as the wild-type strain in this study. All *Cba. tepidum* strains were grown anaerobically in liquid CL media or solid CP media as previously described [24]. Gentamicin was added to medium at a final concentration of 30 μg ml^{-1} as required to select mutant cells. The growth temperature was routinely set at 40ºC to prevent thermal denaturation of the antibiotic resistance gene products. Growth chamber was illuminated at approximately 30 μmole photons m^{-2} s^{-1} by incandescent lamps.

Chemically competent *Escherichia coli* DH5α cells were used as a host for routine molecular biological procedures. 100 μg ml^{-1} of ampicillin, 20 μg ml^{-1} of chloramphenicol and 10 μg ml^{-1} of gentamicin were used to select *E. coli* cells with desired plasmid.

Construction of the plasmid for inactivation of the Cba. tepidum recA gene

Sequences of primers used for PCRs in present study are shown in Table III-1. A 5'-upstream region (1 kbp) of the *Cba. tepidum recA* gene (*CT1930*) were amplified by PCR with recA-4105F and recA-5104R primers, and a 3'-end and downstream region (1 kbp) were amplified with recA-2203F primer and recA-3208R primers. They were sequentially cloned into pKF3 (TaKaRa Bio Inc.) with *Stu*I and *Bam*HI for the 5'-upstream region fragment, and *Sma*I and *Sph*I for the 3'-upstream region fragment, yielding plasmid pKF3-ΔrecA. A 0.8 kbp fragment containing a gentamicin resistance gene, *aacC1* gene, which was obtained from pUCGM [39] by *Sac*II digestion followed by blunting and *Bam*HI digestion, was inserted between *Bam*HI and *Sma*I sites of pKF3-ΔrecA, yielding plasmid pKF3-ΔrecA::aacC1. A 2.8 kbp *Stu*I fragment of pKF3-ΔrecA::aacC1 was ligated with a *Sma*I digest of pHP45 [40] obtaining plasmid pHP45-ΔrecA::aacC1. Sufficient amount of pHP45-ΔrecA::aacC1

prepared from a large scale cultures was linearized with *Ahd*I and used for a transformation of *Cba. tepidum*.

Construction DNA for insertion of the 6xHis-tag-pscA gene into the recA locus

When PscA proteins seemed to be highly produced in *E. coli*, any attempt to clone a full-length *Cba. tepidum pscA* gene was unsuccessful, probably because PscA was potentially toxic to *E. coli*. Therefore, all plasmid constructions involving cloning of the *pscA* gene were performed under limited conditions in which transcription of *pscA* gene was completely or strongly suppressed. To add a His-tag to the N-terminus of PscA, a 3.1 kbp fragment containing a *Cba. tepidum pscAB* gene cluster were amplified by PCR using pscB-948F and pscA-4070BR, and cloned into pET15b (Novagen) with *Bam*HI and *Blp*I in proper reading frame, yielding plasmid pHisAB15b. Another fragment amplified with pscB-1081F and pscA-4435R, which contained a putative promoter as well as the *pscAB* genes, was cloned into the blunt-ended *Bam*HI site of pHP45, yielding plasmid pHP45-AB-P. Using pHP45-AB-P as a template DNA, a 5.7 kbp fragment was amplified by PCR with pscA-4072F and pscA-4070R. After digestion with *Nco*I and *Bgl*II, an amplified fragment was ligated with a 0.3 kbp *Nco*I-*Bgl*II fragment of pHisAB15b, yielding plasmid pHP45-HisAB-P. A 3.5 kbp *Sma*I fragment of pHP45-HisAB-P was inserted into the *Sma*I site of pHP45-ΔrecA::aacC1, as the *6xHis-tag-pscAB* gene cluster and the *aacC1* gene were transcribed in the same direction. However, since all resultant plasmids had a nonsense mutation in the *pscA* coding sequence, megaprimer PCR [41] was employed to obtain a DNA construct with the correct sequence. Using one of the mutated plasmid, pHP45-HisA*B-P, megaprimers were synthesized by PCR with pscA-4095F and HP45-blaF for 5'-flanking region, and pscB-1410R and HP45-ropR for 3'-flanking region. Megaprimer PCR was then carried out according to the previously reported method [41] in a reaction mixture that contained the two gel-purified megaprimers, recA-2203F primer, recA-5104R primer, and pHP45-HisAB-PT. A 6.2 kbp amplification

product with the correct sequence was gel-purified and directly used for a transformation of *Cba. tepidum*.

Transformation of Cba. tepidum and analytical PCR

Natural transformation was performed by the previously described method [24]. Transformants were selected on gentamicin-containing CP plates and restreaked three times onto selective CP plates. To monitor the segregation of wild-type and mutant alleles in each isolation step, analytical PCR was carried out directly using individual colonies as templates (see below). Fully-segregated transformant colonies were inoculated into fresh CL media containing gentamicin and cultivated until early stationary phase. After checking the segregations again, frozen stocks were prepared and used as original mutant strains for further investigations.

Genomic DNA preparation and analytical PCR were performed basically as previously described [14]. For rough tests, a colony or a cell suspension was used as a template for the PCR. A colony was picked with a toothpick and directly soaked into the PCR reaction mixture. When using a cell suspension as a template, cells were harvested by centrifugation and resuspended in water, and then directly added to a PCR reaction mixture at final 50-fold dilution [41].

Steady-state spectral measurement

The steady-state fluorescence emission and absorption spectra were measured with a spectrofluorophotometer RF-1500 (Shimadzu) and spectrophotometer UV-3101PC (Shimadzu), respectively. When measuring the whole cell fluorescence emission and absorbance spectra, the samples were prepared as previously described [14].

Measurement of homologous recombination frequency of Cba. tepidum

The homologous recombination frequency of *C. tepidum* was estimated as the insertional inactivation frequency of the *bchU* gene by the *aadA* streptomycin-spectinomycin resistance cassette [42]. After transformations of the wild-type and *recA* mutant, each frequency was calculated by counting colonies on both selective and non-selective plates. The mean values and standard deviations in the Table III-2 were obtained from at least three independent experiments.

Preparation of the Cba. tepidum His-tagged RC complex

The *Cba. tepidum* cells expressing the His-tagged RC complex were grown in 1.2-liter medium bottles. After 2 days of cultivation, cells were harvested by centrifugations at 12,000*g* for 5 min and stored at -80ºC until use. Unless otherwise indicated, the subsequent processes were carried out in an anaerobic chamber (Coy Laboratory products) at room temperature. All buffers and resins used for preparation were fully degassed by standing in an anaerobic chamber overnight and supplemented with 10 mM L-cysteine and/or 2 mM dithiothreitol for appropriate reductive conditions. Preparation of chlorosome-containing membranes and subsequent solubilization of them were carried out basically as previously reported [43] with a modification as follows: the membranes at 2.5 mg BChl (*a*+*c*) ml^{-1} were solubilized with 50 mM Tris-HCl (pH 8.0), 30 mM n-octyl-β-D-glucopyranoside (β-OG, Sigma), 300 mM NaCl, 2 mM dithiothreitol, and protease inhibitors. After removing unsolubilized materials by centrifugation at 110,000*g* for 1 h, 200 ml of the resultant supernatant was mixed with 60 ml of 50% suspension of the Ni^{2+}-immobilized sepharose resin, His-Accept (Nacalai tesque), which had been pre-equilibrated with the same buffer as used in solubilization. The mixture was gently shaken in a conical flask with a tilt shaker for 1 h, and loaded into an empty column. The

column was washed with 200 ml of wash buffer [50 mM Tris-HCl (pH 8.0), 2 mM sucrose monolaurate (SM-1200, Dojindo laboratories), 300 mM NaCl, 10 mM imidazole, and 2 mM dithiothreitol] to exchange the detergent. The His-tagged RC complex was eluted with elution buffer [50 mM Tris-HCl (pH 8.0), 2 mM sucrose monolaurate, 300 mM NaCl, 300 mM imidazole, and 2 mM dithiothreitol]. For the ESR measurements and further purification by gel filtration, the eluted fraction was concentrated by ultrafiltration with a 15 kDa cutoff membrane (Minicon concentrator, Millipore). SDS-PAGE was performed according to Laemmli's method [44]. The separated protein bands were stained with Coomassie Brilliant Blue.

Time-resolved optical spectroscopy

Flash-induced absorbance changes were measured with a home-built single-beam spectrophotometer. Samples in an air-tight cuvette (1 cm × 1 cm) were continuously probed with a single-wavelength measuring beam isolated from a tungsten-halogen lamp with a 20 cm monochromator. Excitation flashes (decayed within 1 ms) were provided by a Xe flash lamp filtered by suitable band-pass filters, and entered the sample from a perpendicular direction to the measuring beam. The sample was protected from the measuring beam by a shutter until 200 ms prior to the excitation flash. The transmitted measuring beam from the sample was detected by a photomultiplier through suitable long-pass filters and a 10 cm monochromator. The detected signal was amplified by an operational amplifier and stored in a digital oscilloscope. Collected signals were averaged 32-128 scans as required.

nLC-MS/MS

Approx. 4 μM of RC complexes (equal to approx. 0.4 μg/μl of PscA protein) was digested with 20 ng/μl of trypsin at 37°C for overnight under undenaturing condition [50 mM

Tris-HCl (pH 8.0), 2 mM sucrose monolaurate]. The resultant peptides were separated by EASY-nLC (Proxeon, Denmark) and analyzed its mass spectra with micrOTOF-QII (Bruker Daltonics, USA). 10 μl of 1/20-30 diluted trypsin-digested sample was injected into the pre-column, NS-MP-10 BioSphere C18 (5 μm particle size, 120-Å pore size, 100 μm inner siameter, 20 mm length; NanoSeparations, Netherland), with 10 μl/min flow rate using autosampler and washed pre-column with Solution A [0.1% formic acid in double distilled water, HPLC grade]. The desalted peptides were subsequently separated by analytical column, NS-AC-10-C18 BioSphere C18 (5 μm particle size, 120-Å pore size, 75 μm inner diameter, 100 mm length; NanoSeparations, Netherland), at 200 nl/min flow rate. The solvent gradient was started at 5% Solution B [0.1% formic acid in acetonitrile, HPLC grade] and linearly increase to 50% Solution B for 60 min. The separated peptides on a C18 column were introduced into the micrOTOF-QII mass spectrometer with nanoelectrospray ionization under positive mode. The capillary voltage was -4.5 kV and drying gas temperature was set 200°C. The collision energy of the quadrupole for MS/MS fragmentation of each peptide using Ar gas was set from 20-40 eV. Acquired mass spectra in micrOTOF-QII were processed by DataAnalysis 3.4 and Biotools 3.2 (Bruker Daltons).

EPR measurements

Low-temperature EPR measurements were performed using a Bruker ESP-300E spectrometer (Bruker Biospin) equipped with a liquid-helium flow cryostat and a temperature-control system (CF935, Oxford Instruments). Continuous white light for photoaccumulation was provided from a tungsten-halogen lamp through heat-cut glass filters. A Xe flash lamp was used for measurements of flash-induced EPR signals.

Results

Inactivation of the recA gene and insertion of the 6xHis-tag-pscAB gene cluster

Two different *C. tepidum* mutants lacking a functional *recA* (*CT1930*) gene were constructed by the natural transformation method as previously described [24] (Figure III-2A). The *recA::aacC1* strain, in which the *aacC1* gentamicin resistance cassette was inserted into the *recA* region, was used as a control. In another mutant, the *recA::(HisAB-aacC1)* strain, the *6xHis-tag-pscAB* gene cluster was additionally inserted upstream of the *aacC1* cassette. The *6xHis-tag-pscAB* construct contains a putative 365-bp promotor region upstream of the intrinsic *pscAB* gene cluster in order to express the N-terminally His_6-tagged PscA along with the authentic PscA *in vivo*. Segregations of the wild-type and mutant alleles were confirmed by the PCR method using the *recA*-inside and -outside primer set to amplify the *recA* locus (Figure III-2B). No fragment corresponding to the wild-type allele was detected in the amplified products from two mutant cells. The amplified products from the *recA::aacC1* cells were approximately 100-bp smaller than those from the wild-type cells. This size corresponds to the difference in the length between the deleted *recA* gene and the inserted *aacC1* cassette. On the other hand, the amplified products from the *recA::(HisAB-aacC1)* cells were approximately 3.4 kbp larger than those from the *recA::aacC1* cells because of additional insertion of the *6xHis-tag-pscAB* gene cluster. Direct sequencing of these product revealed no unintended alteration of nucleotides, indicating that the *recA* gene was insertionally inactivated with the desired constructs in these two mutants.

Duplication of the *pscAB* gene cluster in the *recA::(HisAB-aacC1)* strain was further confirmed by the PCR method using the *pscA* up-stream primer set (Figure III-2A). The 450-bp fragments amplified from the wild-type, *recA::aacC1* and *recA::(HisAB-aacC1)* cells were derived from the authentic *pscAB* gene cluster (Figure III-2B, panel b). However, an

additional 520-bp fragment was also found only from the *recA::(HisAB-aacC1)* cells. This fragment corresponded in size to the extended region derived from the *6xHis-tag-pscAB* construct inserted into the *recA* locus. These results clearly indicated that the *pscAB* gene cluster was successfully duplicated in the *recA::(HisAB-aacC1)* strain. The *6xHis-tag-pscAB* construct was stably retained in the genome of the *recA::(HisAB-aacC1)* strain since the same PCR results were reproducibly obtained from cultures after several generations (data not shown).

Phenotypes of Cba. tepidum mutant lacking the recA gene

Both *recA::aacC1* and *recA::(HisAB-aacC1)* strains could grow photosynthetically, and showed essentially the same whole cell absorption and fluorescence emission spectra as the wild-type strain (data not shown). Therefore, there seemed to be no serious effect on the photosynthetic system of the *C. tepidum* by the disruption of the *recA* gene as well as the insertion of the *6xHis-tag-pscAB* construct into the *recA* region. The responsibility of the *CT1930* for the homologous recombination was further examined by estimating transformation frequencies of the wild-type and *recA::aacC1* strains. When the wild-type strain was used as a host, about 1% of the total cells could be transformed into the *bchU*$^-$ strain (Table III-2). In contrast, when the *recA::aacC1* strain was used as a host, its transformation frequency was found to be much smaller by 10^{-5}-10^{-6} than the wild type. Since the BchU-less mutant appeared to exhibit a normal phenotype in its growth compared to the wild type [42], the significant decrease of the transformation frequency obtained in the *recA::aacC1* strain was attributable to the complete deficiency of the double-crossover DNA recombination. This result clearly indicates that the *CT1930* is involved in the homologous recombination and that no *orf* other than the *CT1930* would serve as a *recA*-like gene in the *C. tepidum* [26].

Purification of the His-tagged RC complex

A crude fraction containing the RC complex was obtained after extraction with β-OG from chlorosome-containing membranes of the *recA::(HisAB-aacC1)* strain, followed by its isolation using a Ni^{2+} affinity chromatography, as described in experimental procedures. As expected, dark green components were adsorbed onto the Ni^{2+}-immobilized resin. Most of them were retained after a wash procedure with 10 mM imidazole and then eluted with 300 mM imidazole. The eluate contained four major polypeptides of the green sulfur bacterial RC [2], that is, PscA, FMO, PscB, and PscC, although no band corresponding in the apparent molecular mass to the PscD appeared to be observed (Figure III-3A, lane 1). In fact, the further purification step by a gel filtration chromatography with Sephacryl S-300 revealed that these four polypeptides were coeluted from the column and formed a stable complex as the His-tagged RC complex (Figure III-3A, lane 2). A 40-60% fraction of the total extracted RC was supposed to be adsorbed onto the resin, given the absorbance difference between the extract and non-adsorbed fraction. Contrary to this, no RC complex extracted from the wild-type membrane bound to the immobilized Ni^{2+} resin (data not shown). Therefore, the His-tagged RC complex was successfully expressed in the *recA::(HisAB-aacC1)* strain and could be obtained in a single step as well as considerably high purity by a Ni^{2+} affinity chromatography.

The absorption spectrum and the chemically induced oxidized-minus-reduced difference spectrum of the His-tagged RC complex are shown in Figure III-4. There were three major peaks at 815, 671, and 601 nm in the absorption spectrum, which were attributed to characteristic Q bands of BChl *a* and Chl a_{PD} in green sulfur bacterial RC complex [43]. The shoulder around 835 nm, which was ascribable to a specific absorption for a special dimmer of BChl *a* molecules (P840) in the RC core protein, was also observed. The ratio of the absorbance at 815 nm to that at 835 nm was calculated to be 2.2-2.6, which was similar to that of 1FMO-RCC complex comprising a monomer of FMO protein and a RC core protein

[45]. The chemically induced oxidized-minus-reduced difference spectrum showed the negative peak at 830 nm with a shoulder at 840 nm, which was attributed to the oxidation of P840. Assuming the extinction coefficient for BChl *a* at Q_y peak and the difference extinction coefficient for P840 at 830 nm to be 100 mM^{-1} cm^{-1} [46], the apparent antenna size of the present RC preparation was estimated to be 26 BChl *a*/P840, which was also consistent with the estimated value from the 1FMO-RCC complex. The electric-field-induced absorbance change of Chl a_{PD} exhibited an isosbestic point at 665 nm.

The small absorption peak at 551 nm, which disappeared after addition of excess ferricyanide, was attributed to the α peak of cytochrome c_z. Its wavelength was slightly different from 552 nm in a similar RC complex solubilized by the same detergents as in the present study (9), but was identical to that in the one obtained by solubilization with Triton X-100 (18). Cytochrome c_z seems to show its α-peak wavelength from 551- to 553 nm due to some structural modification and/or distortion [47]. The C-terminal soluble domain of cytochrome c_z, which was overexpressed in *Escherichia coli*, exhibited its α peak at 550.5 nm [48] and had almost the same redox potential as in membranes [49]. Assuming the difference extinction coefficient for *c*-type heme of cytochrome c_z at 551 nm to be 20 mM^{-1} cm^{-1} [50], the amplitude of the negative absorption peak at 551 nm in the chemically redox difference spectrum indicated that about 1.7 hemes per P840 were present in the His-tagged RC preparation.

Flash-induced absorption changes of P840 in the His-tagged RC complex

The oxidized primary electron donor, $P840^+$, immediately formed after the flash excitation, is rereduced by cytochrome c_z at the time constant ($t_{1/e}$) of 150 μs in the isolated RC complex at 295 K, and its rereduction rate becomes slower in highly viscous reaction media [9,11]. In the absence of glycerol, the flash-induced $P840^+$ was so rapidly rereduced by cytochrome c_z that its rereduction kinetics could not be fully followed at the present time

resolution of ca. 1 ms and its signal amplitude was apparently too small to be detected (Figure III-3B, trace a). Contrary to this, at least the 10-fold greater intensity of the photooxidized $P840^+$ was observed in the presence of 60% glycerol, which exhibited a monophasic decay kinetics with a relatively larger $t_{1/e}$ = 65 ms (Figure III-3B, trace b). This kinetics seemed to be a mixture of two different ET processes to the $P840^+$; one was from cytochrome c_z and another was from F_A/F_B, because they had been shown to give almost the same time constant in the presence of 60% glycerol at 295 K [11]. The flash-induced difference absorption spectrum at 1 ms after the flash excitation (Figure III-5, open circles) was almost identical to the chemically induced redox difference spectrum of $P840^+$ (see Figure III-4, trace b). The decay associated spectrum with $t_{1/e}$ = 60 ms, which was obtained by a global analysis, was also reasonably fitted to the difference spectrum at 1 ms (Figure III-5, dotted line). These data including subunit compositions described above suggest that the His-tagged RC complex contains all ET components essential for the light-energy conversion reaction to produce reducing power.

LC-MS/MS analyses of the His-tagged RC preparation

In principle, the *recA::(HisAB-aacC1)* mutant cells can expess three kinds of RC complexes: the non-tagged PscA homodimer, the His-tagged PscA homodimer, and the non-/His-tagged PscA heterodimer (Figure III-1, lower). The His-tagged RC preparation obtained in the present study would thus be a mixture of the His-tagged PscA homodimer and the non-/His-tagged PscA heterodimer. This heterogeneity was explored by the LC-MS/MS analysis of peptides produced by a tryptic digestion of the His-tagged RC preparation under non-denaturing conditions (Figure III-6 and III-7A). The N-terminal tryptic peptide of the His-tagged PscA was detected as the 1767.86 Da fragment (m/z = 884.932, accuracy < 10 ppm) at the retention time of 8.2 min in the LC-MS analysis, whose product ion spectrum by the tandem mass spectrometry (MS/MS) further confirmed that it corresponded to peptide

2-13 (GSSHHHHHHSSGLVPR) in the His-tagged PscA (Figure III-8). On the other hand, no ion peak corresponding to every possible N-terminal peptide of the non-tagged PscA could be identified at all in the MS/MS data. There were two conceivable explanations for this: 1) the non-tagged PscA polypeptide was never present in the His-tagged RC preparation, or 2) the amount of the N-terminal peptide recovered from a tryptic digestion of the non-tagged PscA polypeptide was too small to be analyzed by the MS/MS.

In order to resolve this issue, we tried to determine the retention time and the accurate mass of the N-terminal tryptic peptide of the non-tagged PscA using the RC complex isolated from the wild-type strain by our previous methods [9]. The LC-MS/MS analysis revealed that peptide 2-16 (AEQVKPAGVKPK) in the authentic PscA, which was eluted at 17.8 min from the C18 column, was acetylated at the N-terminal alanine residue, giving a molecular mass of 1292.74 Da (accuracy < 10 ppm) (Figure III-7B, upper panel and III-9). This fragment was regarded as the sole N-terminal tryptic peptide of the non-tagged PscA because no peptide fragment subjected to any other potential modification, e.g., an oxidation, formylation, and/or acetylation of the first methionine residue, was never detected. A small but obvious peak with the same mass and retention time could be detected in the tryptic digests of the His-tagged RC preparation in the LC-MS analysis (Figure III-7B, lower panel). This result clearly indicated that the *recA::(HisAB-aacC1)* mutant cells expressed the non-/His-tagged PscA heterodimeric RC complex in addition to the His-tagged PscA homodimeric one.

The amounts of these two kinds of RC complexes in the His-tagged RC preparation were roughly estimated by comparing the intensity of the ion peak corresponding to the non-tagged N-terminal peptide from the His-tagged preparation with that from the authentic RC one. The intensity of peptide 214-225 (Figure III-6), which showed a molecular mass of 1240.609 Da (accuracy < 10 ppm) and was reproducibly detected in both authentic and His-tagged RC preparations (data not shown), was used as the internal standard to calculate a

relative amount of each preparation. The non-tagged PscA polypeptide content in the His-tagged RC preparation was thus estimated to be 8.1 ± 1.7% compared to that in the authentic RC one in three independent measurements. A similar estimation (approx. 10%) was also obtained by the SDS-PAGE analysis; non- and His-tagged PscA polypeptides could be almost, but not quite separated on the gel containing a high concentration of urea to improve its resolution (data not shown). Since non-tagged PscA polypeptide in the His-tagged RC preparation should be derived only from the non-/His-tagged PscA heterodimer, the estimated value implies that the artificial heterodimeric RC complex constitutes about one fifth of the total amount in this preparation.

Light-induced ESR signals of Fe-S centers in the His-tagged RC complex

The ESR measurements were carried out to clarify the intactness of terminal iron-sulfur centers in the His-tagged RC fraction. The illumination for 1 min at 5 K induced a irreversible signal of the reduced Fe-S center with apparent *g*-values of g_z = 2.079, g_y = 1.901, and g_x = 1.863 when measured at 10 K (Figure III-10A). Their *g*-values and temperature dependence (data not shown) closely resembled those of the center F_B^- reported in isolated RC complexes [43,51] as well as membranes [52].

After the illumination for 20 min at 210 K followed by the subsequent cooling to 5 K under the illumination, two other signals with apparent *g*-values of g_x = 1.886 and g_y = 1.948 at 10 K and g_x = 1.754 and g_y = 1.928 at 5 K, respectively, were observed (Figure III-10B). These signals exhibited different temperature dependences (Figure III-10C). The former signal could be assigned to the spin-interacting state of F_A^-/F_B^- and the latter one to the center F_X^- as previously characterized in both membranes [43,51,53] and isolated RC complexes [14,52,53]. All of the above data indicated that there was a complete set of photoreducible Fe-S centers, namely, F_X, F_A and F_B, on the acceptor side in the His-tagged RC fraction.

Photoaccumulated ESR signal of semiquinone radical in the His-tagged RC complex

In order to examine whether quinone molecules were served as an electron acceptor, the photoaccumulated ESR signal of semiquinone radicals was measured, as previously reported in the membrane of *C. parvum* [16] and the RC core complex of *H. modesticaldum* [15]. In the presence of dithionite, the illumination for 1 min at 5 K using the sample frozen in the dark induced an irreversible ESR signal with the apparent *g*-value of $g = 2.0043$ when measured at 30K (Figure III-11, solid line). This signal was attributable mainly to the $P840^+$ in addition to a tiny contribution by semiquinone radical. Contrary to this, the same mesurement using the photoaccumulated sample prepared as in Figure III-10B slightly shifted the *g*-value of the signal to a lower magnetic field at $g = 2.0049$ and broadened its bandwidth (Figure III-11, broken line). The difference ESR spectrum between them showed the *g*-value of $g = 2.0066$ with the broad bandwidth of 12 G (Figure III-11, short-dotted line), indicating that quinone molecules, which could be photoaccumulated in the present conditions, were contained in the His-tagged RC complex.

Spin-polarized ESR signals of the charge-separated state $P840^+F_X^-$

The electron transfer reactions within the His-tagged RC complex were investigated at cryogenic temperature by flash-induced transient ESR measurements. Figure III-12A shows flash-induced transient ESR spectra of the His-tagged RC complex at 10 K in the presence of dithionite. The spin-polarized ESR signal with E/A (E, emission; A, absorption) pattern around 339.4 mT was observed just after the flash excitation and completely converted into the stable ESR signal derived only from $P840^+$ within 4 ms. Almost the same spin-polarized signal was also reported in the membrane preparation and the isolated RC complex of *C. tepidum* at 100 K and assigned to the charge-separated state of $P840^+F_X^-$ [18]. This clearly indicated that the electron transfer reaction from the P840 to F_X proceeded so rapidly in the *Chlorobium* RC complex even at cryogenic temperature as to detect the

spin-polarized signal formed between them. The kinetics at a positive peak of 339.4 mT (Figure III-12A, inset) exhibited a biphasic decay with time constants ($t_{1/e}$) of 1.1, and 7.5 ms whose contributions were estimated to be 75% and 25%, respectively. The fast phase was assigned to the spin relaxation time of the spin-polarized state of $P840^{+}F_X^{-}$ [18]. The slow phase would thus be attributable to the charge recombination rate between $P840^{+}$ and F_X^{-} at 10 K. On the other hand, the transient ESR measurement of the chlorosome-free membrane, which was isolated from the wild-type strain according to the previously described method [10], exhibited almost identical spectral and kinetic properties to those of the His-tagged RC fraction (Figure III-12B). The His-tagged RC complex, therefore, seems to have intrinsic biophysical nature so far described in the wild-type one and could be a useful sample to be prepared easily and in large amount as well.

Discussion

The Cba. tepidum recA mutant as a host for the homologous gene expression

The *recA* gene is involved in homologous recombination to repair the damaged DNA in bacteria [54-56]. Indeed, the disruption of the *C. tepidum recA* gene caused drastic decrease of homologous recombination efficiency (Table III-2). A defect in the *recA*-related repair system is, however, lethal for oxygenic photosynthetic organisms, since an exposure to light produces reactive oxygen radicals including singlet oxygen that would damage chromosomal DNA. The *recA*$^-$ mutant of a cyanobacterium *Synechocystis sp*. PCC6803 accumulated nonviable cells even under low-light intensity (about 10 μmole photons m^{-2} s^{-1}) [56]. In contrast, the mutant of *C. tepidum* was found to be viable judging from colony counts on plates. This may simply imply that no oxidative stress exceeds harmful threshold level in the mutant because *C. tepidum* requires the strictly anaerobic condition for its growth.

A recent study has demonstrated that antioxidant enzymes were constitutively expressed to defense against the oxidative stress in the *C. tepidum* [57]. Other DNA repair system by non-homologous recombination could thus be operative in response to such stress because the phenotype of the mutant was stably maintained after multiple subcultures. Although RecA protein also serves as a trigger for the SOS response to the damaged DNA in many bacterial lineages, the typical RecA-LexA-mediated SOS response system is missing in *C. tepidum* [28]. In conclusion, the *recA*$^-$ strain constructed in the present study would be a desirable host for the stable expression of homologous genes as well as mutated ones those are essential for the photosynthetic growth.

The Cba. tepidum His-tagged RC complex

This is the first report for the affinity purification of green sulfur bacterial RC

complex. The His-tagged RC complex contained a series of functional electron cofactors and exhibited a stable charge separation state between P800 and terminal acceptors F_A/F_B. The addition of $(His)_6$-tag to the N-terminus of PscA was thus effective for a convenient and short-time preparation of the photoactive *C. tepidum* RC complex. Gulis et al. reported a successful purification of PS I by the addition of N-terminal His-tag to PsaA core protein in green alga *Chlamydomonas reinhardtii* [34]. They noted that the N-terminus of PsaA was a desirable portion for the attachment of tags from the point of view of 3D structure; it protrudes to an aqueous phase from membranes and the N-terminal 12 residues are never resolved due to a disorder as seen in the crystal of PS I complex of a cyanobacterium *Thermosynechococcus elongatus*. On the other hand, when the $(His)_6$-tag was attached to the C-terminus of PscA, no RC complex could be adsorbed onto the Ni^{2+}-immobilized resin, presumably because the tag was embedded within complex (data not shown). A similar case was experienced by Tang and Chitnis who failed to attach the $(His)_6$-tag to the C-termini of PsaK and PsaL in cyanobacterium *Synechocystis* sp. PCC6803 [37]. In general, the cytoplsmic/stromal side would be preferable to the periplasmic/lumenal side for the attachment of tags to type I RCs (Table III-3). Especially in green sulfur bacterial RC, the C-teminal water-soluble domain of cytochrome c_z could reduce the accessibility of the tag at the periplasmic/lumen side. In the case of type II RC, successful rapid preparations were achieved by attaching the His-tag not only at the cytoplsmic/stroma side, but also the periplasmic/lumen side. This relationship between RC types and favorable tag-attachment sites might reflect the difference in structure and/or function between each type of RC.

Although the addition of the His-tag did not interfere with the electron transfer activity of RC by all measures, the PscD subunit was not included in the His-tagged RC complex fraction (Figure III-3A). The whole cell fluorescence emission of the *recA::(HisAB-aacC1)* mutant did not show an increase in fluorescence emission like in PscD-less mutant [14] , meaning that the PscD subunit was in the His-tagged RC complex, but

would dissociate during the preparation, especially solubilization of the membranes. Since PscD is estimated to bind to the corresponding side of RC complex to N-terminus of PscA [2,14] , the loss of PscD subunit could be conceivably caused by the change of electrostatic environment around the cytoplasmic side of RC complex due to positive charges of the consecutive 6 histidine residues. Supporting this notion, the His-tagged RC complex had a low content of FMO (1FMO/RC, Figure III-3B and III-4) which also bind to the cytoplasmic side of RC complex [2,7]. However, since PscD would not affect the structure and stability of the RC complex, the loss of PscD subunit would not cause any serious problem on further structural investigations of the His-tagged RC complex. Indeed, the temperature dependence of the spin-interacting ESR signal of F_A^-/F_B^- in present preparation (Figure 6B) was similar to that in membrane of the wild-type rather than the PscD-less mutant whose signal intensity peaks at slightly higher temperature, 12 K [14].

The electron transfer in green sulfur bacterial RC at cryogenic temperature

The author observed the flash-induced spin-polarized ESR signal of $P840^+F_X^-$ in the His-tagged RC complex and the membrane even at cryogenic temperature (Figure III-12). The charge recombination reaction between $P840^+$ and F_X^- was also observed with a time constant of 7.5 ms. This time constant is significantly shorter than that reported in transient ESR signals of *Cba. tepidum* membrane and isolated RC complex at 100 K, $t_{1/e} \sim 30$ ms [18]. A similar temperature dependence has been closely examined in the heliobacterial RC core complex of *Heliobacterium modesticaldum* whose F_X^- lifetime is 12-19 ms at above 200 K, accelerates on cooling, and replaced 3-5 ms at below 150 K [58]. This feature in homodimeric type I RC is completely different from that in PS I [59], in which the charge recombination time is 250 μs at room temperature, slows on cooling and becomes barely detectable below 200 K due to the suppression of the electron transfer from A_1^- and F_X. Another controversy in homodimeric type I RC has been the involvement of quinine as A_1

acceptor in the forward electron transfer. A certain proportion of photoexcited electrons were accumulated on quinones by the preillumination at 200 K in the presence of dithionite (Figure III-11). However, further investigations are required for the elucidation of the functionality of quinones in green sulfur bacterial RC.

A methodological proposal for the site-directed mutagenesis in Cba. tepidum

In this paper, the author examined availability of the *pscA* gene duplication as a mutagenesis method for the *Cba. tepidum* RC (Figure III-1). Our present results clearly demonstrated suitability of the *recA* locus for the introduction of homologous gene and availability of the affinity tag for specific purification of RC complex. In addition, the approximately half of total extracted RCs did not adsorb onto the Ni^{2+}-immobilized resin, indicating that the *recA::(HisAB-aacC1)* mutant strain expressed the non-tagged RC core protein encoded by the authentic *pscA* gene. The non-tagged RC complex is obviously supposed to be same as the wild-type one and retain the proper function, which can complement any growth deficiency suffered due to the nonfunctional mutated RC, affirming the *pscA* gene duplication approach for the construction of the mutated RC. This approach integrating the disruption of *recA* gene and the attachment of affinity tag can be also applicable to purification and biochemical analyses for any other genes, which are likely to play an essential role in *Cba. tepidum*, such as *petCB* genes (*CT0302* and *CT0303*) and *ndh* genes (*CT0766* to *CT0776*) expected to encode homologues of cytochrome *bc* complex and complex I of the respiratory chain, respectively.

Another noteworthy advantage of the *pscA* gene duplication is as a method for construction of the heterodimeric RC with a site-directed mutation (see above). The LC-MS/MS analyses in present study showed that the His-tagged RC preparation contained not only the His-tagged PscA homodimer but also a significant amount of the non-/His-tagged PscA heterodimer (Figure 4B). Thus, construction of the heterodimeric RC is thought to be

really possible by means of the *pscA* gene duplication. However, there are two problems that need to overcome for actual preparation and investigations of the heterodimeric RC. First, since the content of heterodimer in the present His-tagged RC preparation, approx. 15%, is not enough for detailed biochemical and spectroscopic analyses, some improvements for yielding much more heterodimers are required. One possible strategy is regulation of the expression level of the duplicated *pscA* gene. In the *recA::(HisAB-aacC1)* mutant cells, since the *6xHis-tag-pscA* gene could be transcribed by not only the promoter of *pscA* gene but also the endogenous promoter for the *recA* gene (Figure III-1), the expression levels of non-tagged PscA would be lower than that of the His-tagged PscA. This may be improved by driving the authentic *pscA* gene with more effective promoter; however, no promoter sequence analyzed in detail has been available in *Cba. tepidum*. Instead of enhance the expression level of authentic *pscA* gene, a similar improvement can be obtained by same expression levels of two genes at a local point in the cell. This will be achieved by tandemly-arranged wild-type *pscA* and *6xHis-tag-pscA* genes driven with common one promoter. Another reason for lower content of the heterodimer could be a significant loss during the preparation. Indeed, 15-25% of total RCs adsorbed onto the Ni^{2+}-immobilized resin eluted with 10 mM imidazole at the washing stage. Considering that the non-/His-tagged PscA heterodimer has only one His-tag while the His-tagged PscA homodimer has two, the heterodimeric RCs would bind more loosely to the resin than the homodimeric His-tagged RC. Hence, the fraction eluted with 10 mM imidazole might contain the non-/His-tagged PscA heterodimer at higher contents. The improvement strategy for this is related to the second problem.

The second problem in preparation and investigations of the heterodimer is the isolation method for the heterodimeric RC complex. In present study, the His-tagged PscA homodimer and the non-/His-tagged PscA heterodimer could be separated by its affinity to Ni^{2+}, but not completely. The most promising method for complete isolation of the heterodimer is attaching different kinds of affinity tags, such as His-tag and strep-tag, to the

authentic and duplicated *pscA* genes. For example, when the strep-tag and His-tag attach to the authentic and duplicated *pscA* genes, respectively, the Strep-tagged/His-tagged PscA heterodimer can be purified by tandem affinity chromatography using strep-tactin-immobilized resin and Ni^{2+}-immobilized resin. This strategy is also expected to improve yield of the heterodimeric RC because heterodimeric RC complexes in the wash fraction of Ni^{2+}-affinity chromatography can be recovered using the Strep-tag attached to the authentic PscA. Since the His-tag did not cause harmful effect on the structure and function, some small tag similar to His-tag, such as strep-tag [60], would be also available for affinity purification of RC. Indeed, the author has succeeded in constructing the *Cba. tepidum* mutant strains whose authentic *pscA* gene was replaced with *6xHis-tag-pscA* gene or *strep-tag-pscA* gene. These mutants have showed no obvious growth defects and deleterious effects on photosynthetic systems (data not shown). Therefore, in conclusion, the *pscA* gene duplication method would enable us to experimentally explore and investigate mutations that make two symmetric electron transfer pathways asymmetric by the heterodimerization with any given mutation.

Tables

Table III-1: ***Primers used for DNA constructions and analytical PCRs***

Primer name[a]	Sequence[b]
recA-2203F (*Sph*I, *Stu*I)	TTTGCATGCAGGCCTTATTTCTCGCCCTTGTACTCC
recA-3208R	GGGCTGTCGAGTTCGGCATCATC
recA-4105F (*Bam*HI)	TTTGGATCCGTATGGTCCTGGTTTACTGC
recA-5104R	CCTATTCTCATCACCGGTGCAAC
pscA-4070BR (*Bam*HI)	AAAGGATCCGATGGCTGAACAAGTGAAACCC
pscA-4435R	GGTGAAATCGATGTGCATGTC
pscA-4072F (*Nco*I)	TCAGCCATGGTATGTTCTCCTTTGTTTGAACG
pscA-4070R	ATGGCTGAACAAGTGAAACCC
pscA-4095F	TATTTTCAGGTTGAAGAAACCG
pscB-1410R	CTCCGAAAGCCAAGAAGCA
pscB-1081F	CGATTCCTGACTATCTGGCT
pscB-948F (*Blp*I)	AAAGCTCAGCTTTATTCTTTCTGGCCTGTACTGC
HP45-blaF	CAAGGATCTTACCGCTGTTG
HP45-ropR	GCTTACAGACAAGCTGTGAC
recA-inside primers	CGAGCTTTTCAGTGCCATAAC
	CATGTCGTACCGCCCATTC
recA-outside primers	ATTGAGAATCAGTCTGGGCG
	ATTGCGGATGGATTTGGGTG
pscA up-stream primers	GGTGAAATCGATGTGCATGTC[c]
	ATTTGCCTTCGGAGCTGGTG

[a] Restriction enzyme sites attached to primers for cloning are shown in parentheses.

[b] Recognition sequences of restriction enzymes used for DNA constructions are underlined.

[c] This sequence is completely identical to that of pscA-4435R.

Table III-2: ***Comparison of transformation efficiencies for the bchU gene inactivation of between the wild-type and the recA::aacC1 mutant strains of C. tepidum***

Strain	Amount of DNA for the transformation	Number of vial cells (cfu/ml) [a]	Transformation frequency [b]
wild-type	0.1 μg	$5.6 \pm 0.4 \times 10^{9}$	$2.5 \pm 1.2 \times 10^{-4}$
	1 μg	$8.0 \pm 2.0 \times 10^{9}$	$4.9 \pm 1.6 \times 10^{-3}$
	10 μg	$6.2 \pm 2.4 \times 10^{9}$	$1.1 \pm 0.6 \times 10^{-2}$
recA::aacC1	0.1 μg	$4.4 \pm 1.6 \times 10^{9}$	$1.1 \pm 1.9 \times 10^{-9}$ [c]
	1 μg	$9.6 \pm 2.0 \times 10^{9}$	$7.7 \pm 5.7 \times 10^{-9}$ [c]
	10 μg	$6.0 \pm 1.6 \times 10^{9}$	$3.1 \pm 0.6 \times 10^{-8}$ [c]

[a] The number of cells in the liquid culture at late exponential phase.

[b] The ratio of the number of drug-resistant colonies on the selective plate to the total number of colonies (see *Experimental procedures*).

[c] $P < 0.05$, for comparison to the wild-type within the same conditions.

Table III-3: (*His*)$_6$*-tag attachment sites in various kinds of RCs and their membrane topologies*

Topology of the tag position [a]	Type of RC	Attachment site of the His-tag	Comment and Reference
Cytoplasmic/stroma side	Purple bacterial RC	C-terminus of H subunit	Ref. 29
	PS II	N-terminus of D1	decreasing of O2-evolving activity, Ref. 35
		C-terminus of CP43	Ref. 36
		C-terminus of CP47	Ref. 30
		N-terminus of cyt b_{559} (PsbE)	Ref. 32
	PS I	N-terminus of PsaA	Ref. 34
	Grean sulfur bacterial RC [b]	N-terminus of PscA	this study
Periplasmic/lumen side	Purple bacterial RC	C-terminus of M subunit	Ref. 33
	PS II	C-terminus of D2	Ref. 35
		C-terminus of PsbH	Ref. 31
	PS I	C-terminus of PsaK	buring the tag in the complex, Ref. 37
		C-terminus of PsaL	buring the tag in the complex, Ref. 37
	Grean sulfur bacterial RC [b]	C-terminus of PscA	buring the tag in the complex, this study.

[a] The membrane topologies were estimated based on the crystal structures of the purple bacterial RC (PDB ID: 1PRC), cyanobacterial PS II (PDB ID: 3BZ), and PS I (PDB ID: 1JB0).

[b] The membrane topology of PscA was estimated based on the number of predicted transmembrane helices and homology of the amino acid sequence to cyanobacterial PS I (2, 20).

Figures

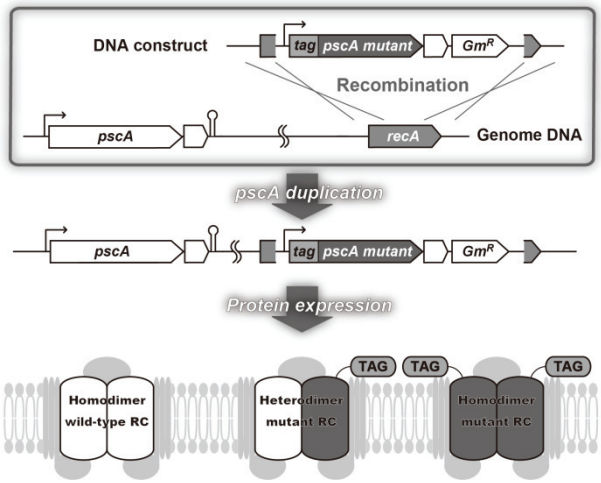

Figure III-1. Mutagenesis strategy for constructing the site-directed mutant of *Cba. tepidum* RC. The *recA* gene is inactivated by insertion of the mutated *tag-pscA* gene together with selection marker such as a gentamicin resistance cassette. All of the mutated RC complexes can be isolated with the affinity tags which are supposed to attach to only mutated PscA core proteins. The authentic *pscA* gene remained untouched is expected to express the native RC core proteins and promise the photosynthetic growth of the *Cba. tepidum* mutant.

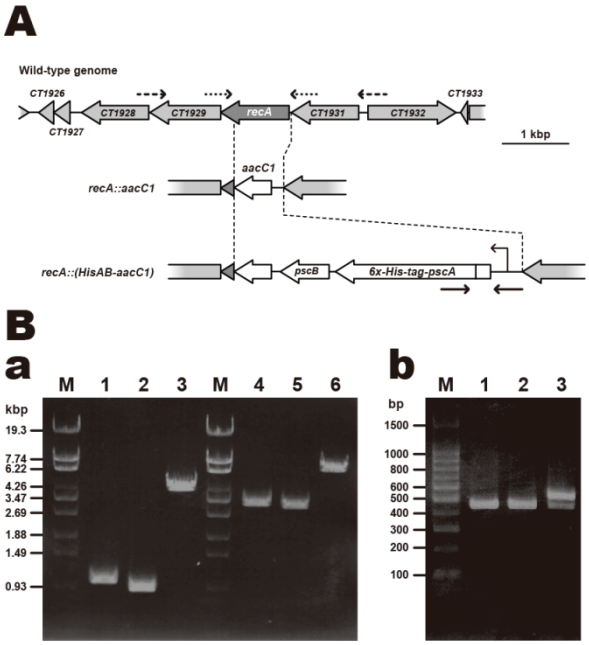

Figure III-2. Insertional inactivation of the *recA* gene and duplication of the *pscA* gene in *Cba. tepidum*. (A) Schematic map for the construction of *recA*-disrupted mutants. The upper map indicates the genomic region of the wild-type *Cba. tepidum* around the *recA* gene. The middle and lower maps indicate the regions of DNA constructs used for homologous recombination. The arrows the oligonucleotide primers used for the PCR analyses in panel B. (B) (a) PCR analyses of the genomes from the wild-type (lanes 1 and 4), the *recA::aacC1* (lanes 2 and 5), and the *recA::(HisAB-aacC1)* (lanes 3 and 6) strains at the *recA* regions. Lanes 1-3 and 4-6 contained the amplification products of the PCRs using the *recA*-inside (short-dotted arrows in panel A) and the *recA*-outside (broken arrows in panel A) primer sets, respectively. Lanes M contained λ/*Sty*I digests as molecular weight makers. (b) PCR analyses for verifying the *pscA* gene duplication. The upstream regions of *pscA* genes were amplified from the genomes of the wild-type (lane 1), the *recA::aacC1* (lane 2), and the *recA::(HisAB-aacC1)* (lanes 3) using the *pscA* up-stream primer sets (solid arrows in panel A). Lane M contained 100 bp DNA ladder makers.

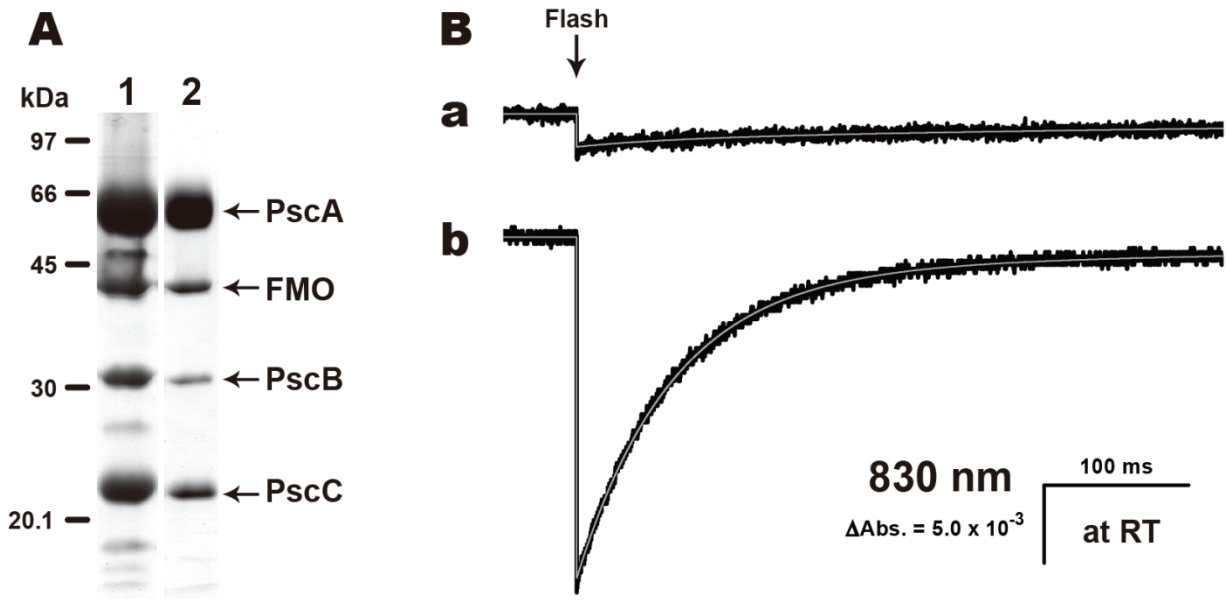

Figure III-3. SDS-PAGE analysis (A) and flash-induced absorption kinetics (B) of the His-tagged RC preparation. (A) Lane 1, the His-tagged RC preparation eluted from the Ni^{2+}-immobilized resin; lane 2, the His-tagged RC preparation purified by gel filtration with Sephacryl S-300. Numders and bars in the left indicate masses and mobilities of polypeptides in LMW protein marker (GE Healthcare), respectively: phosphorylase b (97 kDa), bovine serum albumin (66 kDa), ovalbumin (45 kDa), carbonic anhydrase (31 kDa), trypsin inhibitor (20.1 kDa), and α-lactalbumin (14.4 kDa). (B) The kinetics at 830 nm in the absence (trace a) and presence of 60% glycerol (trace b). Measurements were carried out at room temperature. The concentrations of samples were adjusted to be $Abs._{815} = 1.0$.

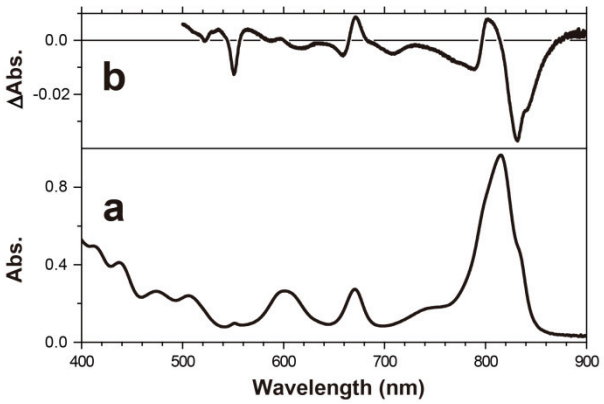

Figure III-4. The absorption (a) and chemically oxidized-minus-reduced different spectra (b) of the His-tagged RC preparation. The gray thin lines indicate the results of kinetic analyses by curve fitting programs. The absorption (trace a) and chemically oxidized-minus-reduced difference spectra (trace b) of the His-tagged RC complex. The difference spectrum was obtained by oxidizing the sample with a small amount of ferricyanide, followed by reducing it again with an excess amount of ascorbate. The sample used for the difference spectrum was same as that for trace a.

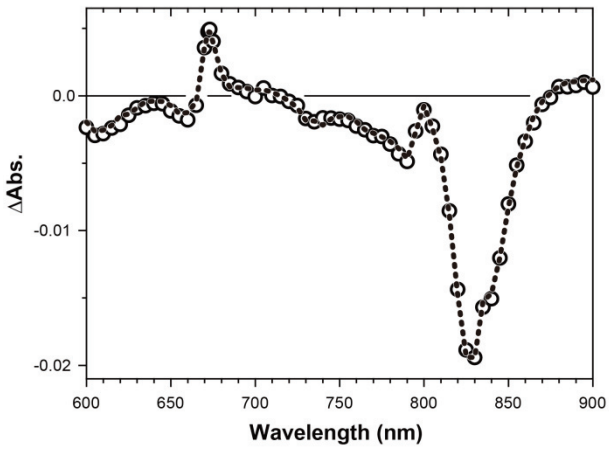

Figure III-5. The flash-induced absorption spectrum of P840 in the His-tagged RC preparation. The flash-induced absorption spectrum (open circles) and the decay associated spectrum of 60 ms components (dotted line) at 600-900 nm. The kinetics at each wavelength was measured in the presence of 60% glycerol at room temperature, and fitted by global analysis with monoexponential function whose time constant was shared in all kinetics. The concentrations of samples were adjusted to be $Abs._{815} = 1.0$.

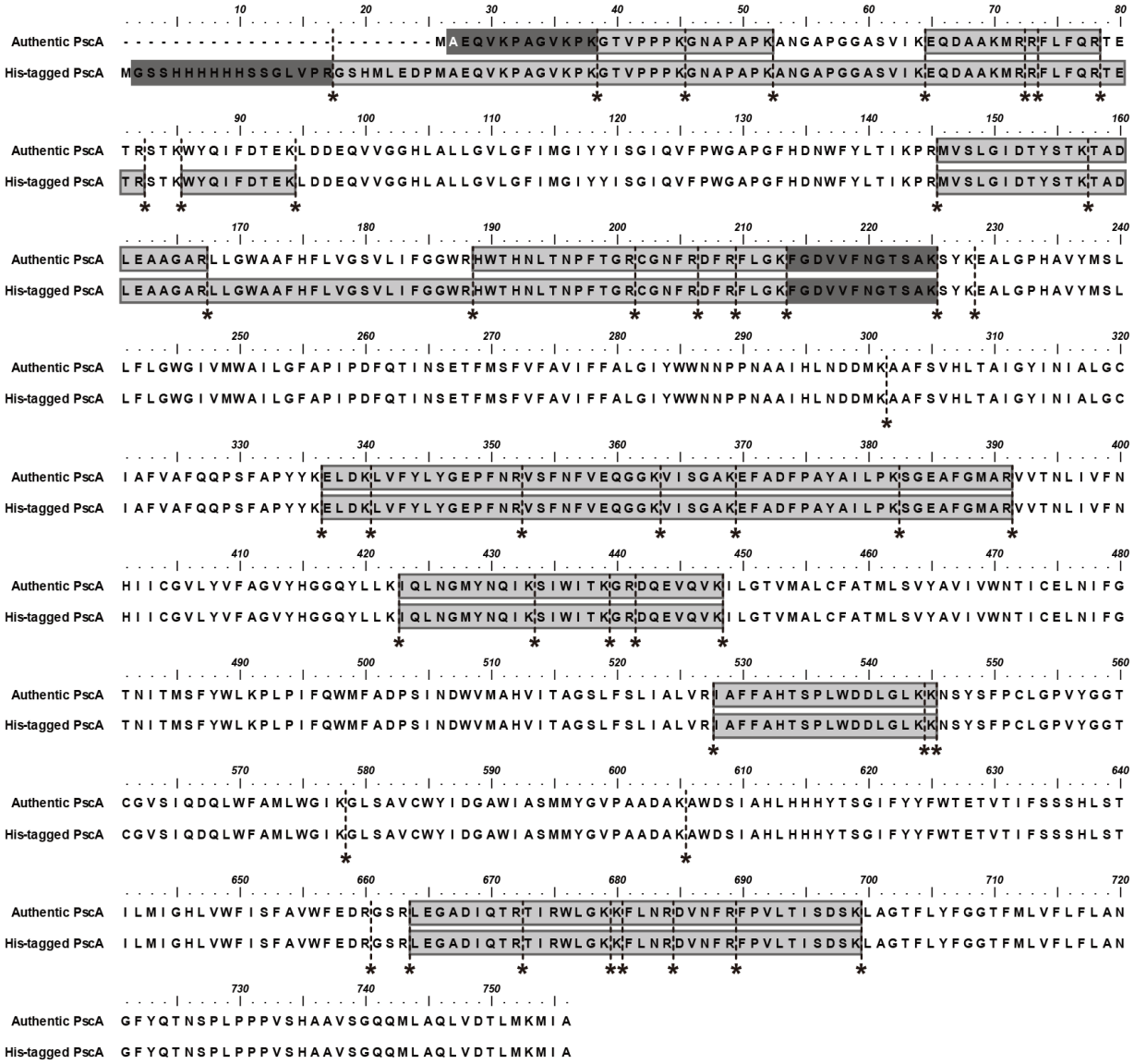

Figure III-6. The overall amino acid sequence alignment of the authentic (non-tagged) and His-tagged PscAs. The trypsin cleavage sites are indicated by broken lines with asterisks. The shaded sequences are N-terminal tryptic peptides detected by LC-MS/MS in the present study. The peptides used for confirmation and quantitation of heterogeneity in the Hi-tagged RC preparation are shaded in dark gray. The alanine having acetylated amino group is written in white.

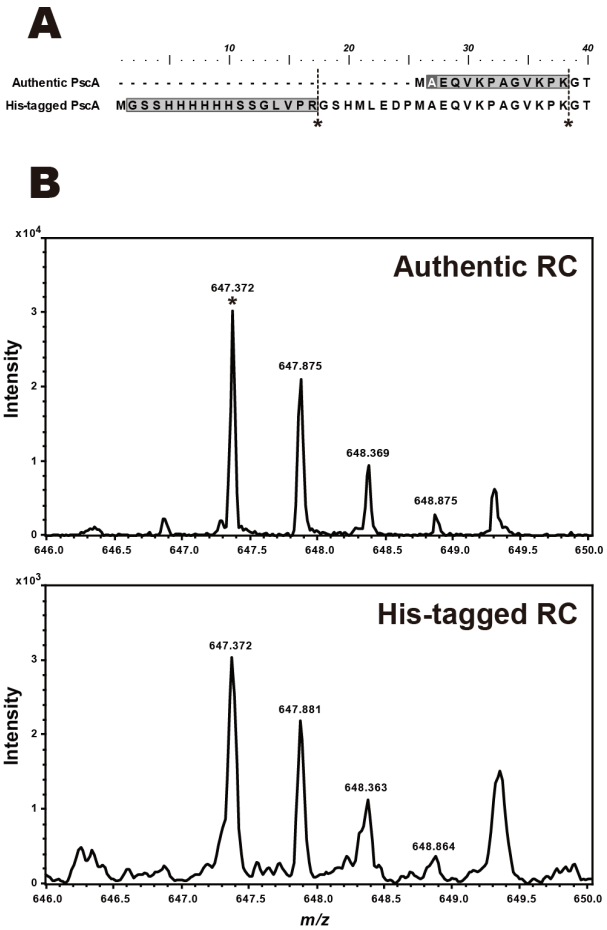

Figure III-7. LC-MS/MS analyses of N-terminal tryptic peptides of the authentic and His-tagged RC preparations. (A) The amino acid sequence alignment of the authentic (non-tagged) and His-tagged PscAs at N-terminal region. The trypsin cleavage sites are indicated by broken lines with asterisks. The shaded sequences are N-terminal tryptic peptides detected by LC-MS/MS in the present study. The alanine having acetylated amino group is written in white and shaded in dark gray. The overall sequence alignment and detected tryptic peptides are shown in Figure S3. (B) Mass spectra of N-terminal tryptic peptides of non-tagged PscAs obtained from the authentic (upper) and Hi-tagged RC preparations (lower) at 646-650 m/z. These peptides were separated with C-18 column and eluted at 17.8 min. The asterisk indicates the 2+-ion peak of the N-terminal tryptic peptides of non-tagged PscA whose amino acid sequence was confirmed by MS/MS (see Figure S5).

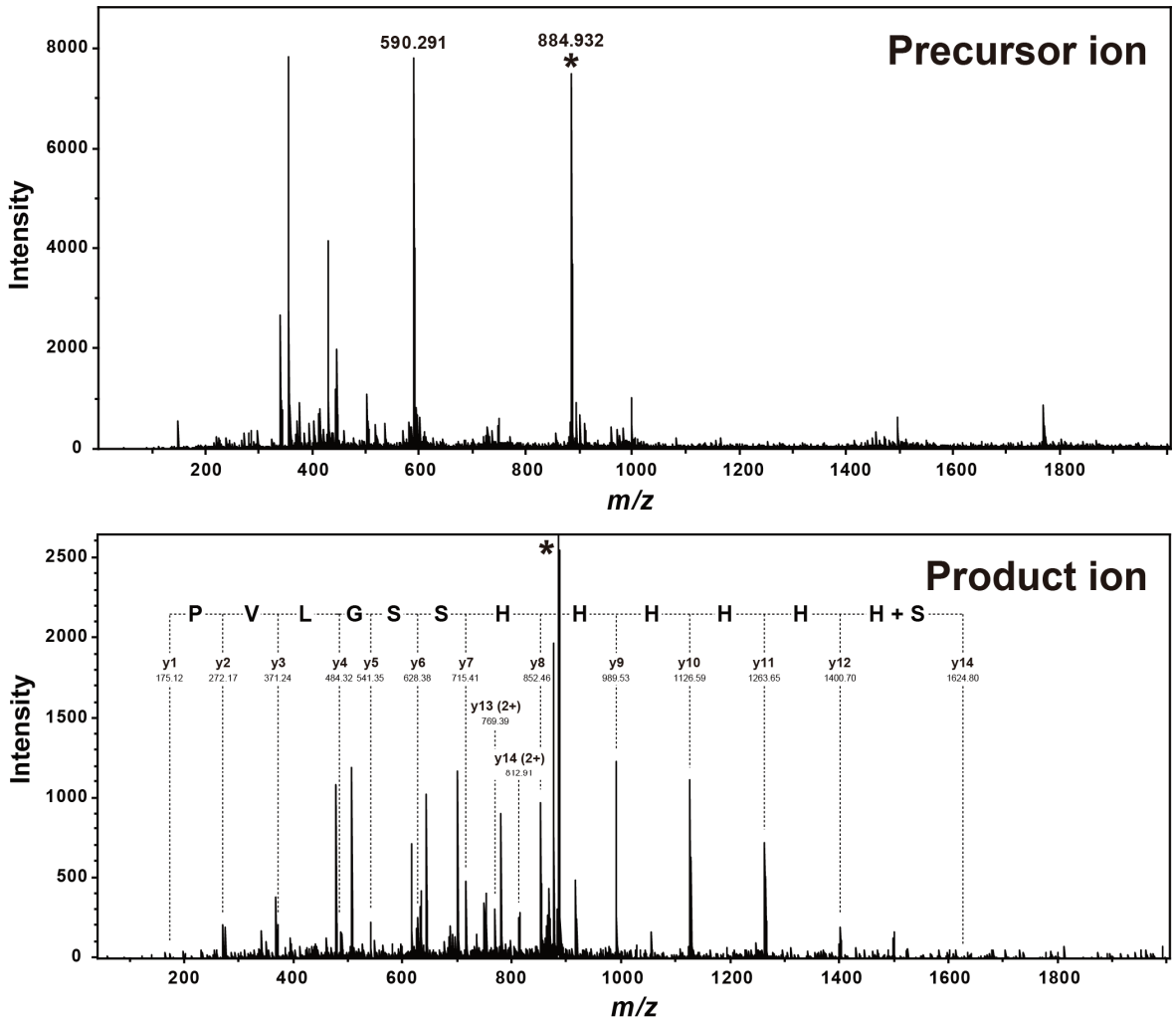

Figure III-8. Mass spectra for the precursor (upper) and product (lower) ions of the N-terminal tryptic peptide of the His-tagged PscA. The peptide for precursor ion was separated from the His-tagged RC preparation with C-18 column and eluted at 8.2 min. The asterisk indicates the 2+-ion peak used for MS/MS. The precursor ion was fragmented by collision induced dissociation with Ar gas. The y-ion peaks and its m/z are shown in product ion spectrum. The amino acid sequence deduced from their mass differences is also shown on the top of them.

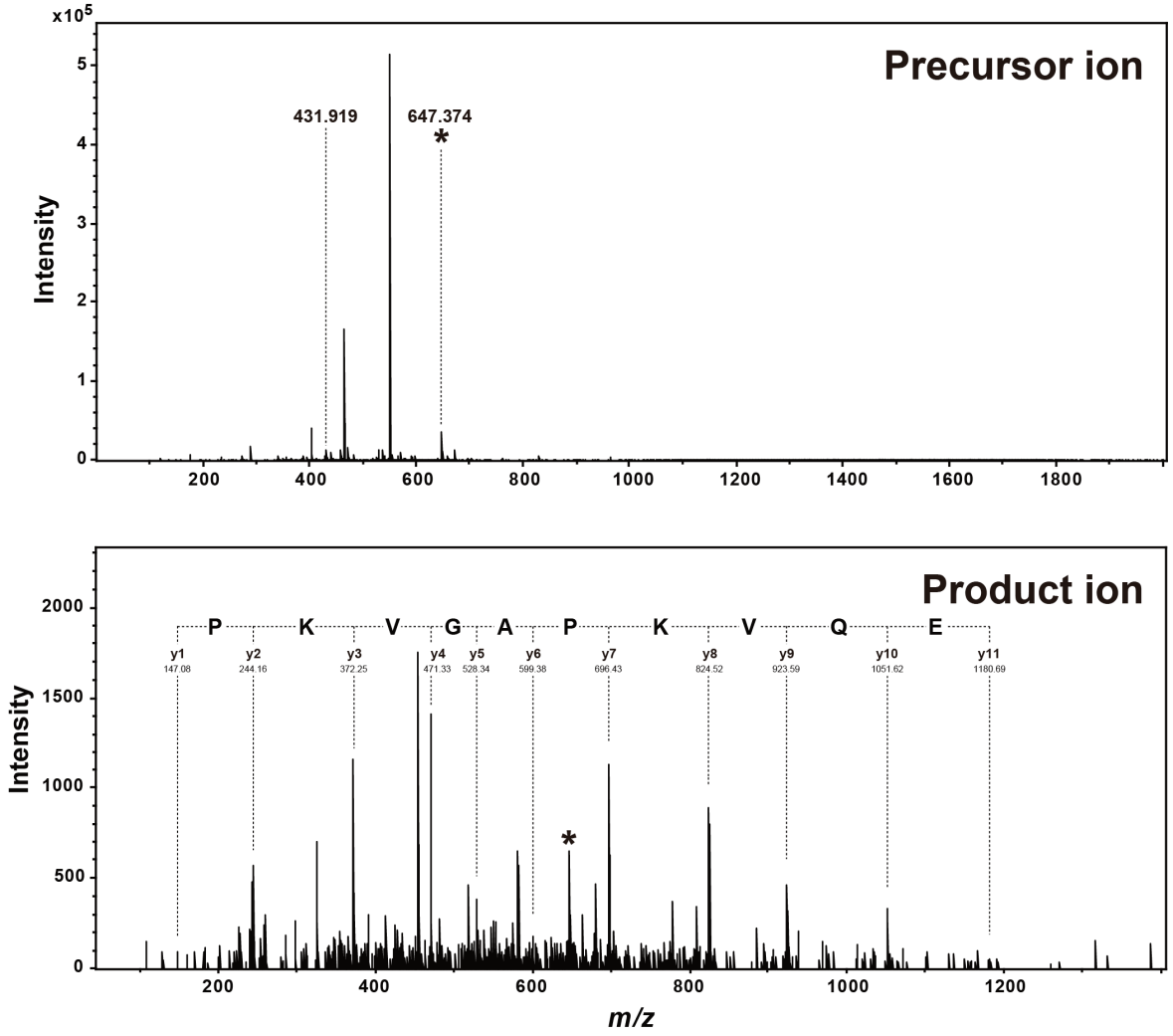

Figure III-9. Mass spectra for the precursor (upper) and product (lower) ions of the N-terminal tryptic peptide of the non-tagged PscA. The peptide for precursor ion was separated from authentic RC preparation with C-18 column and eluted at 17.8 min. The asterisk indicates the 2+-ion peak used for MS/MS. The precursor ion was fragmented by collision induced dissociation with Ar gas. The y-ion peaks and its m/z are shown in product ion spectrum. The amino acid sequence deduced from their mass differences is also shown on the top of them.

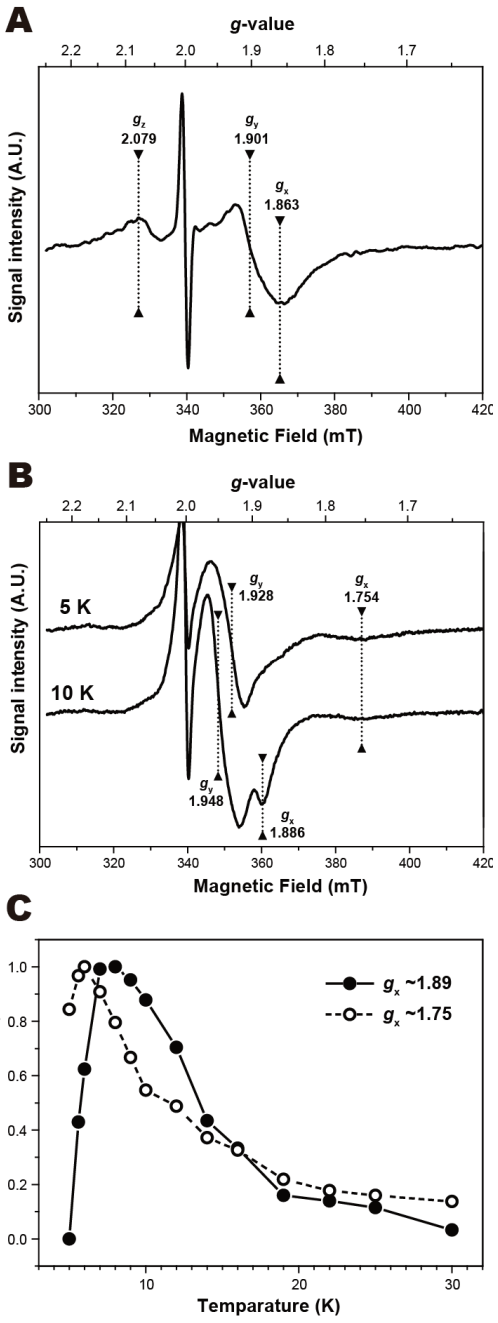

Figure III-10. ESR spectra of iron-sulfur centers and their temperature dependency in the His-tagged RC. (A) The sample was frozen to 5 K in the dark in the presence of an excess dithionite. The light-minus-dark difference spectrum was obtained by subtracting the spectrum measured without illumination from the spectrum measured after the illumination for 5 minutes at 5 K. Conditions of ESR measurements: temperature, 10K; microwave power, 10 mW; microwave frequency, 9.518 GHz; modulation amplitude, 20 G; and modulation frequency, 100 KHz. (B) The photoaccumulated sample was prepared by the preillumination for 20 minutes at 210 K in the presence of an excess dithionite and the subsequent cooling to 5 K under the illumination. The light-minus-dark difference spectra at 5 (upper) and 10 K (lower), respectively, were obtained by subtracting the spectra measured in the sample frozen in the dark from the spectra measured after the illumination for 5 minutes at 5 K in the photoaccumulated sample. Conditions of ESR measurements are the same as in (A) except for temperature. (C) The temperature dependency of ESR signals obtained in (B). The intensities of g_x signals corresponding to g_x values of approx. 1.89 (closed circle) and 1.75 (open circles) were normalized and plotted against temperature.

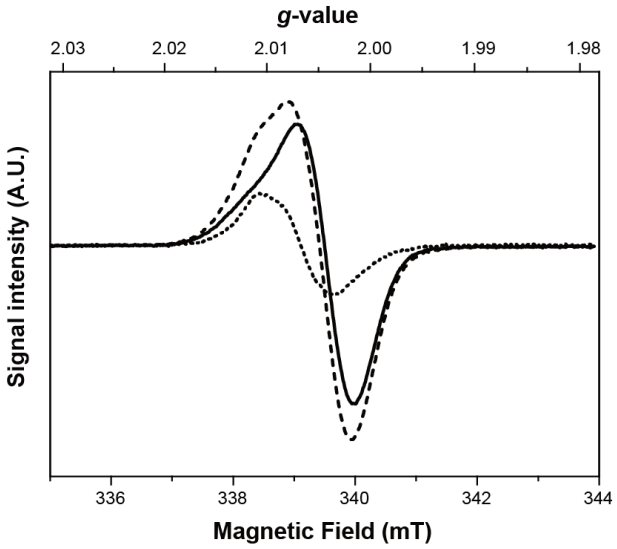

Figure III-11. ESR spectrum of photoaccumulated A_1 semiquinone radicals in the His-tagged RC. The spectra were measured after the illumination for 1 minute at 5 K using the sample frozen in the dark (solid line) and photoaccumulated sample as in Figure III-10 (broken line), respectively. The difference spectrum (short-dotted line) was obtained by subtracting the former from the latter. Conditions of ESR measurements: temperature, 30K; microwave power, 1 mW; microwave frequency, 9.524 GHz; modulation amplitude, 4.1 G; and modulation frequency, 100 KHz.

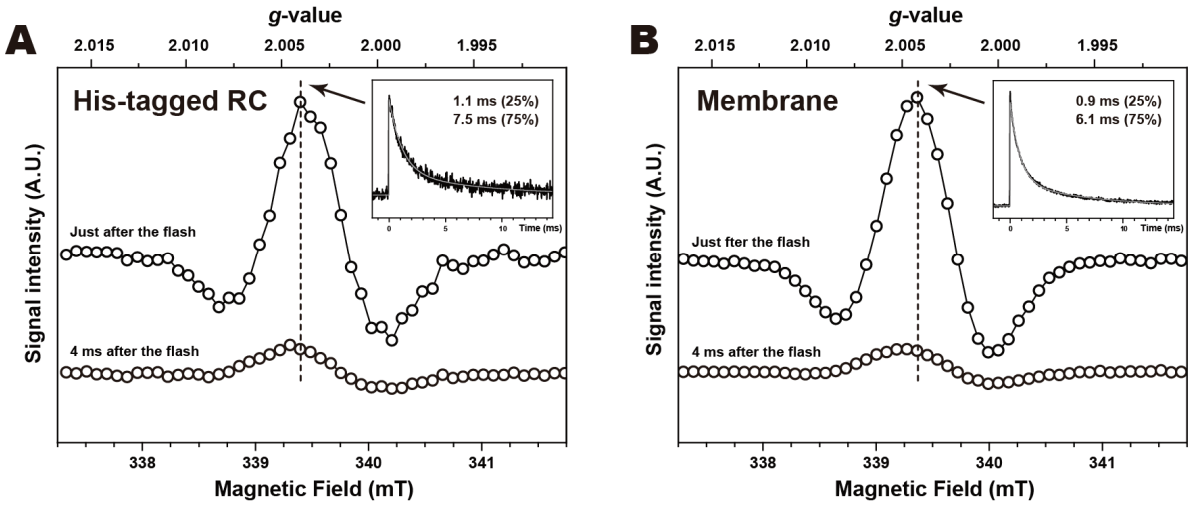

Figure III-12. The flash-induced ESR spectra in the His-tagged RC preparation (A) and the membrane from the wild-type strain (B) at 10 K. The dark-frozen sample was excited with the xenon flash at 10 K. Transient ESR signals of 4 ms (lower) and just after the flash excitation (upper) are plotted against the magnetic field. The decay kinetics at 339.4 mT are shown as inset. The field position corresponding to 339.4 mT was shown as a broken line in spectra. The gray thin line indicates the result of kinetic analysis by a curve fitting program. Conditions of ESR measurements: microwave power, 0.1 mW; microwave frequency, 9.520 GHz; modulation amplitude, 4.0 G; and modulation frequency, 100 KHz.

References

1. Heathcote, P., Fyfe, P. K., and Jones, M. R. (2002) Reaction centres: the structure and evolution of biological solar power, *Trends Biochem Sci* **27**, 79-87
2. Hauska, G., Schoedl, T., Remigy, H., and Tsiotis, G. (2001) The reaction center of green sulfur bacteria(1), *Biochim Biophys Acta* **1507**, 260-277
3. Oh-oka, H. (2007) Type 1 reaction center of photosynthetic heliobacteria, *Photochem Photobiol* **83**, 177-186
4. Li, Y., van der Est, A., Lucas, M. G., Ramesh, V. M., Gu, F., Petrenko, A., Lin, S., Webber, A. N., Rappaport, F., and Redding, K. (2006) Directing electron transfer within Photosystem I by breaking H-bonds in the cofactor branches, *Proc Natl Acad Sci U S A* **103**, 2144-2149
5. Wakeham, M. C., and Jones, M. R. (2005) Rewiring photosynthesis: engineering wrong-way electron transfer in the purple bacterial reaction centre, *Biochem Soc Trans* **33**, 851-857
6. Diner, B. A., and Rappaport, F. (2002) Structure, dynamics, and energetics of the primary photochemistry of photosystem II of oxygenic photosynthesis, *Annu Rev Plant Biol* **53**, 551-580
7. Olson, J. M. (2004) The FMO Protein, *Photosynth Res* **80**, 181-187
8. Jagannathan, B., and Golbeck, J. H. (2008) Unifying principles in homodimeric type I photosynthetic reaction centers: properties of PscB and the FA, FB and FX iron-sulfur clusters in green sulfur bacteria, *Biochim Biophys Acta* **1777**, 1535-1544
9. Oh-oka, H., Kamei, S., Matsubara, H., Iwaki, M., and Itoh, S. (1995) Two molecules of cytochrome c function as the electron donors to P840 in the reaction center complex isolated from a green sulfur bacterium, Chlorobium tepidum, *FEBS Lett* **365**, 30-34
10. Oh-oka, H., Iwaki, M., and Itoh, S. (1998) Membrane-bound cytochrome cz couples quinol oxidoreductase to the P840 reaction center complex in isolated membranes of the green sulfur bacterium Chlorobium tepidum, *Biochemistry* **37**, 12293-12300
11. Oh-oka, H., Iwaki, M., and Itoh, S. (1997) Viscosity dependence of the electron transfer rate from bound cytochrome c to P840 in the photosynthetic reaction center of the green sulfur bacterium Chlorobium tepidum, *Biochemistry* **36**, 9267-9272
12. Fenna, R. E., and Matthews, B. W. (1975) Chlorophyll arrangement in a bacteriochlorophyll protein from Chlorobium limicola., *Nature* **258**, 573-577
13. Tronrud, D. E., Wen, J., Gay, L., and Blankenship, R. E. (2009) The structural basis for the difference in absorbance spectra for the FMO antenna protein from various green sulfur bacteria, *Photosynth Res* **100**, 79-87
14. Tsukatani, Y., Miyamoto, R., Itoh, S., and Oh-Oka, H. (2004) Function of a PscD

subunit in a homodimeric reaction center complex of the photosynthetic green sulfur bacterium Chlorobium tepidum studied by insertional gene inactivation. Regulation of energy transfer and ferredoxin-mediated NADP+ reduction on the cytoplasmic side, *J Biol Chem* **279**, 51122-51130

15. Miyamoto, R., Mino, H., Kondo, T., Itoh, S., and Oh-Oka, H. (2008) An electron spin-polarized signal of the P800+A1(Q)- state in the homodimeric reaction center core complex of Heliobacterium modesticaldum, *Biochemistry* **47**, 4386-4393
16. Kjaer, B., Frigaard, N. U., Yang, F., Zybailov, B., Miller, M., Golbeck, J. H., and Scheller, H. V. (1998) Menaquinone-7 in the reaction center complex of the green sulfur bacterium Chlorobium vibrioforme functions as the electron acceptor A1, *Biochemistry* **37**, 3237-3242
17. Kusumoto, N., Setif, P., Brettel, K., Seo, D., and Sakurai, H. (1999) Electron transfer kinetics in purified reaction centers from the green sulfur bacterium Chlorobium tepidum studied by multiple-flash excitation, *Biochemistry* **38**, 12124-12137
18. van der Est, A., Hager-Braun, C., Leibl, W., Hauska, G., and Stehlik, D. (1998) Transient electron paramagnetic resonance spectroscopy on green-sulfur bacteria and heliobacteria at two microwave frequencies, *Biochim Biophys Acta* **1409**, 87-98
19. Heathcote, P., Jones, M. R., and Fyfe, P. K. (2003) Type I photosynthetic reaction centres: structure and function, *Philos Trans R Soc Lond B Biol Sci* **358**, 231-243
20. Artz, K., Williams, J. C., Allen, J. P., Lendzian, F., Rautter, J., and Lubitz, W. (1997) Relationship between the oxidation potential and electron spin density of the primary electron donor in reaction centers from Rhodobacter sphaeroides, *Proc Natl Acad Sci U S A* **94**, 13582-13587
21. Bylina, E. J., and Youvan, D. C. (1988) Directed mutations affecting spectroscopic and electron transfer properties of the primary donor in the photosynthetic reaction center, *Proc Natl Acad Sci U S A* **85**, 7226-7230
22. Diner, B. A., Schlodder, E., Nixon, P. J., Coleman, W. J., Rappaport, F., Lavergne, J., Vermaas, W. F., and Chisholm, D. A. (2001) Site-directed mutations at D1-His198 and D2-His197 of photosystem II in Synechocystis PCC 6803: sites of primary charge separation and cation and triplet stabilization, *Biochemistry* **40**, 9265-9281
23. Krabben, L., Schlodder, E., Jordan, R., Carbonera, D., Giacometti, G., Lee, H., Webber, A. N., and Lubitz, W. (2000) Influence of the axial ligands on the spectral properties of P700 of photosystem I: a study of site-directed mutants, *Biochemistry* **39**, 13012-13025
24. Frigaard, N. U., and Bryant, D. A. (2001) Chromosomal gene inactivation in the green sulfur bacterium Chlorobium tepidum by natural transformation, *Appl Environ Microbiol* **67**, 2538-2544
25. Frigaard, N. U., and Bryant, D. A. (2004) Seeing green bacteria in a new light: genomics-enabled studies of the photosynthetic apparatus in green sulfur bacteria and filamentous anoxygenic phototrophic bacteria, *Arch Microbiol* **182**, 265-276

26. Eisen, J. A., Nelson, K. E., Paulsen, I. T., Heidelberg, J. F., Wu, M., Dodson, R. J., Deboy, R., Gwinn, M. L., Nelson, W. C., Haft, D. H., Hickey, E. K., Peterson, J. D., Durkin, A. S., Kolonay, J. L., Yang, F., Holt, I., Umayam, L. A., Mason, T., Brenner, M., Shea, T. P., Parksey, D., Nierman, W. C., Feldblyum, T. V., Hansen, C. L., Craven, M. B., Radune, D., Vamathevan, J., Khouri, H., White, O., Gruber, T. M., Ketchum, K. A., Venter, J. C., Tettelin, H., Bryant, D. A., and Fraser, C. M. (2002) The complete genome sequence of Chlorobium tepidum TLS, a photosynthetic, anaerobic, green-sulfur bacterium, *Proc Natl Acad Sci U S A* **99**, 9509-9514

27. Kowalczykowski, S. C., Dixon, D. A., Eggleston, A. K., Lauder, S. D., and Rehrauer, W. M. (1994) Biochemistry of homologous recombination in Escherichia coli, *Microbiol Rev* **58**, 401-465

28. Erill, I., Campoy, S., and Barbe, J. (2007) Aeons of distress: an evolutionary perspective on the bacterial SOS response, *FEMS Microbiol Rev* **31**, 637-656

29. Abresch, E. C., Axelrod, H. L., Beatty, J. T., Johnson, J. A., Nechushtai, R., and Paddock, M. L. (2005) Characterization of a highly purified, fully active, crystallizable RC-LH1-PufX core complex from Rhodobacter sphaeroides, *Photosynth Res* **86**, 61-70

30. Bricker, T. M., Morvant, J., Masri, N., Sutton, H. M., and Frankel, L. K. (1998) Isolation of a highly active photosystem II preparation from Synechocystis 6803 using a histidine-tagged mutant of CP 47, *Biochim Biophys Acta* **1409**, 50-57

31. Cullen, M., Ray, N., Husain, S., Nugent, J., Nield, J., and Purton, S. (2007) A highly active histidine-tagged Chlamydomonas reinhardtii Photosystem II preparation for structural and biophysical analysis, *Photochem Photobiol Sci* **6**, 1177-1183

32. Fey, H., Piano, D., Horn, R., Fischer, D., Schmidt, M., Ruf, S., Schroder, W. P., Bock, R., and Buchel, C. (2008) Isolation of highly active photosystem II core complexes with a His-tagged Cyt b559 subunit from transplastomic tobacco plants, *Biochim Biophys Acta* **1777**, 1501-1509

33. Goldsmith, J. O., and Boxer, S. G. (1996) Rapid isolation of bacterial photosynthetic reaction centers with an engineered poly-histidine tag, *Biochim Biophys Acta* **1276**, 171-175

34. Gulis, G., Narasimhulu, K. V., Fox, L. N., and Redding, K. E. (2008) Purification of His6-tagged Photosystem I from Chlamydomonas reinhardtii, *Photosynth Res* **96**, 51-60

35. Sugiura, M., Inoue, Y., and Minagawa, J. (1998) Rapid and discrete isolation of oxygen-evolving His-tagged photosystem II core complex from Chlamydomonas reinhardtii by Ni2+ affinity column chromatography, *FEBS Lett* **426**, 140-144

36. Sugiura, M., Rappaport, F., Brettel, K., Noguchi, T., Rutherford, A. W., and Boussac, A. (2004) Site-directed mutagenesis of Thermosynechococcus elongatus photosystem II: the O2-evolving enzyme lacking the redox-active tyrosine D, *Biochemistry* **43**, 13549-13563

37. Tang, H., and Chitnis, P. R. (2000) Addition of C-terminal histidyl tags to PsaL and PsaK1 proteins of cyanobacterial photosystem I, *Indian J Biochem Biophys* **37**, 433-440
38. Wahlund, T. M., and Madigan, M. T. (1995) Genetic transfer by conjugation in the thermophilic green sulfur bacterium Chlorobium tepidum, *J Bacteriol* **177**, 2583-2588
39. Schweizer, H. D. (1993) Small broad-host-range gentamycin resistance gene cassettes for site-specific insertion and deletion mutagenesis, *Biotechniques* **15**, 831-834
40. Prentki, P., and Krisch, H. M. (1984) In vitro insertional mutagenesis with a selectable DNA fragment, *Gene* **29**, 303-313
41. Frigaard, N. U., Sakuragi, Y., and Bryant, D. A. (2004) Gene inactivation in the cyanobacterium Synechococcus sp. PCC 7002 and the green sulfur bacterium Chlorobium tepidum using in vitro-made DNA constructs and natural transformation, *Methods Mol Biol* **274**, 325-340
42. Maresca, J. A., Gomez Maqueo Chew, A., Ponsati, M. R., Frigaard, N. U., Ormerod, J. G., and Bryant, D. A. (2004) The bchU gene of Chlorobium tepidum encodes the c-20 methyltransferase in bacteriochlorophyll c biosynthesis, *J Bacteriol* **186**, 2558-2566
43. Oh-oka, H., Kakutani, S., Matsubara, H., Malkin, R., and Itoh, S. (1993) Isolation of the photoactive reaction center complex that contains three types of Fe-S centers and a cytochrome *c* subunit from the green sulfur bacterium *Chlorobium limicola* f. *thiosulfatophilum*, strain Larsen, *Plant Cell Physiol* **34**, 93-101
44. Laemmli, U. K. (1970) Cleavage of structural proteins during the assembly of the head of bacteriophage T4, *Nature* **227**, 680-685
45. Francke, C., Permentier, H. P., Franken, E. M., Neerken, S., and Amesz, J. (1997) Isolation and properties of photochemically active reaction center complexes from the green sulfur bacterium Prosthecochloris aestuarii, *Biochemistry* **36**, 14167-14172
46. Olson, J. M., Philipson, K. D., and Sauer, K. (1973) Circular dichroism and absorption spectra of bacteriochlorophyll-protein and reaction center complexes from Chlorobium thiosulfatophilum, *Biochim Biophys Acta* **292**, 206-217
47. Azai, C., Tsukatani, Y., Itoh, S., and Oh-Oka, H. (2010) C-type cytochromes in the photosynthetic electron transfer pathways in green sulfur bacteria and heliobacteria, *Photosynth Res*
48. Higuchi, M., Hirano, Y., Kimura, Y., Oh-oka, H., Miki, K., and Wang, Z. Y. (2009) Overexpression, characterization, and crystallization of the functional domain of cytochrome c(z) from Chlorobium tepidum, *Photosynth Res* **102**, 77-84
49. Hirano, Y., Higuchi, M., Azai, C., Oh-Oka, H., Miki, K., and Wang, Z. Y. (2010) Crystal structure of the electron carrier domain of the reaction center cytochrome c(z) subunit from green photosynthetic bacterium Chlorobium tepidum, *J Mol Biol* **397**, 1175-1187
50. Meyer, T. E., Bartsch, R. G., Cusanovich, M. A., and Mathewson, J. H. (1968) The

cytochromes of Chlorobium thiosulfatophilum, *Biochim Biophys Acta* **153**, 854-861

51. Feiler, U., Nitschke, W., and Michel, H. (1992) Characterization of an improved reaction center preparation from the photosynthetic green sulfur bacterium Chlorobium containing the FeS centers FA and FB and a bound cytochrome subunit, *Biochemistry* **31**, 2608-2614
52. Nitschke, W., Feiler, U., and Rutherford, A. W. (1990) Photosynthetic reaction center of green sulfur bacteria studied by EPR, *Biochemistry* **29**, 3834-3842
53. Vassiliev, I. R., Ronan, M. T., Hauska, G., and Golbeck, J. H. (2000) The bound electron acceptors in green sulfur bacteria: resolution of the g-tensor for the F(X) iron-sulfur cluster in Chlorobium tepidum, *Biophys J* **78**, 3160-3169
54. Clark, A. J., and Margulis, A. D. (1965) Isolation and characterization of recombination-deficient strains of Escherichia coli K-12, *Proc Natl Acad Sci U S A* **53**, 451-459
55. Chen, I. P., and Michel, H. (1998) Cloning, sequencing, and characterization of the recA gene from Rhodopseudomonas viridis and construction of a recA strain, *J Bacteriol* **180**, 3227-3232
56. Minda, R., Ramchandani, J., Joshi, V. P., and Bhattacharjee, S. K. (2005) A homozygous recA mutant of Synechocystis PCC6803: construction strategy and characteristics eliciting a novel RecA independent UVC resistance in dark, *Mol Genet Genomics* **274**, 616-624
57. Li, H., Jubelirer, S., Garcia Costas, A. M., Frigaard, N. U., and Bryant, D. A. (2009) Multiple antioxidant proteins protect Chlorobaculum tepidum against oxygen and reactive oxygen species, *Arch Microbiol* **191**, 853-867
58. Miyamoto, R., Iwaki, M., Mino, H., Harada, J., Itoh, S., and Oh-Oka, H. (2006) ESR signal of the iron-sulfur center F(X) and its function in the homodimeric reaction center of Heliobacterium modesticaldum, *Biochemistry* **45**, 6306-6316
59. Golbeck, J. H., and Bryant, D. A. (eds). (1991) *Photosystem I*, Vol. 16, Academic Press, Inc., San Diego
60. Skerra, A., and Schmidt, T. G. (1999) Applications of a peptide ligand for streptavidin: the Strep-tag, *Biomol Eng* **16**, 79-86

List of publications

1. Parallel electron donation pathways to cytochrome c(z) in the type I homodimeric photosynthetic reaction center complex of Chlorobium tepidum
   Tsukatani, Y., Azai, C., Kondo, T., Itoh, S., and Oh-Oka, H. (2008), *Biochim Biophys Acta* **1777**, 1211-1217

2. Accumulation of chlorophyllous pigments esterified with the geranylgeranyl group and photosynthetic competence in the CT2256-deleted mutant of the green sulfur bacterium Chlorobium tepidum
   Harada, J., Miyago, S., Mizoguchi, T., Azai, C., Inoue, K., Tamiaki, H., and Oh-oka, H. (2008), *Photochem Photobiol Sci* **7**, 1179-1187

3. Sulfur oxidation in mutants of the photosynthetic green sulfur bacterium Chlorobium tepidum devoid of cytochrome c-554 and SoxB
   Azai, C., Tsukatani, Y., Harada, J., and Oh-oka, H. (2009), *Photosynth Res* **100**, 57-65

4. Crystal structure of the electron carrier domain of the reaction center cytochrome c(z) subunit from green photosynthetic bacterium Chlorobium tepidum
   Hirano, Y., Higuchi, M., Azai, C., Oh-Oka, H., Miki, K., and Wang, Z. Y. (2010), *J Mol Biol* **397**, 1175-1187

5. C-type cytochromes in the photosynthetic electron transfer pathways in green sulfur bacteria and heliobacteria
   Azai, C., Tsukatani, Y., Itoh, S., and Oh-Oka, H. (2010), *Photosynth Res*, (*in press*)

6. Affinity purification and characterization of the His-tagged reaction center complex of the photosynthetic green sulfur bacterium *Chlorobaculum tepidum* expressed by the gene duplication method
   Azai, C., Kim, K., Kondo, T., Itoh, S., and Oh-Oka, H., in preparation.

Acknowledgements

This thesis would not have been accomplished without hearty assistance and cooperation of many people. I would like to express my deepest gratitude to all of them.

Before all, I would like to thank Dr. Hirozo Oh-oka (Osaka University). He supported me with his critical suggestions, fruitful discussion, and encouragement throughout my research. I really thank Prof. Keiichi Fukuyama (Osaka University). He provided me with the opportunity for this study, and helped me with his kind guidance and expertise on structural biology. I greatly thank Dr. Yusuke Tsukatani (Pennsylvania State University) and Dr. Jiro Harada (Kurume University) for their collaboration and deep discussions. They taught me the ABC's of the study of green sulfur bacteria, and gave me careful and constructive advices at every step of my research. I am deeply grateful to Prof. Shigeru Itoh (Nagoya University) for his support, stimulating discussions, and useful suggestions. I am sincerely grateful to Mr. Toru Kondo (Nagoya University) for his collaboration and valuable discussions on spectroscopic experiments, especially on ESR measurements. I am thankful to Dr. Kwang Kim (Osaka University) for his incomparable skill in mass spectrometric analysis of proteins. I also thank Prof. Susumu Takakuwa (Kyoto Women's University) for his technical advice to estimate the quantity of sulfur compounds, and Mr. Hirofumi Omori (Osaka University) for technical assistance for nucleotide sequencing. I note special thanks to all members of Fukuyama laboratory for invaluable supports to carry out this study.

Finally, I would like to give my warmest appreciation to my parents, Hajime Azai and Hisako Azai, and all other members of my family, as well as my future wife, Ayumi Yamada. They have a profound understanding of my way of thinking and allowed me to lean 'science'.